FINAL REPORT

LOW EMISSION BURNER FOR RANKINE CYCLE ENGINES FOR AUTOMOBILES

U.S. Environmental Protection Agency

Low Emission Burner for Rankine Cycle Engines for Automobiles

FINAL REPORT

By

T. E. Duffy
J. R. Shekleton
R. T. LeCren
W. A. Compton

Prepared for

Department of Motor Vehicles
Research and Development
Air Pollution Control Office
Environmental Protection Agency

SOLAR
DIVISION OF INTERNATIONAL HARVESTER COMPANY
2200 PACIFIC HIGHWAY · SAN DIEGO, CALIFORNIA 92112

RDR 1695

FOREWORD

This Final Report covers the work performed under EPA/APCO during the work period, July 1, 1970 to March 31, 1971. It is published for information only, and does not necessarily represent the recommendations, conclusion, or approval of the Environmental Protection Agency, National Air Pollution Control Administration.

The contract with the Research Laboratories of Solar Division of International Harvester Company, San Diego, California, was initiated by the EPA/APCO under contract number EHS 70-106, monitored by Mr. F. Peter Hutchins, Project Officer.

The program was under the general direction of Mr. W. A. Compton, Assistant Director-Research, who served as Program Director. Mr. R. T. LeCren, Group Engineer was the principal investigator at Solar. Mr. Thomas E. Duffy, Research Staff Engineer was the specialist on controls and systems. Mr. Jack R. Shekleton, Engineering Specialist was the leader in combustion system development.

This report is identified by Solar as RDR 1695.

CONTENTS

CONTENTS (Cont)

ILLUSTRATIONS

ILLUSTRATIONS (Cont)

ILLUSTRATIONS (Cont)

ILLUSTRATIONS (Cont)

ILLUSTRATIONS (Cont)

TABLES

1

INTRODUCTION

Much of the air pollution in the United States is a result of undesirable emissions from automotive Otto cycle engines. Each day thousands of tons of toxic gaseous and particulate pollutants are dumped into the limited volume of the atmosphere over the United States. Because of the highly complex and transient nature of combustion combined with the cold walls of an automotive spark ignition engine, direct control of emissions in the combustion process is a difficult and possibly insoluble problem. Control by various post combustion schemes appears to offer considerably more potential. Several methods have been demonstrated and show promise. However, potential maintenance, service life, and high cost problems make it necessary to also consider alternatives to the internal combustion engine if these methods fail to achieve the goals. Systems utilizing continuous flow external combustors have been demonstrated to have low emission levels under steady-state operation. A Rankine Cycle engine has one of the best potentials of any of the continuous combustion engines for automotive application. The EPA is presently supporting basic research studies to optimize the low pollution features of burner designs for Rankine engines.

The basic problem resolved by this program was the demonstration that a Rankine cycle combustor system designed to be integrated into a "family car" could meet the 1980 Advanced Automotive Power Systems (AAPS) goals. A major portion of the effort for such a system has been devoted to the development of a full scale (2,000,000 BTU/hr) prototype combustor system and controls with the desired low emission characteristics. Automotive requirements for duty cycle, compactness, cost and efficiency are the constraints that challenge the present state-of-the-art for combustors. Rapid starts, high response, frequent shutdown, with large and frequent transients of power level demand, are required automotive performance factors that cause existing combustor designs to fall short of emission goals.

This program addressed itself to these problems by applying a new and novel fuel atomization and precise air-fuel ratio control concept to the automotive Rankine combustion system problem. Rotating cup atomization with a full range air-fuel ratio control is ideally suited to the wide fuel flow variations necessary for automotive duty cycles requiring low emissions because of all the various methods of fuel injection, it has the widest possible range of operation with a single fuel atomizer. Experience has indicated a major portion of the emissions result from load transients in conven-

tional combustors. The problem of making an on-off system emission-free is technically difficult, if not impossible. A combined on-off and modulated system share some of the problems of both and has greater complexity. Thus, this program developed a fully modulated system incorporating a rotating cup fuel atomization system and all necessary controls to supply and regulate both fuel and air at high response rates while maintaining the optimum air-fuel ratio for lowest emissions.

The purpose of this program was to apply modern analytical and experimental tools to the design, fabrication, development and demonstration of a low emission combustor system for an automotive Rankine cycle engine. The result of this study has been two-fold. First, the capability of meeting the emission goals has been demonstrated. Second, areas, which require further development in order to make the system usable in an automobile, have been identified.

2

SUMMARY

The primary objective of this program was to apply modern analytical and experimental techniques to the design and demonstration of a low emission combustor for an automotive Rankine engine. Results would show if the 1980 AAPS emission goals could be achieved and determine technology requiring advancement to equip a "family car" with a low emission combustor. Excellent progress had previously been made with combustors to obtain low unburned hydrocarbons (HC) and carbon monoxide (CO) at rated steady state operation but they could not meet the nitric oxide (NO) emission levels nor could they operate over the wide fuel flow range and rapid transients required for the automotive Rankine cycle engine.

Two approaches are open for emission control from automobile engines -- limit NO formation during combustion or eliminate NO after it is formed. Spark ignition engines can generate reducing exhaust gases and therefore eliminate NO by catalytic reduction with CO. Rankine cycles, gas turbines, and diesels cannot run fuel rich because of smoke production, inefficiency and overtemperature, and therefore cannot generate the necessary reducing exhaust gases. Thus the limit NO formation approach must be employed in the combustion zone.

The Solar approach has been to obtain low NO emissions through air-fuel ratio-control in combustion zones. A schematic shows the air-fuel ratio control and residence time for the primary, secondary, and tertiary zones of the combustor which were demonstrated to perform well within the established 1980 AAPS emission goals.

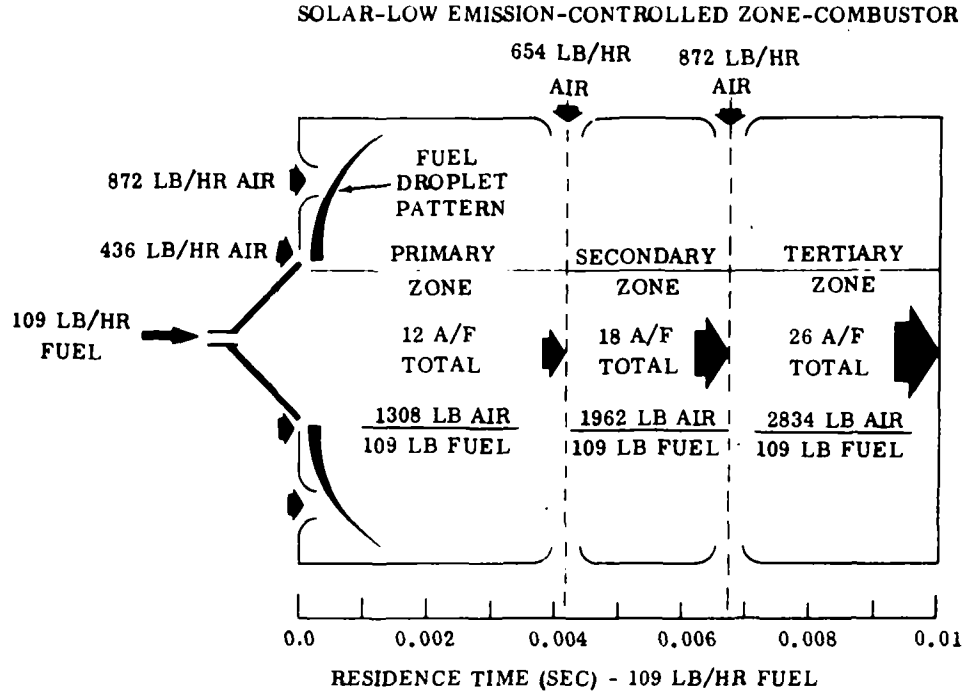

The rotating cup atomization system yields precision fuel droplet size and pattern independent of fuel flow. Precision air and fuel metering values allows scheduling of the desired air-fuel ratios over the 100 to 1 heat release estimated as a maximum range necessary to cover all engine systems.

The volume of the demonstrated combustor would be 1.1 cubic feet for the optimum design which included an optimum fan, demonstration controls and combustor. This corresponds with an initial goal of 1.3 cubic feet. The parasitic power is computed at 1.25 horsepower without the vaporizer and can be substantially reduced at part load with minor modifications of the demonstrated control system. Fan and combustor noise was above acceptable limits during many test conditions. An analysis of the noise indicated that noise could be reduced to acceptable limits by use of special design approaches for both the fan and combustor.

A fully modulated air-fuel control system has been designed and was demonstrated in integrated combustor emission tests. All major components of the system except the fan were specifically designed to obtain accurate control of air-fuel ratios. Design emphasis has also been placed upon high response capabilities necessary for low emission city traffic operations of automotive vehicles. Stop and start duty cycles require an almost continually fluctuating heat release rate from the combustor system. On-off control modes, although simple, were rejected because of their potential for higher emissions during the frequent start-up and shutdown transients required in automotive Rankine engines. The system developed basically consists of a variable area air valve mechanically linked to a variable area fuel valve. Integrated with the

basic area control is the air supply (electric fan) and the pressure control system (air by-pass valve). A fuel supply (electric pump) and fuel pressure regulator subsystem are incorporated in a manner that allows for compensation of fan motor voltage reductions or other changes that tend to vary the desired air-fuel ratio. High response to power level demands is provided, while a prescheduled air-fuel ratio is maintained to minimize emissions.

In both the air and fuel metering systems, a constant (or proportionally controlled) pressure differential is maintained across the variable area valves. Thus the 100 to 1 flow range is obtained by providing a 100 to 1 area ratio in each valve. A low fuel supply pressure, 10 psig, has been selected to minimize the system's sensitivity to contamination and allow the use of inexpensive pumps. A fuel pressure regulator is integrated into the system to allow the air-fuel ratio to be essentially independent of fan motor voltage (or fan efficiency, leakage, brush wear, etc.). An important feature of incorporation of this fuel pressure control scheme is that part load parasitic power demands of the fan motor can be reduced by as much as 65 percent by scheduled voltage reductions while still maintaining the air-fuel ratio independent of the inertial lags of the fan motor.

A series of demonstration tests at various steady state and transient power levels were performed on the integrated combustion system. Emissions monitored during transients and indicated that the peak levels of emissions would remain below the limits at a transient rate of 50 percent power level change per second (54 lbs/hr per sec). In most transient ranges the rate of change of power level could go as high as 150 percent per second without significant emission peaks. However, decreasing power transients below 30 lbs/hr at rates of slightly above 50 percent per second were observed to produce emission peaks of CO above the limits for three or four seconds. Startup from cold to maximum firing rate in three seconds or less appeared to present no significant emission peaks. Steady state emission levels were in general significantly below the 1980 AAPS goals. Measured values across the entire heat release range were on an average 61 percent below the goal for CO, 90 percent below the goal for HC and 37 percent lower in the case of NO. The only condition that caused an emission level above the goal was at 1 pound per hour fuel flow. At this low flow condition CO levels were above the limit. It should be noted that 1 pound per hour fuel flow is an extreme boundary normally outside the range of typical engine systems.

Basically the component and system demonstration tests have indicated the system can provide the necessary degree of air and fuel regulation for a low emission combustion system that has imposed on it a wide heat release range and frequent high response power level changes. Construction, size, weight, and reliability features of the system have the potential to be incorporated into inexpensive mass production automotive engines.

3

CONCLUSIONS

This program has demonstrated that a Rankine cycle combustor with a two million BTU per hour heat release in a 1.33 cubic foot volume operating on JP-5 fuel can meet the 1980 AAPS emission level goals over a 100 to 1 heat release range at steady state or during rapid transients. The transients include startup to full power in three seconds and a 50 percent power rate change per second.

The program has further demonstrated that the package size and power requirements of combustors need not be excessive. The components used are not complex and are capable of being mass produced at low cost. All of the components employed proven concepts that appear capable of a high degree of reliability.

The novel fuel atomization system assures that the fuels can be rapidly ignited in even the coldest weather and does not need warm up to maintain low emission as do the current spark ignition engines. Further the fuels used need no special additives for combustion control and a wide variety of currently available fuels can be used (however, leaded gasoline is not acceptable).

The novel rotating cup has been shown to be essential for low emission control over the 100 to 1 heat release range. The precision air and fuel metering valves and controls have also been shown to be essential to maintain the low emissions over the 100 to 1 heat release range.

Fan and combustor noise was shown to be a problem, thus special attention must be given to its elimination in future development programs.

4

RECOMMENDATIONS

The demonstrations were conducted to show that given certain boundary conditions, such as heat release range, fuel and emission levels, a Rankine cycle combustor could perform satisfactorily and provide incentive for further Rankine cycle engine development. All major components except fan and cup drive motor were specially designed and developed to conduct this investigation. Further development is necessary, especially in regard to integration with other engine components because they effect both the shape and final performance of the combustor. The principal component having the greatest effect on emission levels will be the vaporizer. The temperature boundary conditions on the combustor will be altered by the addition of the vaporizer and thus need special development. Further the emission levels will be altered because of boundary conditions, heat up times required, response time, and stability of the vaporizer. All of these factors must be considered when coupling the vaporizer with the low emission combustor. The work conducted on the program has demonstrated that these problems are solvable and that a combustor with emissions well under the goals can be expected.

Minimum fan power must also be demonstrated for the optimum design Rankine cycle combustor. Fan power, system volume and uniform air distribution (air-fuel ratio control) require the design of a fan that is aerodynamically and geometrically integrated with both the air valve and combustor. The fan motor represents one of the largest inherent cost factors in the Rankine cycle combustor control system. Minimum fan power becomes a prominent factor in a continued development program. Elimination of a separate cup motor by using an extension shaft on the fan motor will also be necessary to minimize cost and volume. Additional development testing is necessary to match the cup and fan speeds to obtain satisfactory atomization and fan aerodynamic design at the same shaft speed. The combustor pressure drop must be held at a minimum. However, if the pressure drop is too low emissions and temperature distribution into the vaporizer and exhaust system will become a problem and can cause hot spots and low reliability of the vaporizer. Further test analysis, using a vaporizer and optimum fan should be conducted to establish engineering requirements necessary for minimum emissions with a reliable automotive vapor generator.

Vaporizer air side pressure drop must be held at minimum to conserve fan power. However, the weight and response time for the vaporizer becomes excessive

if the pressure drop is too low. An optimum balance will require an integrated development program.

Transient performance of the combustor-vaporizer system must be further demonstrated. One of the critical items is the start and warm up period to roadload power of the complete Rankine cycle engine. Time must be maintained at a minimum and therefore will require optimum performance of each component during this period, while still maintaining minimum parasitic power. Further development and integrated system tests are essential to demonstrate transient and warm up characteristics with a vaporizer.

A final but important consideration is the development and demonstration of an integrated vapor generator and fuel control system. Response, temperature distribution, heat flux, wall temperature, flame radiation, thermal inertia, feed control, fluid hot spots, and stability must be considered in a high response control system. It is necessary to demonstrate that fuel and air flows can be made to respond rapidly and accurately enough to regulate the vapor pressure and temperature within acceptable limits as vapor flow rates respond to automotive duty cycles. A low cost control system must be developed without sacrificing the inherent low emission characteristics of the combustion system.

5

SYSTEM REQUIREMENT DISCUSSION

The purpose of this program was to design, fabricate and test a full scale combustion system suitable, with minor modifications, for installation in a Rankine cycle engine powered vehicle. Included in the system was the combustor, fan, controls, ignition system and fuel pump.

5.1 SYSTEM PERFORMANCE GOALS

The performance goals of the combustion system are as follows:

- Maximum heat release of 2,000,000 BTU/hr (which corresponds to 109 pounds per hour fuel flow) and a minimum heat release of 20,000 BTU/hr which results in a 100 to 1 turndown ratio. The maximum heat release was stated as a time averaged rate, thus permitting use of an on-off or modulating system or a combination of both.

- Steady state emissions - 1980 AAPS goals

Pollutant	gm Pollutant Kilogram of Fuel	Corresponding gram pollutant per mile (assuming 10 mpg)
Carbon monoxide	16.25	4.7
Unburned hydrocarbons reported as $CH_{1.85}$	0.48	0.14
Oxides of nitrogen reported as NO_2	1.38	0.4
Particulates	0.10	0.03

In addition no visible smoke is allowed at any operating condition. Meeting these goals results in high combustion efficiency, which was also listed as a goal.

- The steady state emission goals are to be met within 2 seconds after any change in fuel flow. There is to be no severe degradation of emission levels during a transient.

- Startups and shutdowns are to be as clean as possible since they are included in the latest automotive emission test procedure.

The combustion system is to have the following constraints:

- Maximum combustor volume - 1.33 cubic ft.
- Maximum parasitic power - 2.0 HP (without the vaporizer)
- Test fuel - Kerosene, #1 Diesel, Jet A
- Test conditions - ambient pressure and temperature

5.2 DESIGN APPROACH

Reviewing the requirements the major problem was identified as maintaining low emission levels over a wide range of heat release rates or fuel flows. To obtain low emission levels of CO, HC and NO simultaneously involves a careful trade-off of combustor parameters such as local and overall air-fuel ratios, peak temperatures, residence time and velocity. In general the factors which contribute to low NO promote high CO and HC and vice versa. This will be discussed in greater detail in Section 7. One conclusion established was that the air-fuel ratio must be closely controlled over the entire operating range. The air control valve and fuel control valve are linked together in such a way as to provide the desired overall air-fuel ratio at each fuel flow. The local air-fuel ratios are determined by location, size and number of the combustor air entry holes.

Based on published data and our own experience that startups and shutdowns, i.e., turning the combustor on and off, would result in substantial emissions, it was concluded that the system must be completely modulating over the entire range. In order to accomplish full modulation a fuel atomizing device which would atomize the fuel adequately at flow rates from 1 to 109 pounds per hour was required. Not only is the wide turndown ratio a problem but so is adequate atomization of a fuel flow as low as 1 pound per hour. Our investigation indicated that the rotating cup fuel atomizer was the most likely device to fulfill the requirement.

The major components of the demonstration system are the air supply system, air control valve, fuel control valve, fuel pressure regulator valve, and the combustor with its rotating cup fuel atomizer. The selection and/or development of these components is discussed in the following sections.

6

CONTROL SYSTEM

6.1 AIR AND FUEL CONTROL SYSTEM DESIGN

Low emissions were the main design criteria used to synthesize the control system. Analysis and experience determined that a fully modulated control of both air and fuel across the full range of heat release rates would offer the optimum low emissions approach. Inherent with this design concept was the necessity to maintain the ideal air fuel ratio at any heat release rate from one percent to 100 percent. In addition to the wide range of heat release rates necessary in automotive systems, the very frequent and high response demands for power level changes dictates that air-fuel ratio control must be free of fan motor inertia time lags. A fully modulated control system independent of inertial lags of fan motor was designed with simple hydromechanical control components that have the potential of being incorporated into low cost automotive type engine systems.

6.1.1 System Analysis

Experience and analysis has shown that the optimum air flow control and combustion air delivery system requires a high degree of symetry to provide uniform flow (and consequent correct air-fuel ratios) into the combustor. Figure 1 schematically describes the overall air and fuel control system. Air mass flow is controlled by varing the flow area of 12 orifice ports leading directly into the combustor outer casing. To ensure that fuel flow is directly proportional to air flow, a mechanical coupling syncronizes the control of fuel flow area to air flow area. Once the area ratios have been fixed, it is only necessary to regulate pressure drops to maintain the desired weight flow ratios.

For low pressure rise, air compression can be neglected and the weight flow relationships can be written as:

$$W_a = K_a A_M \sqrt{\frac{P_1}{T_1} (P_1 - P_2)} \qquad (1)$$

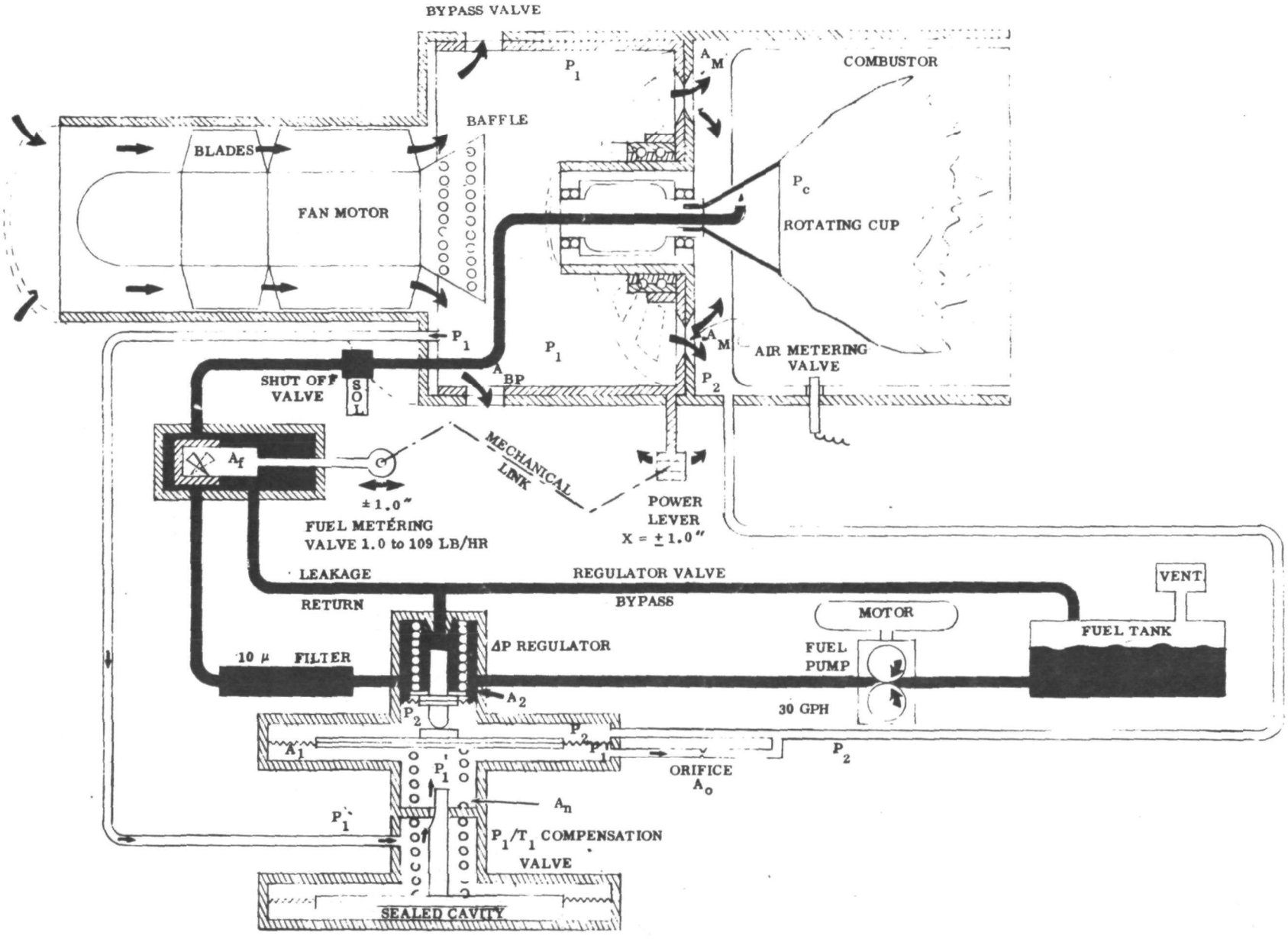

FIGURE 1. CONTROL SYSTEM SCHEMATIC

$$W_f = K_f A_f \sqrt{\Delta P_f} \tag{2}$$

where W_a = mass air flow into combustor

A_M = air metering valve area

P_1 = upstream pressure (fan discharge)

P_2 = downstream pressure

T_1 = air temperature at metering valve

W_f = fuel mass flow

ΔP_f = pressure drop across fuel valve

A_f = fuel metering valve area

If the inlet pressure (altitude) and temperature are constant, a simple relationship can be written for the air-fuel ratio:

$$\frac{W_a}{W_f} = K\sqrt{\frac{P_1 - P_2}{\Delta P_f}} \tag{3}$$

To ensure the air fuel ratio remains a function of flow area only, the pressure drop across the fuel valve is controlled proportional to the pressure drop across the air metering ports. A ΔP_f regulator valve performs this function by a force balance across diaphragms. Operation of this component is illustrated in Figure 1. P_1 pressure is connected (through a density compensator) to the bottom side of diaphragm A_1. Downstream pressure (P_2) is connected to the opposite side of the diaphragm. Fuel system pressure is regulated by a flapper valve that by-passes excess fuel to the tank. A small diaphragm on the fuel side balances the pressure difference across the air metering ports A_M against the fuel pressure. If the air pressure drop increases (causing W_a to increase), the force across the system becomes unbalanced and the fuel pressure regulator moves up; reducing the by-pass flow, and thus increasing the fuel pressure and its mass flow across the fuel metering valve. Since the force balance must be maintained across the ΔP_f regulator, we have:

$$\Sigma \text{Forces} = A_2 (\Delta P_f - P_2) = A_1 (P_1' - P_2)$$

where P_1' = P_1 adjusted for inlet air density and where ΔP_f is large compared to P_2

we have $$\Delta P_f = \frac{A_1}{A_2} (P_1' - P_2) \tag{4}$$

thus equation (3) can be rewritten as

$$\frac{W_a}{W_f} = K\sqrt{\frac{(P_1 - P_2)\,A_2}{(P_1' - P_2)\,A_1}} = \text{constant}$$

Fan speed changes due to voltage or load variations, fan efficiency reductions due to fouling or wear, and by-pass valve leakage variations are automatically compensated by maintaining the ΔP_f as a function of the air valves pressure differential.

It can be seen from equation (1) that the air flow is a function of

$$\sqrt{\frac{P_1}{T_1}} \quad .$$

Thus, an altitude and inlet air temperature correction can be incorporated by adding a P_1/T_1 compensator (Fig. 1). Fan discharge pressure (P_1) is admitted to the ΔP regulator by a contoured needle valve. This valve is positioned by a force balance across a diaphragm having P_1, T_1 on one side and cavity sealed with air at standard conditions. Thus, as the air temperature increases, the sealed air will expand and move the valve upwards. This action will increase the pressure drop across the contour valve and thus reduce P_1 to a corrected value of P_1' on the bottom side of diaphragm A. As P_1' decreases, the fuel pressure will drop producing the desired fuel flow reduction as the ambient air temperature increases.

6.1.2 Air Metering Valve Analysis

Air to the combustor is metered across a series of twelve ports cut into two plates (Fig. 2). An input lever rotates one plate with respect to the stationary backup plate. The metering port areas are caused to open or close as the input power lever rotates matched ports in each plate. Figure 3 shows one of the 12 port configurations. The area is established by maximum mass air flow requirements of the system:

Maximum Power = 2×10^6 BTU/hr.

Let LHV of fuel = 18,350 BTU/lb for JP-5

$\therefore$ fuel flow = 109 lbs/hr or 1.82 lbs/min.

Air fuel ratio at maximum rated heat release = 26 (See Sec. 7)

$\therefore$ Maximum Air Flow = (26) (1.82) = 47.3 lbs/min = 630 SCFM

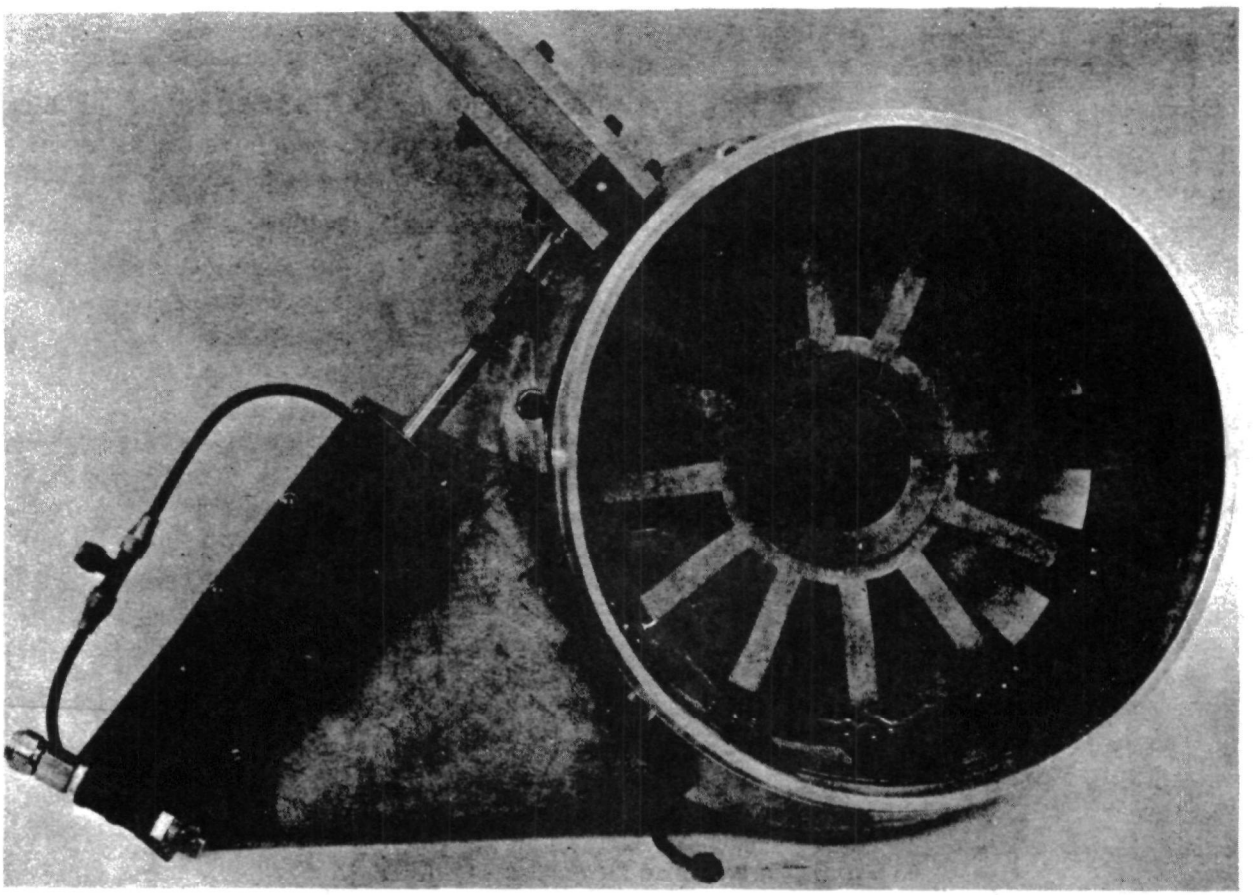

FIGURE 2. AIR METERING VALVE

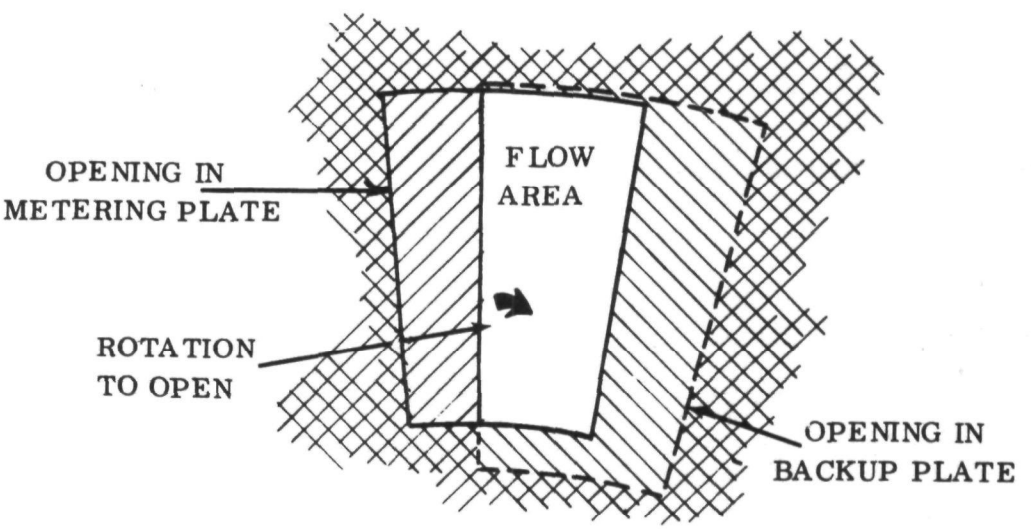

FIGURE 3. AIR METERING VALVE PORT SHOWN IN THE 60 PERCENT POWER POSITION

The area to flow this quantity of air depends upon the selection of a design pressure drop across the metering valve. It is desirable to maintain this loss as low as possible to reduce parasitic power requirements. However, very small pressure differences require larger and heavier valves. A tradeoff analysis indicated that a ΔP of 2 inches of H_2O results in a valve size that is within the dimensional envelope of the combustor:

Flow relationship =

$$W_a = 7.617\ KA_M \sqrt{\gamma(P_1 - P_2)}$$

where A_M = $in.^2$ (area of orifice)

γ = lb/ft^3 (density at standard conditions)

W_a = lbs/min.

P = in. of H_2O

Allow ΔP = 2 in. of H_2O

Assume K = 0.6 discharge coefficient

For γ = 0.075 and a maximum flow rate condition of 47.3 lbs/min.

$$47.3 = 7.617\ (0.6)\ A_M \sqrt{(0.075)\ 2}$$

$$A_M = 26.8\ in.^2$$

Since a constant ΔP will be maintained, the area will be varied proportional to the power lever position, X, (1 to 100%) modified to allow leaning of air-fuel ratio at low heat release rates (Fig. 3). (Combustor tests had indicated leaning out was necessary for minimum emissions.)

Delta-P, Voltage Compensation System

The pressure differential across the fuel metering valve can be regulated to maintain the correct air-fuel mass flow ratio regardless of inlet air temperature or absolute pressure (altitude). Initially the system was designed to respond to relatively small variations of voltage ±10 percent (equivalent to ±10% flow variation from the fan). A regulator capable of compensating for voltage changes of ±10 percent was considered adequate for a simple constant voltage motor concept. As component testing progressed it became evident that modifications to the regulator could extend its range sufficiently to accommodate a two speed fan. By incorporating this into the system, a 65 percent reduction of parasitic power at normal driving ranges can be achieved along with a substantial noise level reduction. This modification was incorporated and tested at a

component level in the delta-P regulator. However, since a two speed fan system requires a redesigned by-pass valve, program schedules required that the emission demonstration tests be conducted with the single speed system.

An analytical estimate of the part load power reduction presently possible can be made from component test results. Development tests on the regulator valve have shown it capable of accurately regulating the fuel pressure directly proportional to pressure differential at the air metering valve across the range of 1.0 to 2.5 inches of H_2O. This wide range control allows the fan motor voltage to be reduced as a function of power lever position. If the air by-pass valve is maintained closed for the power lever position range from 100 to 70 percent, the air flow into the combustor can be controlled by proportionately lowering the voltage to the fan while the regulator compensates for the reduced pressure differential across the air metering valve. Since a mechanical linkage maintains a known ratio of air valve area to fuel valve area, the regulator will automatically maintain the air-fuel ratio as the power is reduced. A limitation on this system is the lowest pressure differential signal that can be utilized as an actuator input to the simple diaphragm regulator. Analysis and test results have shown that 1.0 inch of H_2O is a reasonable lower limit. Using this value, the part load power demands of the combustor system can be established. Although the combustor requirements are moderate (1.25 HP for the optimum configuration and 2.3 HP for the demonstration system), addition of a boiler can make parasitic power losses at part loads unacceptable. If a boiler had a high delta-P (as recommended by some designers*), an additional 2.4 horsepower would be required. Total parasitic power levels would then be as high as 3.65 horsepower. If the system were to require this high power level from full power down to idle condition, a highly undesirable condition would exist. Lowering the input voltage across a voltage range that allows accurate ΔP compensation by the regulator will eliminate the motor inertial speed lags since the air-fuel ratio changes are continually maintained by the regulator. Power reduction by operating at 1.0 inch of H_2O can be estimated by simple calculations based on fan laws for a series wound motor. For voltage changes of approximately 2 to 1, the following relationships give reasonably accurate results.

For a given voltage change V_1 to V_2

flow Q: $Q_1/Q_2 = V_1/V_2$

pressure p: $P_1/P_2 = (V_1/V_2)^2$

fan BHP is: $BHP_1/BHP_2 = (V_1/V_2)^3$

By maintaining the by-pass valve closed and reducing the voltage to the motor, the flow through the metering valve will drop as a function of both the motor voltage and the area change of the metering valve. Pressure will drop as a function of the square

* "Condensers and Boilers for Steam-Powered Cars: A Parametric Analysis of Their Size, Weight, and Required Fan Power", by William C. Strack, NASA TN D-5813, May 1970.

of flow. By using 1.0-inch as the lower limit of adequate control, the by-pass valve can be maintained in a closed position until the voltage is reduced to $\sqrt{1/2}$ or $0.707V_1$. Since power is approximately a cubic function, we will obtain $(0.707)^3$ (BHP), or a 65 percent reduction in power. With the optimum system and a relatively high air side boiler pressure drop, a parasitic power loss reduction of approximately 2.4 horsepower occurs. Total power with this high pressure drop boiler would be approximately 1.25 horsepower at vehicle power demands below 35 percent. One problem with this approach is that it is more difficult to make the system linear. However, since this is not a driver input command, linearity is of secondary importance if the correct air-fuel ratios can be maintained.

6.1.3 Fan Selection

Fan pressure requirements are established by the selected metering ΔP of 2 inches of H_2O added to the combustor maximum rated pressure drop of 8 inches of H_2O. A number of fan designs were investigated but program schedules required the use of an off-the-shelf unit. A Joy P/N X702-93 was selected based upon its immediate availability and performance. To match the fan's output characteristics to the combustor flow and pressure requirements, the fan was operated above its design voltage level. In Figure 4 the characteristics at both design (27V) and the increased voltage (33V) used to match the fan indicates a significant electrical input power increase. Final electrical power inputs were approximately 2.4 HP at the less efficient 33V overload operation point. This power includes all losses associated with distribution, air turning, air valve friction and combustor. This power can be reduced by a large percentage by use of a fan specially designed and matched to the aerodynamics of the air valve and combustor. It should be noted that in an integrated system, the pressure drop across the vapor generator and its associated ducting would also have to be added to these pressure rise requirements. A general characteristic of fans is to increase flow as the output pressure decreases. In order to meter the air from 100 to 1 percent at a high response rate independent of motor inertial effects, a by-pass valve has been incorporated. It allows excess fan air at low power settings to be returned to the atmosphere thereby establishing the correct pressure characteristics across the air metering valve and combustor.

6.1.4 By-Pass Valve Analysis

The by-pass valve is designed to regulate the delta-P across the air metering valve at a constant 2 inches of H_2O regardless of power lever settings (1 to 100% range). As the power is reduced from 100 percent, the required combustion air flow must be reduced proportionately. The corresponding pressure drop across the combustor varies as a function of flow squared as shown in Figure 5. Since the by-pass valve is designed to maintain a constant air delta-P of 2 inches of H_2O across A_M, the pressure drop across the by-pass valve is equal to the combustor

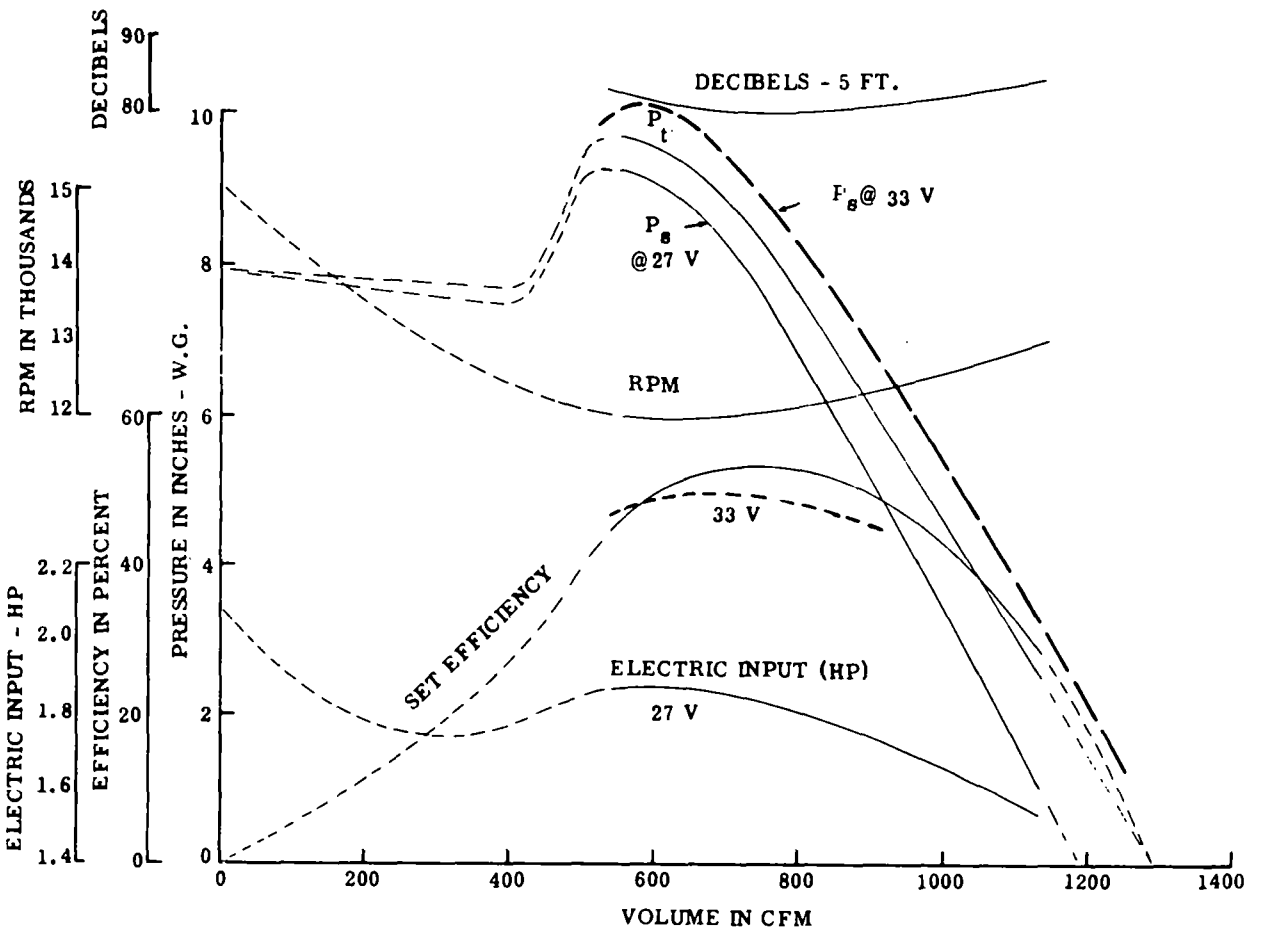

FIGURE 4. FAN CHARACTERISTICS (ALL CURVES AT 27V INPUT EXCEPT AS NOTED) - JOY, MODEL NUMBER P/N 702-93

pressure drop plus 2 inches of H_2O (shown in Fig. 5). As the back pressure on the fan is reduced, its output flow increases (Fig. 4) and must be accommodated in the design of the by-pass valve ports. This increasing flow characteristic causes a significant increase in the dynamic head in the fan annular flow passage (Fig. 6). A baffle mounted immediately downstream of the fan discharge is designed to reduce the effects of the dynamic head by turning and directing the flow into the larger plenum-like space containing the valve elements.

By means of this baffle arrangement, it was possible to establish the by-pass valve size as a function of static pressure rise.

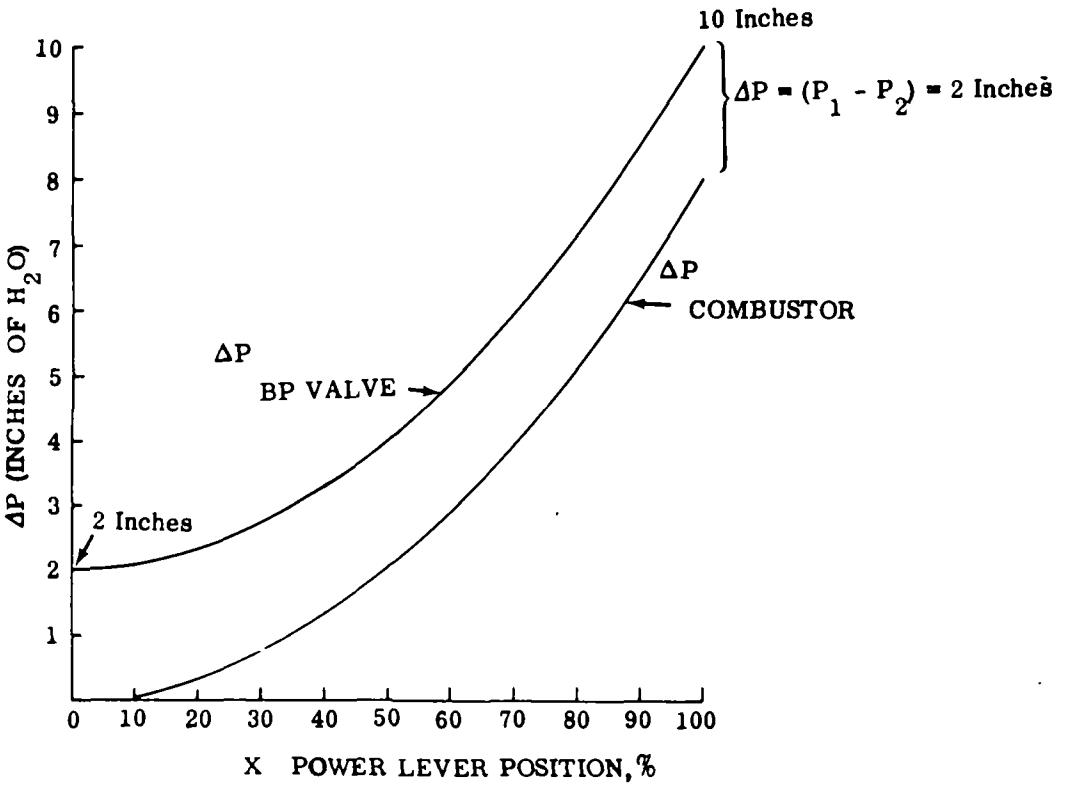

FIGURE 5. COMBUSTOR AND BY-PASS VALVE PRESSURE DROP VERSUS POWER DEMAND

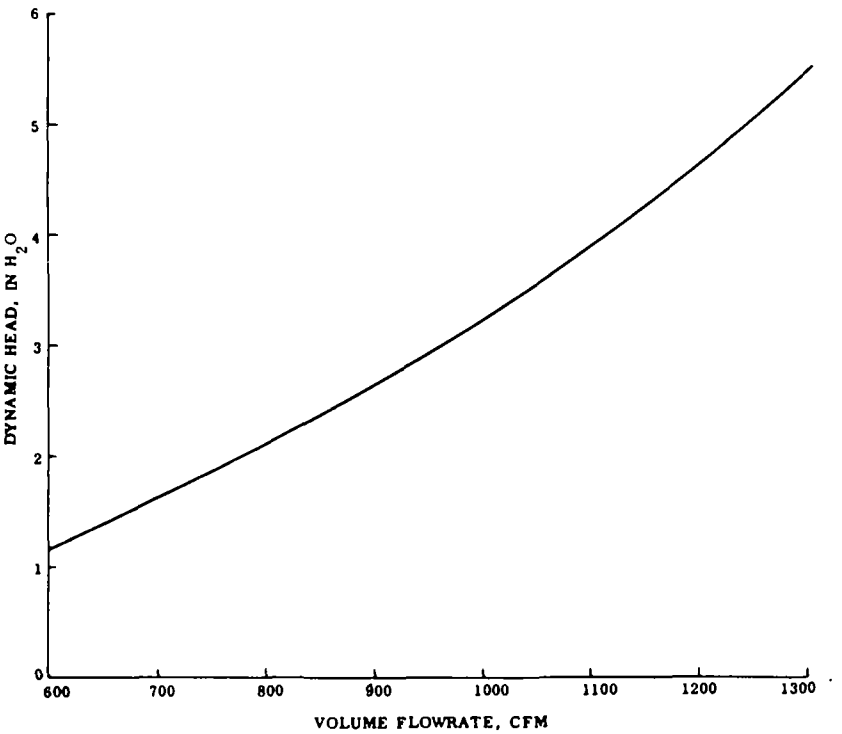

FIGURE 6. DYNAMIC HEAD IN ANNULUS

Air flow across the by-pass valve is equal to the difference between fan flow and the combustor flow (Fig. 7). A plot of air flow through the by-pass valve (Fig. 8) is obtained by subtracting the two curves plotted in Figure 7. By-pass valve area versus power lever position can now be calculated from the known pressure drop and required weight flow. Figure 9 shows the resultant area requirements. It can be seen that the area deviates only slightly (~5 percent) from a linear valve flow area across the entire 100 to 1 flow range. At the maximum power conditions (X = 100%), the valve is fully closed and progressively opens to its full area of 52 square inches at the 1 percent position. This action is exactly opposite the air metering valve sequence, thus both are mechanically coupled to ensure correct high response matching.

6.1.5 Fuel Pressure Regulator Analysis

The fuel pressure regulator serves the basic function of maintaining the correct air fuel ratio in conjunction with the fuel and air flow area control valves. Its incorporation into the design allows the system to operate across the 100 to 1 fuel flow range with sufficient accuracy to minimize emissions. Inertial effects of fan motor leakage, blade fouling, motor performance degradation, air cleaner blockage, and pressure gradients across the fan inlet can be compensated as can scheduled voltage reductions to lower parasitic power demands at reduced loads. The demonstration system incorporates the basic delta-P regulation system that allows the valve to regulate the fuel pressure in proportion to the volumetric air flow. This feature allows compensation for the factors described above. Although a secondary to the primary goal of the program, a design has been completed to provide an additional compensation for altitude and inlet air temperature. This added compensation has not been incorporated into the demonstration system, but analysis indicates a simple mechanical system will perform the task.

Delta-P Compensation System

Delta-P compensation can be obtained with a single diaphragm actuated regulator valve. Static pressure upstream (P_1) and downstream of the air metering valve is sensed and transmitted to either side of the delta-P diaphragm actuator (Fig. 1). Neglecting the small correction between P_1 and P_1' (discussed in the next section) we can analyze the action of the delta-P regulator by letting $P_1' = P_1$. The differential pressure $P_1 - P_2$ across the large diaphragm produces a force which is opposed by the differential pressure across a smaller diaphragm, one side of which is subjected to fuel pressure upstream of the fuel metering valve, and the other, to P_2. Neglecting the effect of the springs which function only to provide stability and centering action of the movable diaphragm assembly, the forces will be in equilibrium if:

$$(P_{fuel} - P_2) A_2 = (P_1 - P_2) A_1 .$$

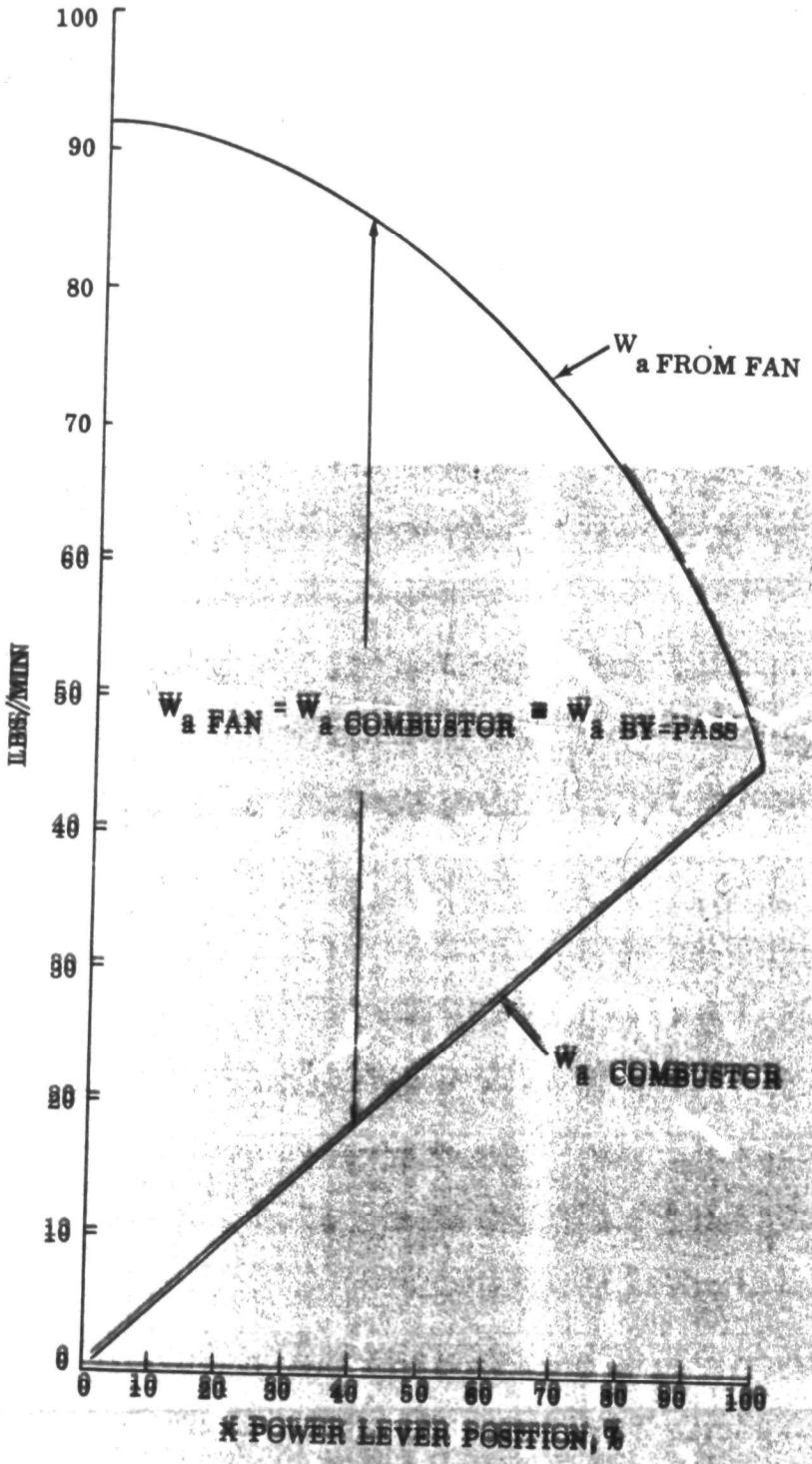

FIGURE 7. FAN AND COMBUSTOR FLOW VERSUS POWER LEVER POSITION

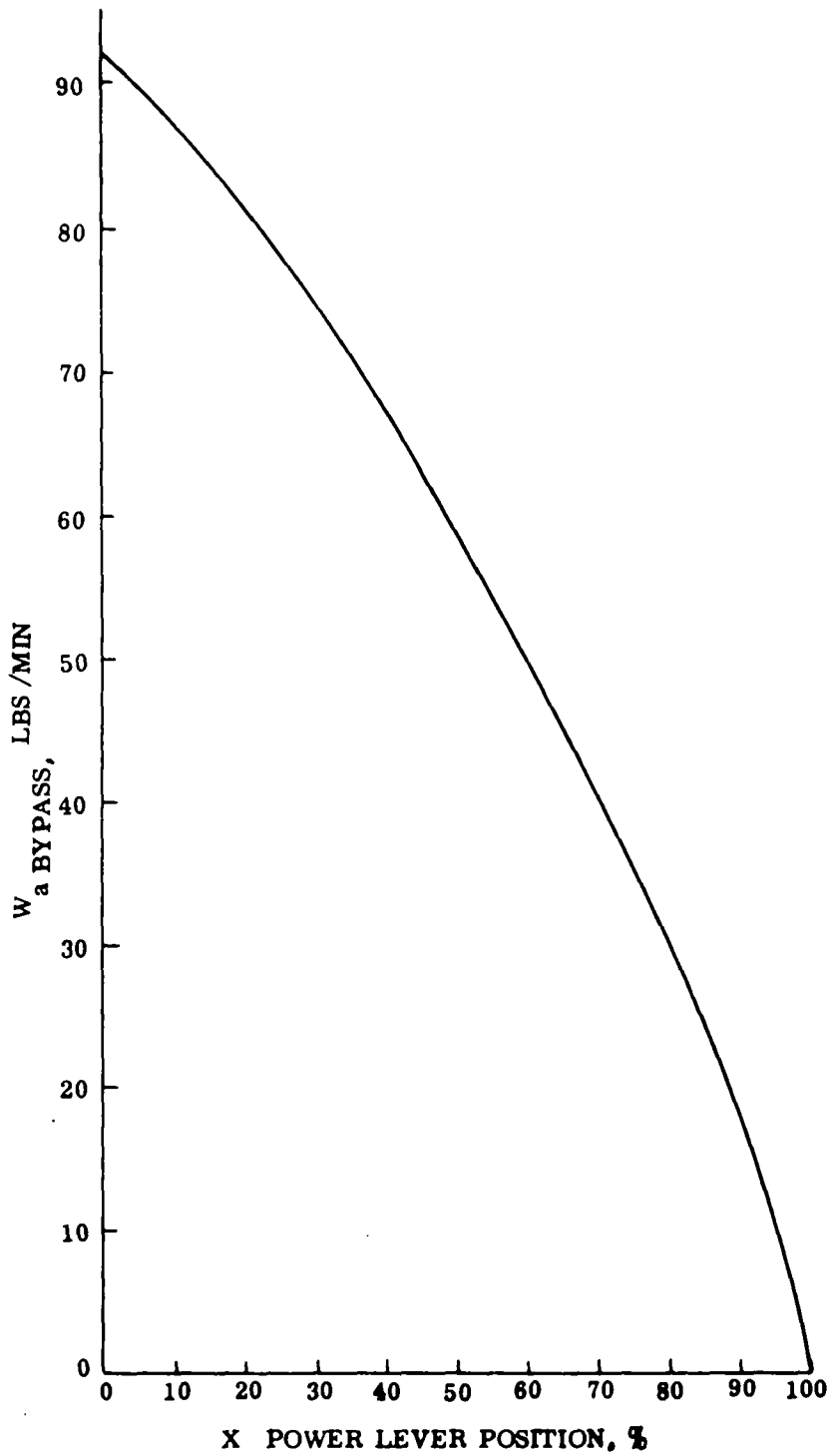

FIGURE 8. BY-PASS FLOW AS A FUNCTION OF POWER REQUIRED

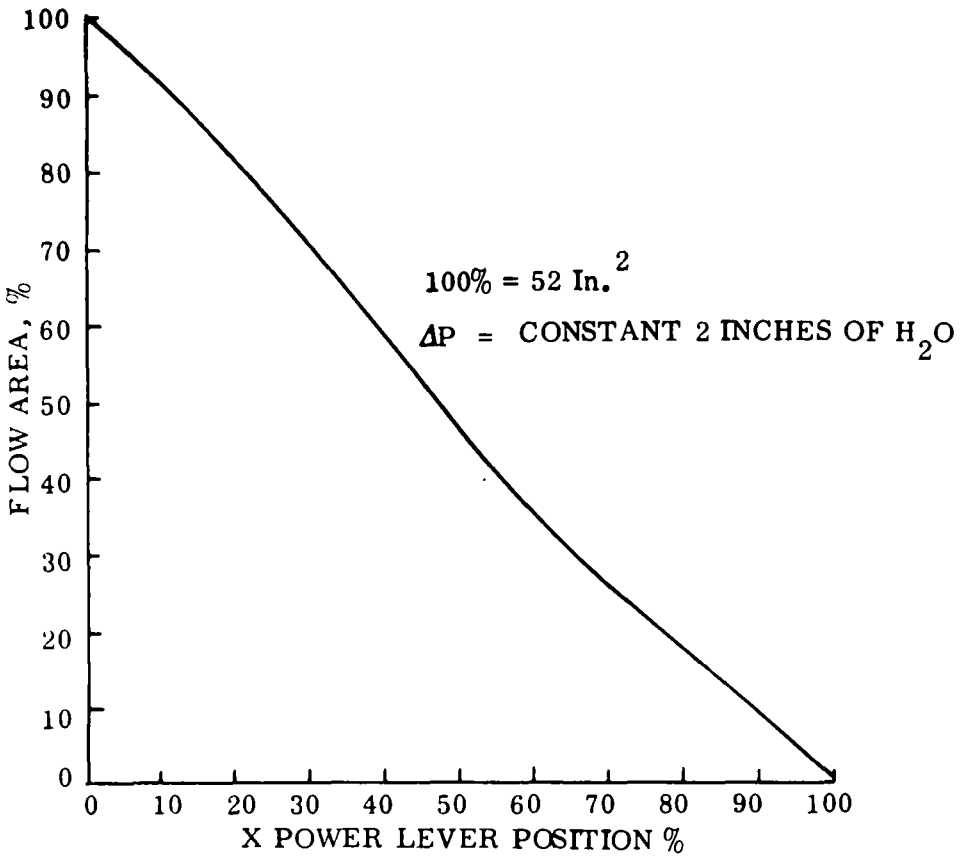

FIGURE 9. BY-PASS VALVE AREA VERSUS POWER REQUIRED

The system is so designed that fuel delta-P across the metering valve will always remain relatively high (approximately 10 psid). On the other hand, fuel pressure downstream of the metering valve enters the burner through the rotating cup at a pressure substantially equal to combustor pressure, P_c. Thus, the pressure drop across the metering valve equals:

$$\Delta P_f = P_{fuel} - (P_{loss} + P_c)$$

where P_{loss} = fractional flow loss between fuel valve and combustor.

Since P_{loss} varies from 0 to 0.5 psi and P_c differs from P by approximately 0.3 psi (for a low loss boiler), the total error is 0.8 psi or ±0.4 psi. Since pressure variation about 10 psig is ±0.4 psi if bias springs are incorporated flow error is thus equal to:

$$\pm \sqrt{\frac{10 \pm 0.4}{10}} = \pm 2\% \text{ flow accuracy} .$$

Thus, for purposes of analysis, we can set the equilibrium to:

$$\Delta P_f = \frac{A_1}{A_2} (P_1 - P_2) .$$

Fuel entering the small diaphragm cavity leaves through a flapper-type valve which opens or closes as the diaphragm moves in response to changes in the sensed pressures, and by passes the fixed-displacement pump output back to the tank, thereby controlling the fuel pressure so that force equilibrium is always maintained. To a high degree of accuracy, therefore, the fuel delta-P is controlled proportional to the applied air delta-P, according to the above equation. The large diaphragm (A_1) is 7.15 inches in diameter and has an effective area of 40 square inches. Small diaphragm (A_2) is 0.6 inch diameter and has an area which is only about 0.28 square inch. Thus fuel delta-P will be 140 times as great as the air delta-P. The air throttle valve delta-P, $P_1 - P_2$, is nominally 2 inches H_2O. With voltage reductions of as great as 30 percent, the normal range of operation will be 1 to 2 inches of H_2O with corresponding fuel pressures of 5 to 10 psig.

Caution has been taken in the design to eliminate sources of friction whenever possible, even when this is at slight sacrifice in theoretical accuracy. A balanced design of the by-pass flapper valve was considered and was rejected because it would have introduced possible hysteresis. The design shown is not balanced, but the forces due to the imbalance contribute a flow error of less than 1/2 percent.

Air Density Compensator

Although not incorporated into the demonstration system, a design analysis has been completed that indicates a simple mechanical system could be used to obtain inlet air density compensation. The variable air pressure, P' applied to the delta-P control, is modulated by the air density compensator in such a way that the following relationship is obtained:

$$P_1' - P_2 = K' \frac{P_1}{T_1} (P_1 - P_2)$$

A small amount of air at pressure, P_1, sensed upstream of the air throttle valve, flows through a variable orifice, controlled by movement of a density-responsive diaphragm, and into the delta-P control valve diaphragm cavity at the pressure P', finally leaving through a fixed orifice, where it connects to the P_2 pressure sense line downstream of the air metering valve. This small amount of air which effectively by-passes the A_M is a negligible fraction of the burner flow, even at minimum power levels.

For low air delta-P's, the air flow equations for the first and second orifices (areas A_n and A_o, see Fig. 1) and steady state continuity of mass required that

$$K_a A_n \sqrt{\frac{P_1}{T_1}(P_1 - P_1')} = K_a A_o \frac{P_1}{T_1} \sqrt{(P_1' - P_2)}$$

This can be solved for $P_1' - P_2$ in terms of $P_1 - P_2$ as follows:

$$P_1' - P_2 = \left[\frac{1}{\left(\frac{A_o}{A_n}\right)^2 \frac{P_1'}{P_1} + 1} \right] (P_1 - P_2)$$

On the basis of absolute pressures, P_1' is never more than one part in 200 different from unity, thus we can simplify to:

$$P_1' - P_2 = \left[\frac{1}{\left(\frac{A_o}{A_n}\right)^2 + 1} \right] (P_1 - P_2)$$

Therefore, the necessary density correction can be achieved simply by contouring the variable orifice needle so that

$$\frac{1}{\left(\frac{A_o}{A_n}\right)^2 + 1} = K' \frac{P_1}{T_1}$$

Now, the density compensator consists, essentially, of a sealed cavity, closed at one side with a flexible air-tight member, within which is trapped a predetermined weight of air (neglecting the effect of the spring which serves only to apply a gently loading action to eliminate diaphragm slack), the pressure inside the sealed cavity will always be substantially equal to P_1 applied to the opposite of the diaphragm. Similarly, for steady state conditions, considering the variations in temperature are due almost entirely to changes in day temperature, the temperature of air inside the sealed cavity will be substantially the same as the temperature, T_1, of the air flowing across the opposite side of the diaphragm and surrounding the control. It will be required that the temperature of the air flowing across the diaphragm be representative of the actual air

temperature at the metering valve. Although the air is being bled directly from upstream of the valve (P_1 cavity) it may not be of sufficient mass flow to rapidly compensate for hot soak conditions under the hood. By insulating the sealed cavity and an additional bleed of air from P_1 around the bottom of this cavity, a much faster adjustment to inlet temperature variations could be made without undue error resulting from underhood temperature gradients. The volume of the expandable cavity will be

$$V = \omega \frac{R\,T_1}{P_1}$$

where R is the gas constant, and ω is the weight of entrapped air. Since the volume is proportional to depth of the cavity, Y, which varies with diaphragm position, we have

$$Y = \left(\frac{\omega R}{A_D}\right) \frac{T_1}{P_1}$$

The desired contour for the variable needle is, therefore, given by

$$\frac{A_n}{A_o} = \sqrt{\frac{1}{\frac{A_D}{K'\omega R}\,(Y - 1)}}$$

Since density varies only by about 20 percent over the complete range of operation, the variable orifice configuration can be selected to operate in a fairly linear range. Once the appropriate contour has been established, any required periodic readjustment of the density compensator is easily achieved by removing the compensator assembly so as to expose the end of the contoured needle protruding through the variable orifice. Then, while the plug in the sealed cavity is opened, the needle is held in a prescribed position, depending on day temperature and altitude, and the cavity is then resealed. With the correct adjustment, the net differential pressure applied to the delta-P control valve will be properly compensated for air density so that fuel delta-P becomes:

$$\Delta P_f = \frac{A_1}{A_2}\, K' \frac{P_1}{P_2}\, (P_1 - P_2)$$

then the fuel-air ratio to the burner will be constant from equations (1) and (2)

$$\frac{W_a}{W_f} = \frac{A_a K_a}{A_f K_f} \sqrt{\frac{P_1}{P_1} \frac{P_1 - P_2}{P_f}} = \frac{A_a K_a}{A_f K_f} \sqrt{\frac{P_1}{P_2} \frac{(P_1 - P_2) P_2 A_a}{P_1 A_1 (P_1 - P_2) K'}}$$

or $$= \frac{W_a}{W_f} = \frac{K_a}{K_f} \sqrt{\frac{A_2}{A_1 K'}} = \text{constant } \frac{A_a}{A_f}$$

Thus, the optimum air-fuel ratio will be maintained as a function of the area ratios selected for the air and fuel valves.

6.1.6 Fuel Metering Valve

Fuel must be metered from 109 to 1.0 pounds per hour. At low power settings (1 pound per hour), the flow is approximately two drops per second. Standard valves do not have sufficient range to accommodate these severe requirements with sufficient accuracy for a low emission combustor. Additionally, the valve should not be sensitive to temperature induced fuel viscosity changes. A new approach to this problem has been taken by the application of a dual slotted shear valve (Fig. 10). Two flat (ground and lapped) plates with matched contour slots 90 degrees to each other. At the intersection of the two slots, a square orifice is formed whose area is a function of the relative position of the top movable plate. The square shape (and thus the discharge coefficient) can be maintained constant throughout the entire 100 to 1 area ratio. Since the plates are in contact, fuel will flow only through the slot in each plate and not between the plates, thereby reducing the clearance leakage path to the microfinish of the contacting surfaces. A drain groove is provided between the upstream pressure and the metered outlet fuel passage, thereby reducing the leakage pressure potential to the level of the frictional flow loss to the rotating cup. Since this is normally less than 0.5 psid, resulting leakage of metered fuel into the drain system will be negligible.

The size of the orifice slots used is a trade-off between four factors.

- Fabrication capabilities - requires large dimensions
- Contamination - requires large dimensions
- Backpressure sensitivity - requires high pressure and thus, small sizes
- Temperature sensitivity - it is desired that changes in fuel temperature have little effect on the coefficient of discharge. This factor requires a high Reynolds number and thereby small orifice dimension.

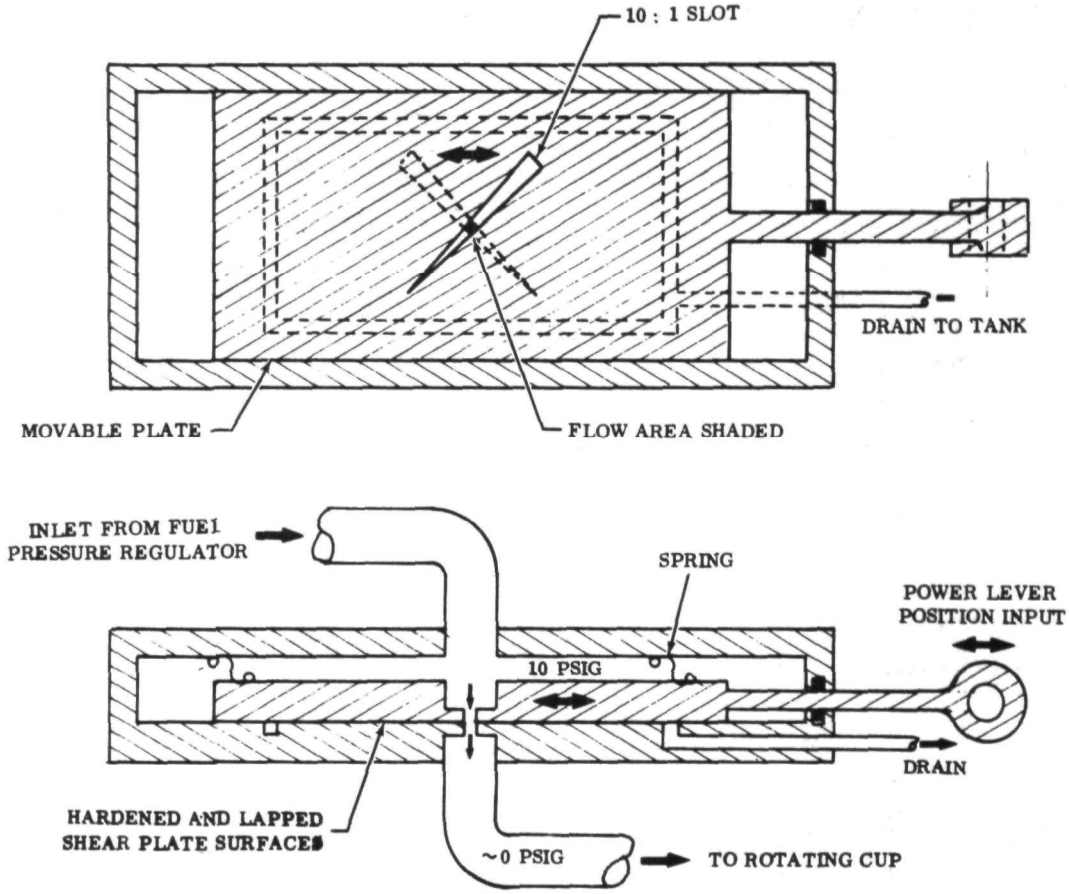

FIGURE 10. FUEL METERING VALVE CONCEPT FOR 100:1 TURNDOWN

Figures 11 and 12 show the effect of orifice size on Reynolds number and its consequent effect upon the discharge coefficient. These curves indicate the dimension of the orifice should be approximately 0.005 inches on a side at the one pound per hour flow rate to minimize viscosity effects.

A pressure difference of 10 psi will produce the desired minimum flow in a 0.0057 inch square orifice and has been selected as the design point. Each slot varies in width from 0.0057 to 0.057 inch according to a square root contour for flow linearization with power lever position.

6.2 CONTROL SYSTEM COMPONENT TESTS

Each of the control component designs was evaluated in a series of tests. Development of the units and final calibration was accomplished at a component level prior to integration into the complete combustor system for low emission demonstrations. Final fuel metering valve performance at 10 psid is 61 pounds per hour per inch stroke with a linearity of ±2.5 percent across a range of 3 to 115 pounds per

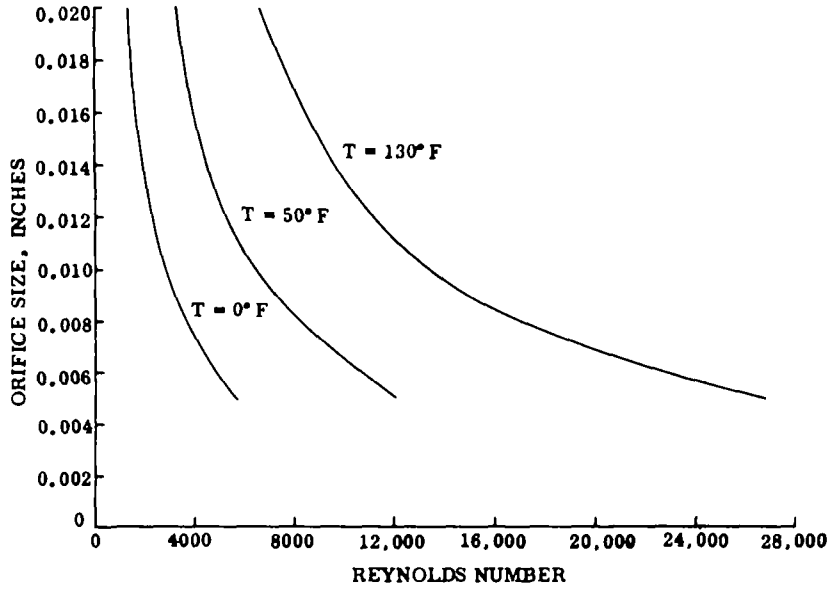

FIGURE 11. REYNOLDS NUMBER AS A FUNCTION OF TEMPERATURE AND ORIFICE SIZE AT 1 LB/HR FOR KEROSENE THROUGH A SQUARE ORIFICE

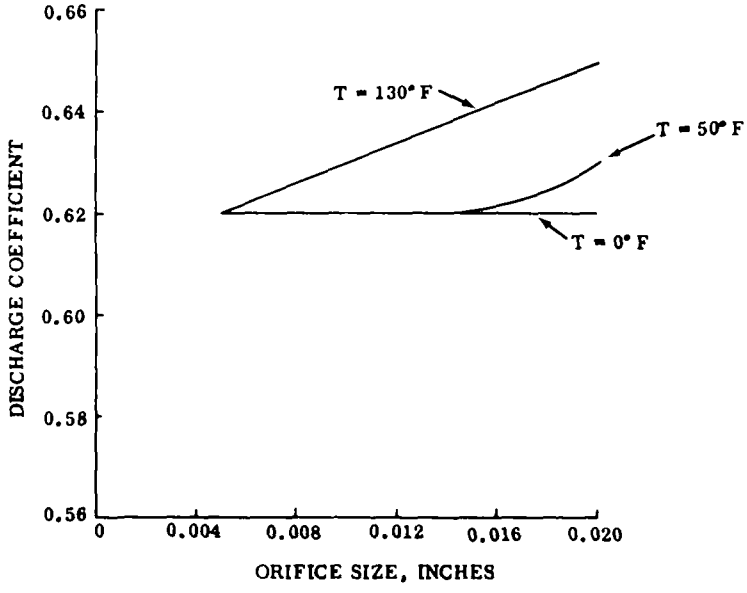

FIGURE 12. DISCHARGE COEFFICIENT AS A FUNCTION OF ORIFICE SIZE FOR KEROSENE

hour. Good repeatability and flow control to as low as 0.5 pounds per hour has demonstrated the valve has a dynamic range greater than 200 to 1. Fuel pressure regulator test results show a useful input actuator range from 1.0 to 2.5 inches of H_2O while regulating fuel flow within ±4 percent. Air metering valve performance calibrations have shown a problem with aerodynamic matching to the fan discharge air. Swirl, dynamic head and turning losses required the incorporation of baffles and flow straightners. Although these devices have given reasonably linear control down to 2 percent of flow, they produced an undesirably high pressure loss. For the final demonstration tests, aerodynamic matching between the fan and air valve was simplified by the use of a plenum created by extending the ducting 36 inches. Although this provided good control of air flow down to 1 percent, it also indicated the importance of correct aerodynamic matching that would be necessary for a minimum volume system. An optimum configuration of fan to air valve design has been established from this experience and is discussed in Section 8.

6.2.1 Fuel Metering Valve Calibrations

In order to obtain linearity and reproducibility over the unprecedented 100 to 1 dynamic range requirements, a new approach to fuel metering was taken. To minimize the effects of air valve to fuel valve linkage distortions (which directly change air fuel ratio) due to actuation load, backlash, or thermal expansion, the valve gain was made as low as practical by making the stroke long. Rigidity was also emphasized for both its mounting flange and actuation rod. These features can be seen in Figures 2 and 13. The rigid mounting flange with five bolt holes and the large diameter actuator are shown in this photograph. Rigidity and freedom from distortion are essential with a valve that must regulate from 1 percent to 100 percent flow, since a linkage blacklash or distortion of 1 percent at the low flow end can change the air fuel ratio by 100 percent. It requires a change of 0.018 inch for a 1 percent flow variation. The air valve lever is connected directly to the fuel valve actuator rod, permitting overall allowances in backlash to be kept below ±0.002-inch (±0.001 at each pinned joint) or approximately ±10 percent flow at the 1 percent valve position. Design analysis indicated that standard metering spool, needle, or flapper configurations could not be expected to provide repeatable flow regulation as a function of stroke from 109 down to one pound per hour.

Calibrations were made by a total weight versus elapsed time to obtain a true weight flow measurement independent of viscosity and accuracy errors associated with flow meters. A precision laboratory balance determined the mass of fuel metered by the test valve with 10 psi pressure differential across the valve housing. Tests were

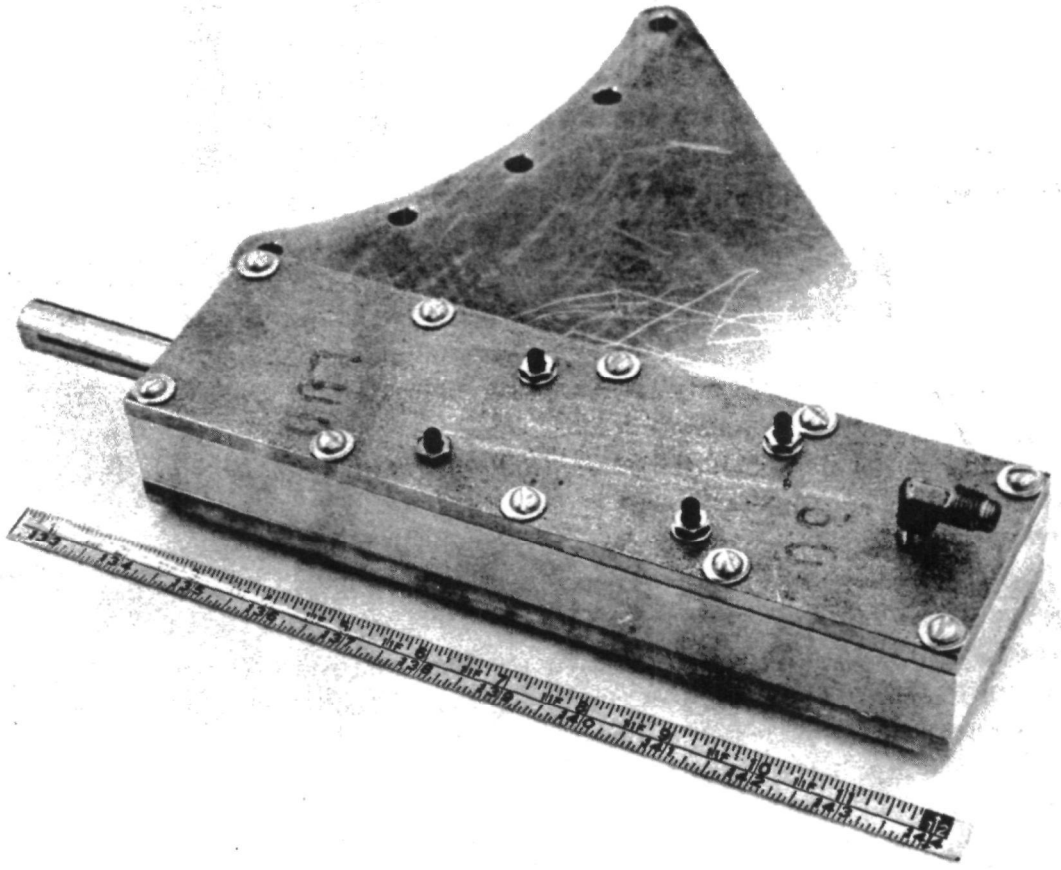

FIGURE 13. FUEL METERING VALVE ASSEMBLY

conducted with all major components of the fuel system connected as on the combustor system. Fuel was pumped by the system's electric driven gear pump to 12 psig. Using shop air supply a constant 2.15 inches of H_2O was maintained across the delta-P regulator simulating the pressure drop across the air control valves metering plates. Differential air pressure across the actuator controls the fuel pressure by-pass valves position to maintain 10 psid across the fuel valve at all flows. A slight increase in air pressure (0.15 inches of H_2O above the nominal 2) was necessary to maintain the fuel pressure at a constant 10 psid from 1 to 115 pounds per hour. All fuel not being metered by the test valve was bypassed by the regulator back to the fuel tank. From the discharge side of the valve the fuel passed either through the flow meter or directly into a container on the scale.

Data obtained as a final calibration of the value is listed in Table I. At 21 different valve stroke positions the weight of fuel that flowed into the container was determined to the nearest thousandth of a pound. A digital timer recorded the elapsed time within 1 second with the lowest time span being 300 seconds. The greatest source of error was associated with the valve position measurement method.

TABLE I

FUEL METERING VALVE WEIGHT FLOW CALIBRATIONS

Test Point	Weight (pounds)	Elapsed Time (sec)	Calculated Flow Rate (pph)	Upstream Pressure (psig)	Downstream Pressure (psig)	Temp. Fuel °F	Valve Stroke (inch)	Date
1	0.267	1800	0.53	10.8	0.80	76	0.006	12/15/70
1A	0.222	1800	0.44	10.8	0.80		0.0065	12/11/70
2	1.032	1800	2.06	10.8	0.80	75	0.031	12/15/70
3	1.695	1500	4.06	10.8	0.79	75	0.063	12/15/70
4	2.450	1500	5.88	10.8	0.80	78	0.0915	12/15/70
5	2.634	1200	7.90	10.8	0.62	78	0.120	12/15/70
5A	1.426	600	8.55	10.8	0.80		0.131	12/11/70
6	3.832	1500	9.20	10.8	0.80	78	0.141	12/15/70
7	6.853	1200	20.56	10.8	0.80	77	0.324	12/15/70
8	10.688	1200	32.06	10.8	0.80	77	0.521	12/15/70
9	7.182	600	43.09	10.7	0.72	78	0.704	12/15/70
10	8.882	600	53.29	10.62	0.68	77	0.862	12/15/70
10A	10.518	600	61.30	10.60	0.62		1.021	12/11/70
11	11.132	600	66.79	10.62	0.62	77	1.096	12/15/70
12	6.114	300	72.10	10.65	0.62	77	1.210	12/15/70
13A	6.934	300	83.10	10.75	0.75		1.382	12/11/70
13	6.980	300	83.80	10.70	0.75	78	1.397	12/15/70
14	7.775	300	93.30	10.70	0.70	78	1.538	12/15/70
15	8.556	300	102.80	10.70	0.70	78	1.729	12/15/70
15A	8.600	300	103.2	10.75	0.75		1.746	12/11/70
16A	9.458	300	113.6	10.80	0.80		1.898	12/11/70
16	9.488	300	113.6	10.85	0.85	78	1.900	12/11/70

A two inch stroke dial indicator was rigidly clamped to the valve body with its probe zeroed against a rigid metal plate bolted to the input rod on the valve (see Fig. 14). A simple screw jack arrangement locked the valve stem into each test position. Accuracy of the dial indicator should be well within ±0.0005 inch but a total hysteresis of 0.0015 inch was observed. Backlash within the valve actuator shaft and in the dial indicator caused the hysteresis. This small amount of backlash has no significant effect on valve performance until flow values of less than two pounds per hour are being controlled.

Fuel backpressure was approximately 0.8 psig throughout the test due to the height (approximately 25 inches) that the fuel was required to be raised into the measurement container. Inlet pressure was compensated to account for this head effect. Additionally both the inlet and pressure gages were located at the same height as the fuel valve to eliminate pressure head errors.

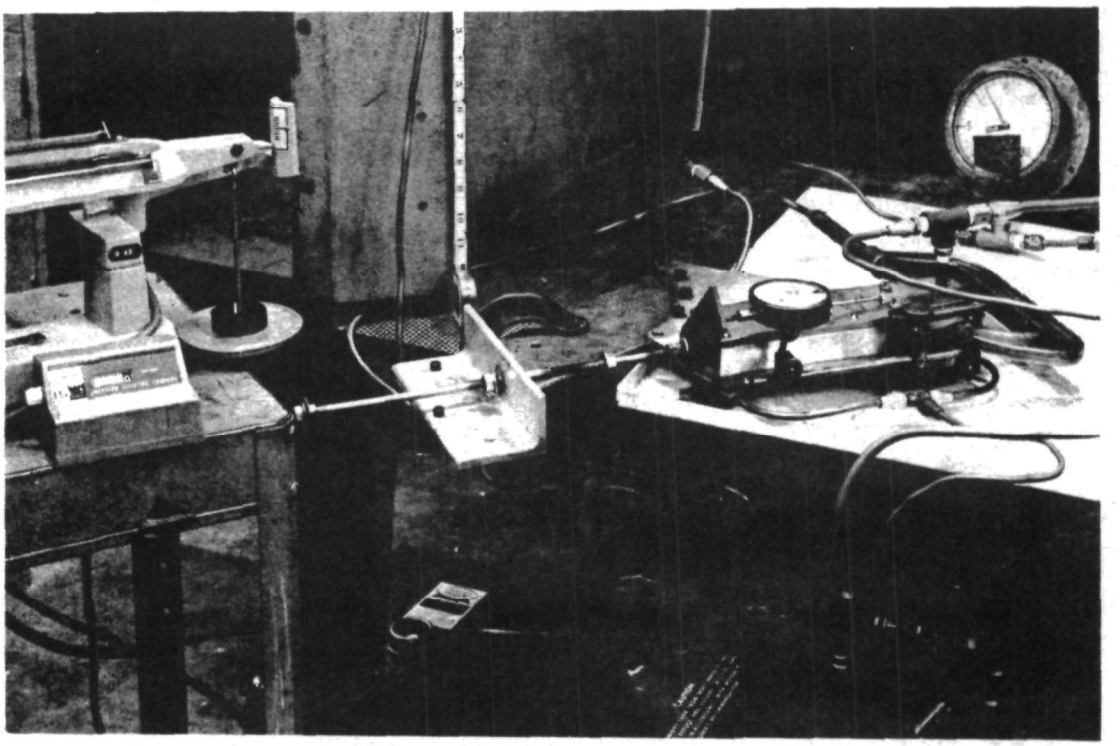

FIGURE 14. FUEL METERING VALVE STROKE MEASUREMENT ARRANGEMENT

Data from Table I is plotted in Figure 15 for a range of flows from 0.5 to 115 pounds per hour. A good degree of linearity is exhibited over this very wide range. At high flow the deviation is approximately 2.5 percent below a true linear operating line. An expanded scale plot of the data from 0.5 to 10 pounds per hour (Fig. 16) shows an excellent degree of linearity across this low flow range. These data points determine a linear operation with a slope of 64.2 pounds per hour per inch of stroke. The overall slope across the entire operating range is 61 pph/in. as indicated by the dashed line in Figure 16. By establishing 0.011 inch stoke equal to one pound per hour flow, we can define the valves performance as linear within ±2.5 percent from 3 to 115 pounds per hour with a gain of 61.0 pounds per hour per inch. Below 3 pounds per hour the absolute deviation is a maximum of 0.2 pounds per hour at the lower range limit (1 pph). Although small in absolute terms, it is a large percentage of the relative flow. However, since it was repeatable, slight modifications in the flow area of the air valve allowed correct air-fuel ratios to be adjusted at low fuel rates.

6.2.2 Air Metering Valve Development Tests

The air metering valve required more extensive development testing than any of the other control components. Figure 17 functionally describes the configuration of the integrated air valve and fan used for development tests. Air is pumped axially

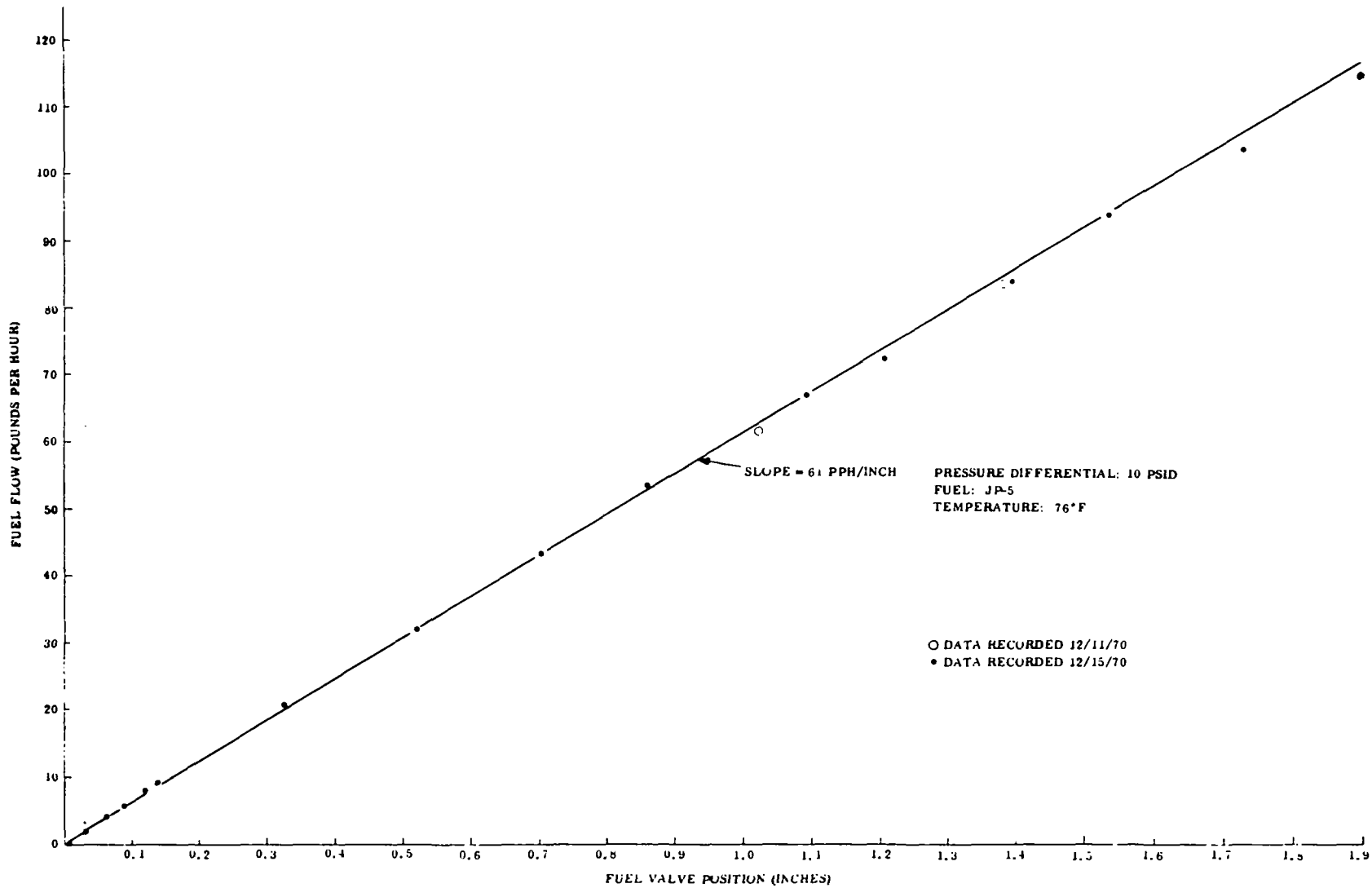

FIGURE 15. FUEL METERING VALVE FINAL WEIGHT FLOW CALIBRATION

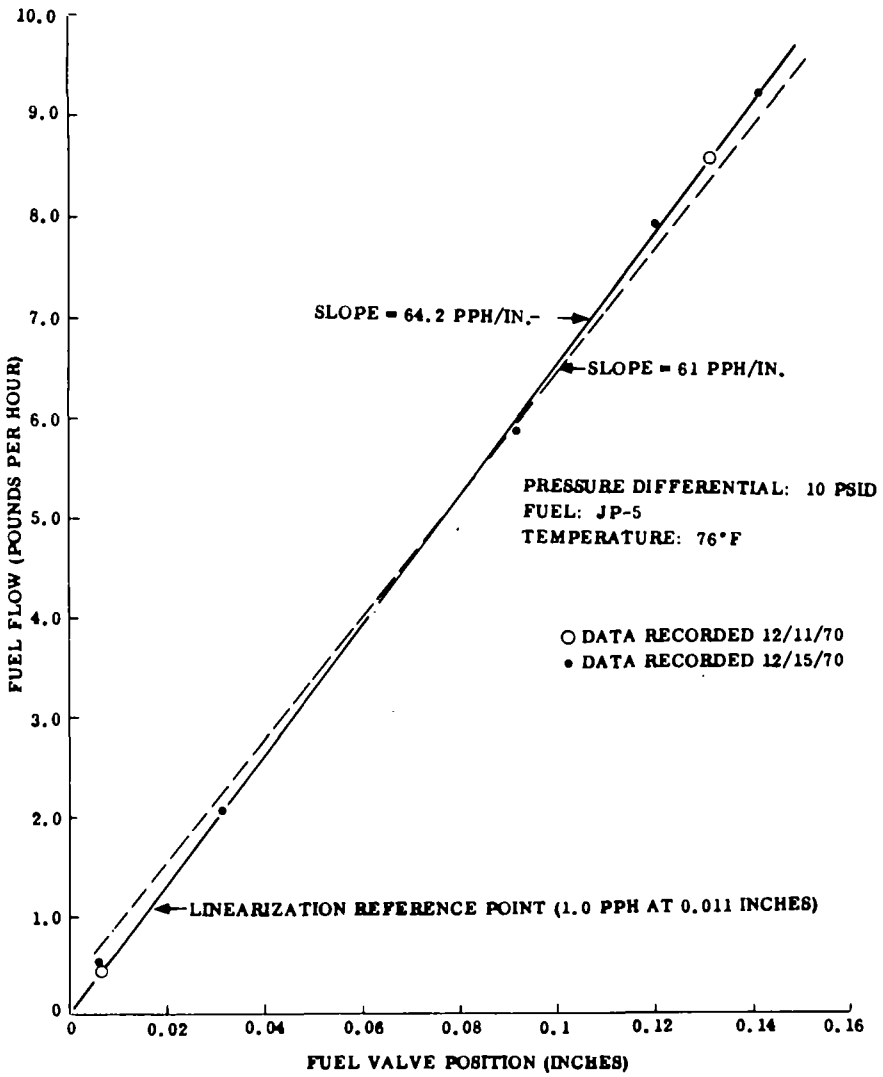

FIGURE 16. FUEL METERING VALVE PERFORMANCE FROM 0.5 TO 10 POUNDS PER HOUR (FINAL WEIGHT FLOW CALIBRATION)

across the fan motor case by a single stage four blade fan operating at 13,000 rpm. Stationary vanes were incorporated immediately downstream of the fan blades to recover the rotational energy in the fan discharge. A cavity formed by the fan on one side and the air valve chamber on the other provides a plenum for air distribution. As testing progressed, data indicated that special attention to uniform distribution of static pressure and velocity gradients would be necessary to obtain uniform air flow circumferentially around the combustor. Flow straightners and baffles were incorporated at the component test level to reduce swirl and provide uniform static and dynamic pressure fields across each of the 12 symetrical parts.

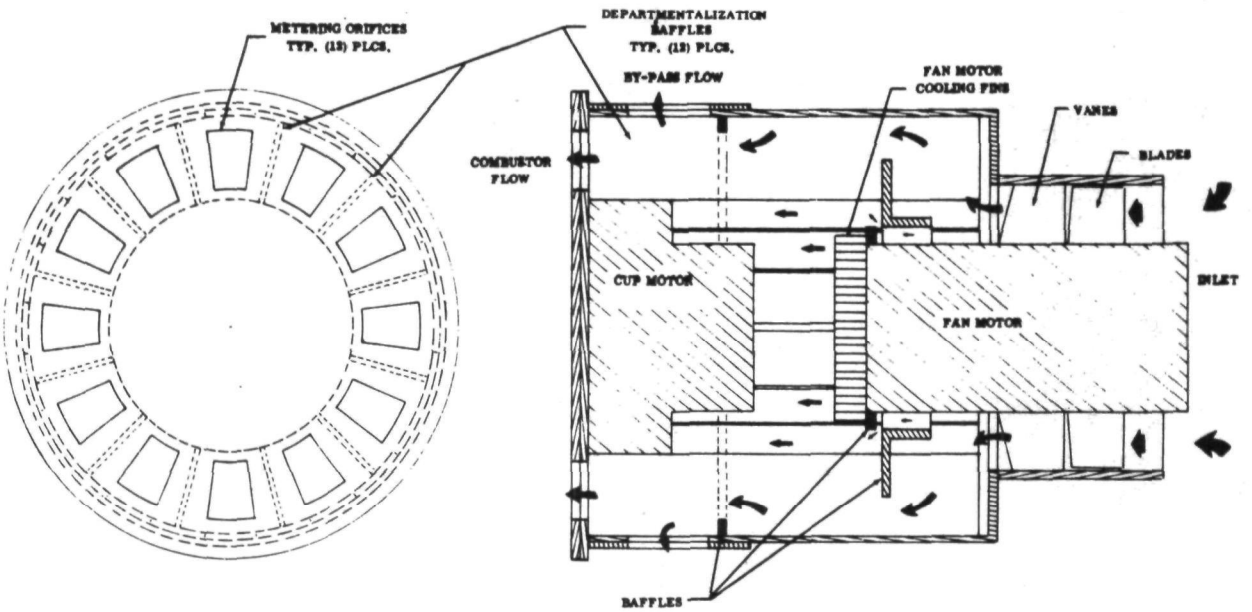

FIGURE 17. AIR VALVE AND FAN FLOW TEST MOCK-UP SCHEMATIC

A variable geometry sheet metal mock-up of the air flow configuration (Fig. 18) of the valve was tested to establish performance characteristics. The sheet metal test valve had all of the functional flow features that were incorporated when the final design unit was fabricated. It was fabricated of light gage sheet metal to facilitate rapid rework for the comparison of different port, baffle, and instrumentation configurations. From the photograph, it can be seen that the valve is in approximately the 10 percent flow metering position since the by-pass ports are approximately 90 percent open. Metering is accomplished by the plates immediately downstream of the by-pass ports. The 12-inch diameter section in the center represents the combustor interface with the air valve. Figure 19 is the schematic arrangement of the flow test rig. Actual test component arrangement and instrumentation is shown in Fig. 20. Air is pumped by the fan into the air valve cavity. Because of wide variations in the dynamic head, three static pressure probes located on the face of the air metering valve proved to give the most consistent results. The average of these three manometer readings was reported at P_1. In a similar manner, P_2 readings were picked up by three flush mounted static probes located in the wall of the 12-inch diameter cavity immediately on the discharge side of the air metering orifice ports. P_3 and P_5 measurements were made by a total of 5 additional static probes (see Fig. 19), designed to determine flow pressure loss in flow duct and across the calibrated metering orifice plate. The metering orifice plate is designed to have 60 (1/2-inch diameter) holes. This arrangment allows rapid matching of the calibration orifice pressure drops to the characteristic pressure drop of the combustor. Initial design point at 100 per cent flow requires the back pressure on the metering valve to be 8 inches of H_2O (design combustor pressure drop). The area of the calibration orifice

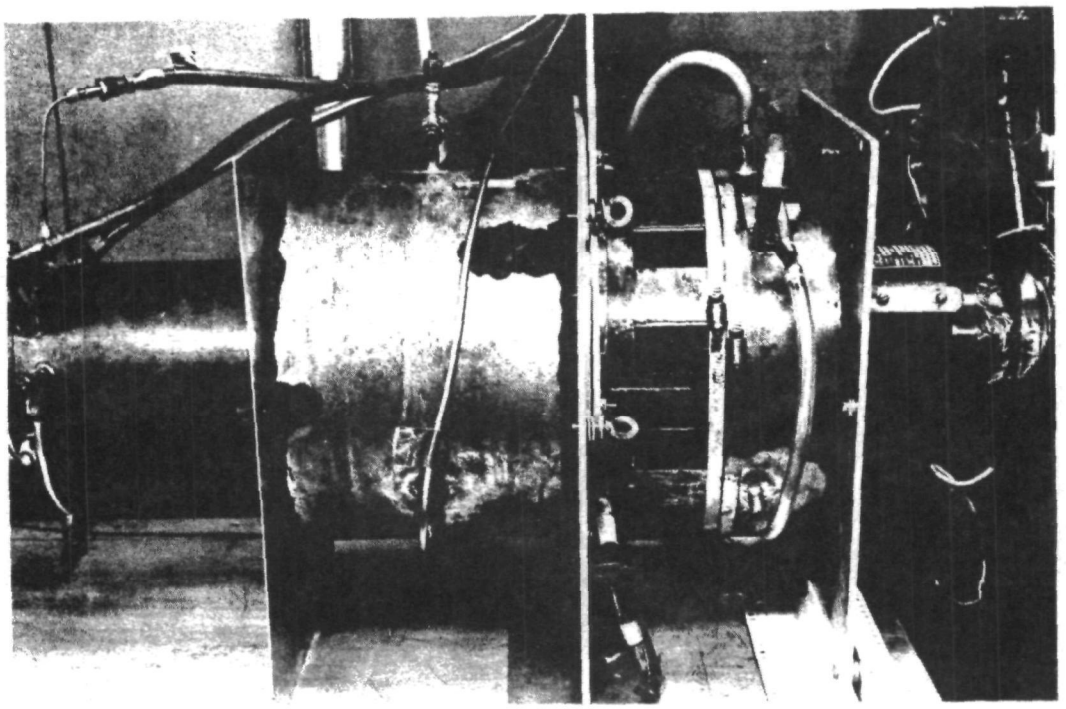

FIGURE 18. AIR VALVE FLOW TEST MOCK-UP

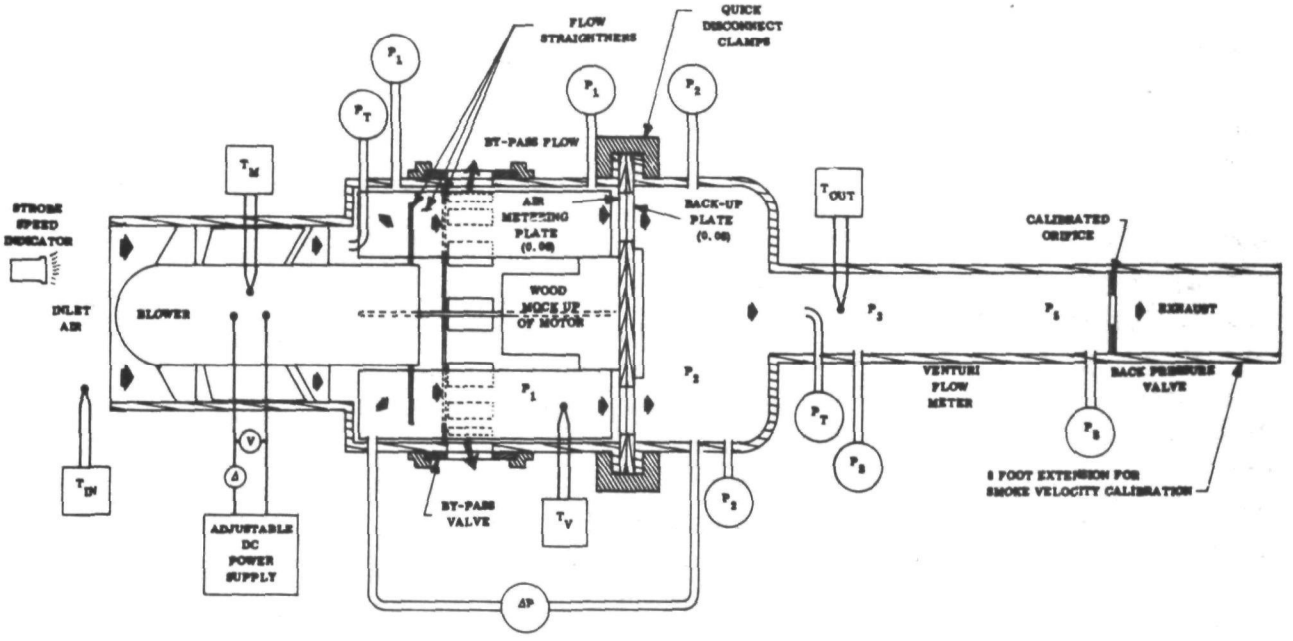

FIGURE 19. AIR VALVE FLOW TEST SCHEMATIC

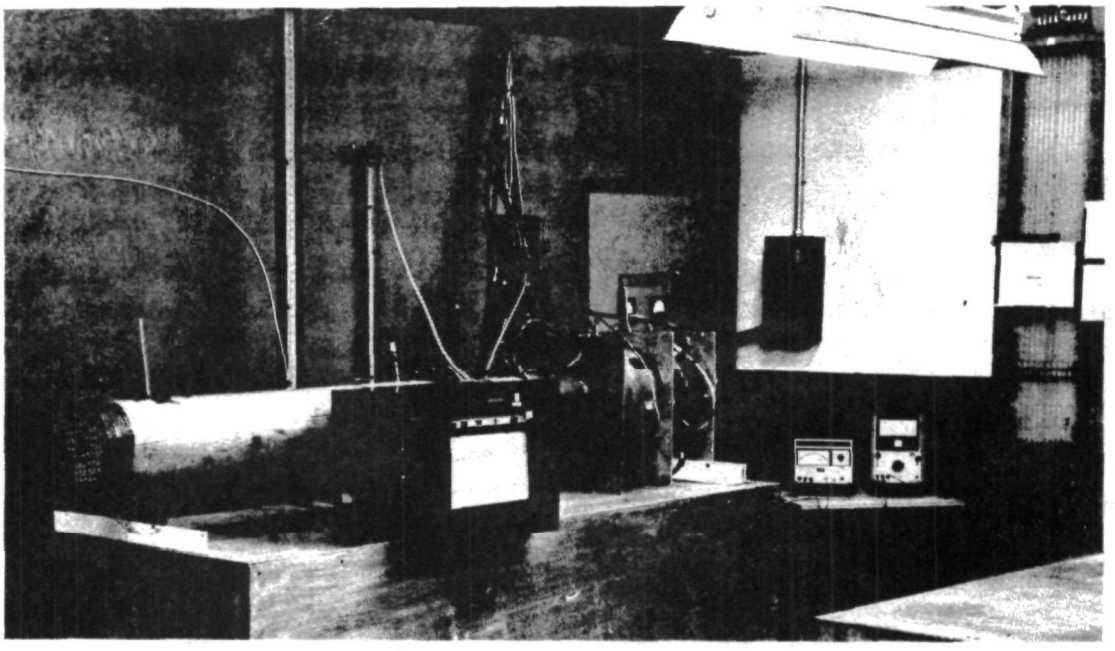

FIGURE 20. AIR FLOW TEST BENCH

plate was adjusted by covering ports in conjunction with cross calibrations against a venturi meter until the desired 8 inches of H_2O was obtained at a flow of 47 pounds per minute.

Procedures for all tests were similar. The valve would be positioned to the 100 percent power lever position and the fan motor operated at a voltage necessary to obtain 10 inches static pressure at P_1. The power lever position would be then adjusted to lower power setting to determine the flow characteristics from 100 to 10 percent flow. At each lever position setting, the pressure distribution and the flow in the test rig were measured to determine the characteristic performance of the valve. When indicated by test results, design changes were incorporated to adjust the performance toward the established goals. Results from concurrent emission monitoring tests being performed on the combustor rig revised air fuel ratios during these tests. These tests indicated that the valve should be designed to produce a lean condition at lower power settings rather than the rich air-fuel ratios incorporated in the original port configuration. As a consequence, the nonlinear cutout in the orifice ports were removed and the valve was designed to produce a constant air-fuel ratio of 25.5 across the range from 100 to 10 percent.

A rich condition (small flow areas) was intentionally maintained to facilitate optimization of the valve air-fuel ratio during combined combustor air yalve emission tests. Leaning of the ratio required only metal removal from the orifice plates by means of simple hand file operations in the range of 10 to 100 percent. Below 10 percent, the design allows the backup plate to be rotated with respect to the housing to provide a wide adjustment of air-fuel at the low heat release rates.

Initial tests were performed with a single conical baffle on the outlet of the fan. Correct flow, pressure levels, and pressure distributions were obtained down to a 50 percent power lever position with electrical input power at 2.02 HP (29.2 volts and 51.5 amps). Unsatisfactory results were obtained below the 50 percent flow position. Investigation isolated the problem to swirl resulting from the air valve-fan combination. Static pressure readings in the system were severely affected and biased toward the high side by the swirl conditions. A venturi meter initially used for flow measurement was particularly sensitivie to swirl induced errors. Since swirl of any significant magnitude can cause serious maldistribution of air in the combustor (in addition to the instrumentation problem), a series of configuration modifications were made and tested to reduce this aerodynamic problem. The edge configuration of the rotating and stationary plates were found to be a prime factor in the swirl condition as was the apparent high and unstable dynamic pressures in the air valve cavity. Metering edges were made as sharp as possible and a number of baffle configurations were tested. Although not optimum, the present configuration has appeared to reduce swirl to acceptable levels. Baffle arrangements are shown in Figure 17. Three radial baffles were found to be necessary to reduce the high dynamic head (4 inches of H_2O pressure) to allow linear valve control. Although these baffles permitted linear operation of the air valve, the pressure difference across the metering ports was not a constant 2 inches of H_2O as is required for accurate operation of the compensation system. Swirl was reduced by use of 12 axial baffles that compartmented the air valve cavity into 12 separate flow passages supplying air to each of the variable orifice ports. Although the valve functioned well in flow bench tests with this configuration, an additional pressure loss (approximately 3 inches of H_2O) has been required. As a consequence, the fan must be matched to the system by operating at 33 volts (14,200 rpm and 2.3 HP).

Flow Metering Test Results

Component level test results with a calibrated orifice are listed in Table II. Power lever position has been used as the main parameter for these tests and has been established by dividing the total stroke between 10 and 100 percent into 9 equal divisions. An 8-foot long, 8.5-inch diameter, extension to the calibration orifice duct was added to obtain an accurate flow calibration below 10 percent by means of a smoke velocity calibration. A puff of smoke was introduced at a port 12 feet from the end of the duct. From the elapsed time it takes to traverse the duct length (37 seconds for 1%), accurate flow measurements were obtained. This was necessary since at 10 percent the back pressure on the air valve must be maintained at $8(0.1)^2$ or 0.08 inch of H_2O. At the 1 percent flow, the back pressure must be maintained at 0.0008 inch of H_2O. Thus, the smoke velocity method appears to be the best approach for accurate flow calibrations down to the 1 percent level. Below the 10 percent position of the power lever, smoke velocity calibrations were made to determine the 7, 5, and 2 percent flows. These positions were recorded and compared with the 10 to 100 percent valve gain on a linear basis to determine accuracy.

TABLE II

AIR CONTROL VALVE TEST RESULTS WITH 2.25 INCH WIDE BY-PASS VALVE (0.5-INCH BAND ON ORIFICE SIDE OF BY-PASS)

Power Lever Position	100	90	80	70	60	50	40	30	20
P_1 (In. of H_2O)	9.60	8.37	6.85	5.70	4.70	3.92	3.43	3.13	2.95
P_2 (In. of H_2O)	8.27	6.75	5.25	4.02	2.97	2.09	1.45	.90	.52
$P_1 - P_2$ (In. of H_2O)	1.33	1.62	1.60	1.68	1.73	1.83	1.98	2.23	2.43
$\left[\sqrt{\frac{P_1 - P_2}{2}} - 1\right] 100\%$ *	-18.0%	-10.0	-11.0	-8.0	-7.0	-4.0	-5.0	-5.0	-11.0
P_3 (In. of H_2O)	7.91	6.66	5.08	3.84	2.78	1.90	1.24	0.74	0.40
P_5 (In. of H_2O) (Main Man.)	8.02	6.73	5.11	3.85	2.77	1.80	1.14	0.7	0.35
P_5 (In. of H_2O) (6° Man.)						1.76	1.145	0.67	0.30
Measured Flow %	100.0	91.5	79.5	69.2	58.6	46.8	37.8	28.8	19.3
$\left(1 - \frac{\text{Position}}{\text{Flow}}\right) 100\%$ Deviation From Linear	0	+1.8	-0.5	-1.1	-2.4	-6.5	-5.8	-4.2	-3.5
Overall Air Fuel Ratio, ΔP - Metering Accuracy	30.0	28.4	28.2	27.3	26.7	24.8	24.2	23.3	22.3

* ΔP Compensation Effect on Fuel

A plot of Table II results and smoke velocity calibrations is presented in Figure 21. The 100 percent position was made to be correct by adjusting motor voltage and valve by-pass port configurations to simulate combustor pressure drop at P_2. It can be seen that the valve has a high degree of linearity across a wide flow range. Cross plotted with valve position is the main parameter which is to be controlled, air fuel ratio as affected by the air metering valve performance. From 100 percent flow down to 6.5 percent, the air-fuel ratio remains within the initial design established limits of ±10 percent. Below this flow setting, the air flow is below the limits, indicating larger flow areas are necessary. This final flow adjustment has been accomplished in combined valve and combustor emission tests. A comparison of preliminary emission test results shows that to meet the optimum air-fuel ratio in the low power setting, the valve required an increased flow area to lean it down to 34:1 air fuel at 1 percent. Since the total area open at 1 percent is 0.2 inch^2, increasing flow area at low power settings was accomplished by rotation of the backup plate by approximately 0.010 inch. A pressure drop across metering valve ports proportional to flow is important for proper functioning of the fuel pressure compensation system. If fan voltage inadvertently changes, or if it is intentionally reduced at part loads to

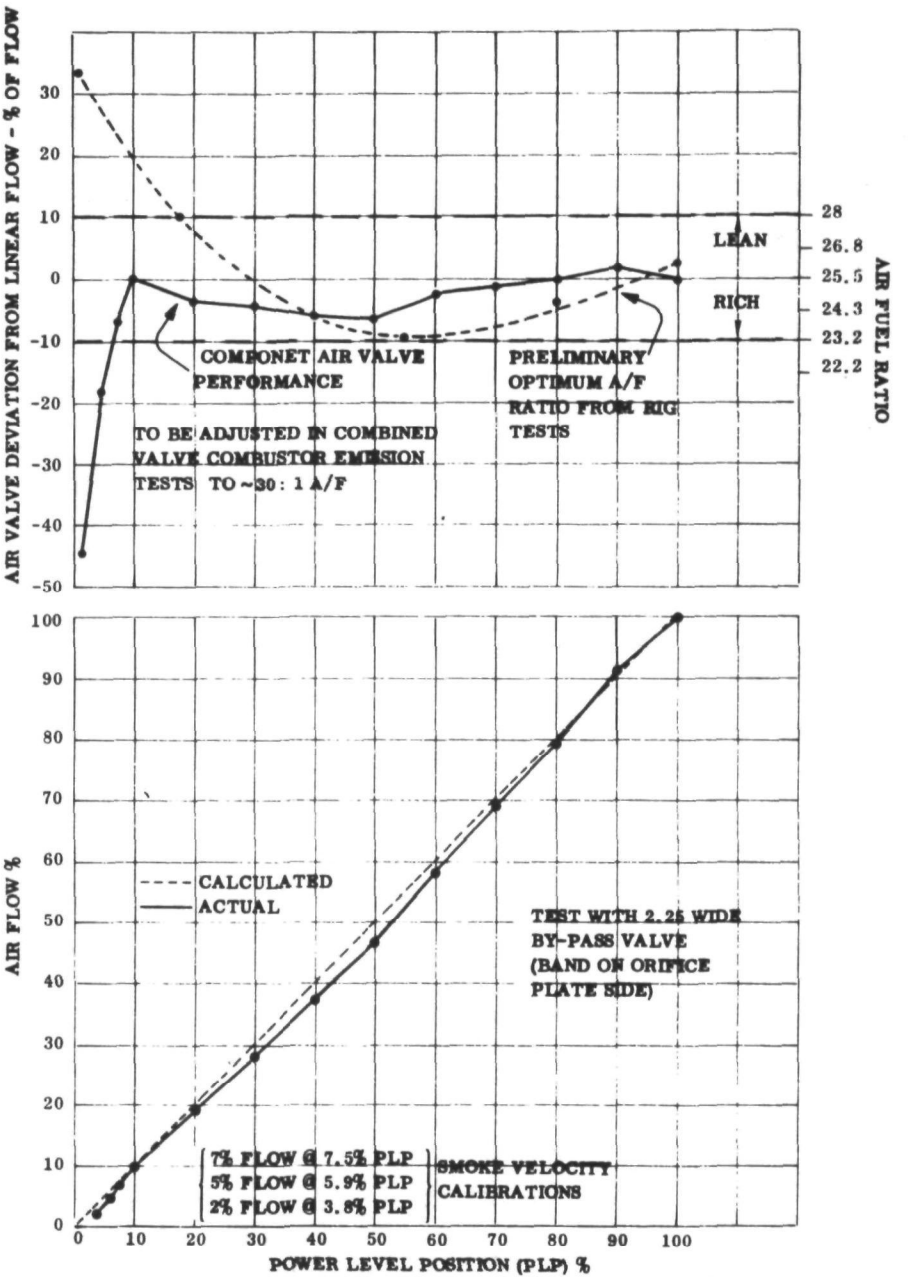

FIGURE 21. FLOW CONTROL PERFORMANCE OF AIR METERING VALVE

lower power losses, the fuel pressure regulator is designed to automatically reduce flow proportional to air flow. To achieve accurate air-fuel ratio control, it is necessary that a pressure difference across the metering ports be maintained at 2 inches of H_2O. Figure 22 shows the pressure differential as a function of valve position. At high flows, the $P_1 - P_2$ is less than calculated and at low flows, it is approximately the same amount (~0.5 inch of H_2O) above the 2 inches of H_2O design point. Assuming perfect fuel pressure regulator and fuel metering valve, the effect on fuel flow and air-fuel ratio are also plotted in Figure 22. It is seen that the air-fuel ratio exceeds the 10

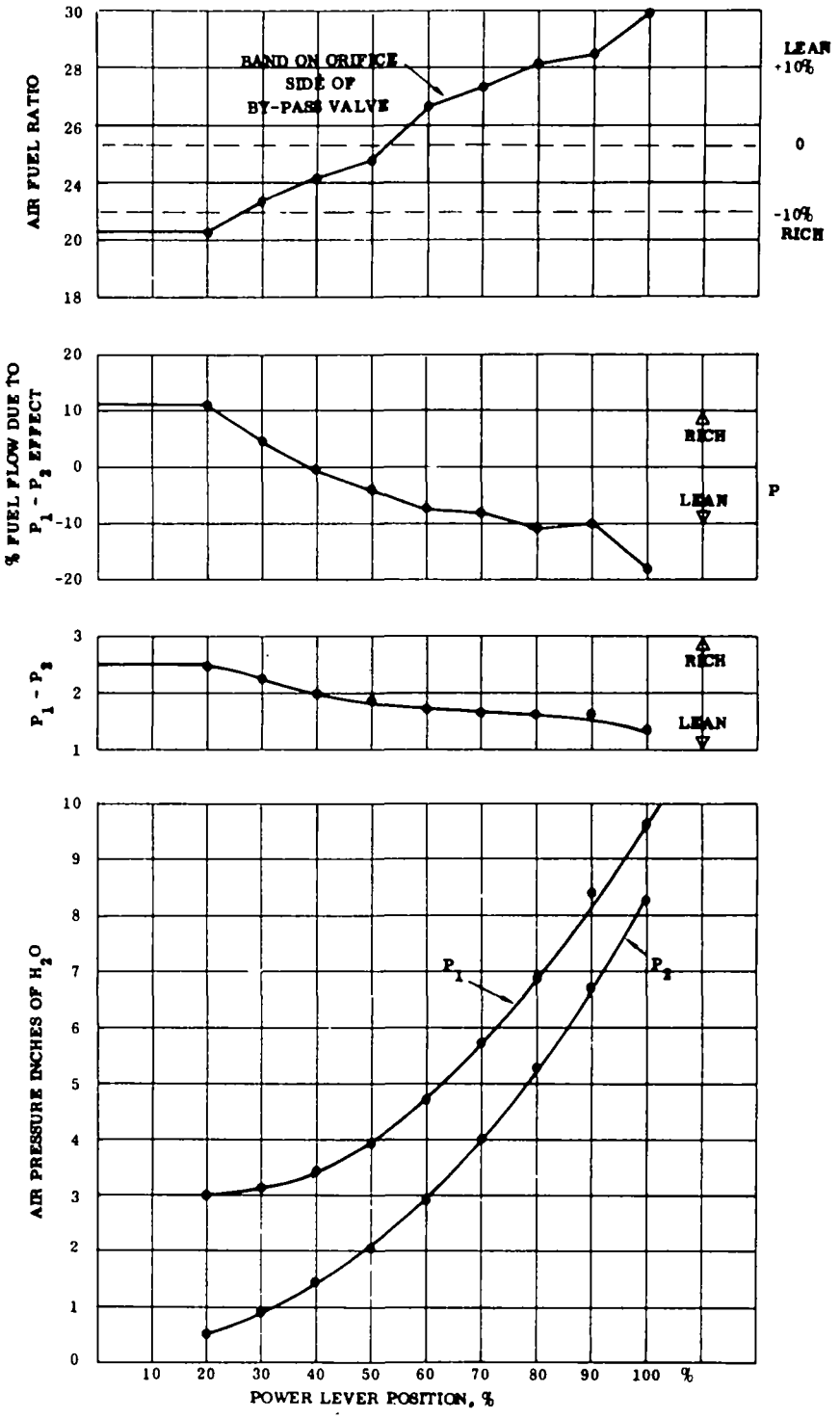

FIGURE 22. AIR VALVE ΔP TEST RESULTS WITH MOCK-UP AIR VALVE

percent lean band at high flows and the 10 per cent rich band at low flows. It appears that the cause of this large difference between calculated and actual pressure differences at the metering port is associated with the high dynamic head in the small diameter fan discharge annulus. High velocity jets must change their direction as a function of geometry and the amount of flow required. Several approaches to the problem exist. The optimum method would be to specially design a fan to match the large diameter geometry of the combustor and air valve and thereby have lower speeds and dynamic turning losses. Schedule and scope limitations of the program have not allowed the design and incorporation of an optimum fan. An extension duct to allow a larger plenum has been used in most of the final emission demonstration tests as a simulation of the aerodynamics expected in a matched fan-combustor system.

An even greater effect upon the pressure distribution across the metering port can be obtained by baffle and flow straightener configuration changes. Another significant factor is the location of the static pressure probes for P_1. An apparent pressure gradient across the face of the valve plate has been observed and found to vary with power lever position. By optimizing by-pass valve geometry, baffle configurations and static probe location, significant reductions in variations of $P_1 - P_2$ with power lever setting were obtained. A major portion of the valve development tests were directed toward this, since a stable $P_1 - P_2$ not only can be used to compensate for operating variations in fan voltage but can form the basis for major flow changes accompanying voltage reductions to save on parasitic losses.

From these test results the final configuration of the valve was fabricated. Figures 2 and 23 show the final design prior to installation into the demonstration system. Mechanical functioning is very simple as the air metering port moveable parts are mechanically fastened to the by-pass port fingers. Air pressure and springs force the sliding valve elements against the valve housing and backup plate. Capability to change the low flow rate air-fuel ratio is provided by allowing the backup plate to be rotationally indexed with respect to the power lever position and by an adjustable linkage between the power lever and the fuel valve (See Fig. 2 and 23). Adjustments to the final air-fuel ratio were made in integrated systems tests to minimize emissions from the combustor (See Section 7).

Fan Noise

Due to the high dynamic turning and straightening losses, the fan has been operated at 33 volts to match it to the system requirements. As a consequence, the noise level was above the 80 db at fan rated conditions. An analytical and experimental investigation of the problem and its potential solutions has been initiated.

Sound pressure levels of the Rankine burner fan section operating separately from combustor were taken with and without inlet guide vanes. The results were 102 db

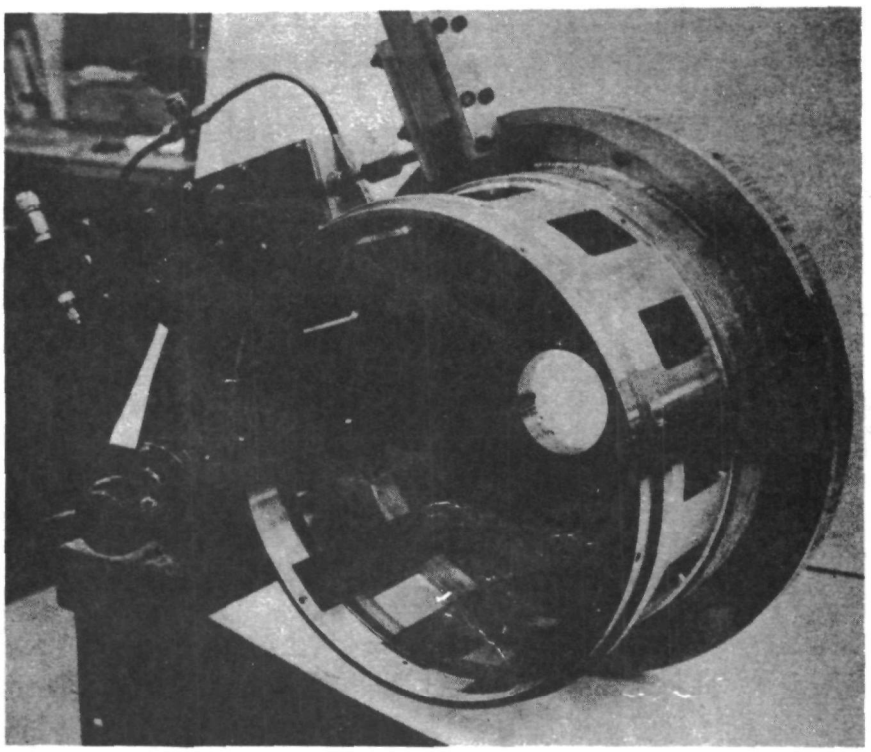

FIGURE 23. DEMONSTRATION SYSTEM AIR VALVE

(ref. $20\mu N/m^2$) overall sound pressure level with inlet guide vanes and 94 db overall sound pressure with the inlet guide vanes removed. A 1/10 octave frequency analysis of noise with guide vanes removed, is given in Figure 24. Test details are given below:

- Blower Power Setting: 31 Volts, 53 amps
- Blower Speed: 14,000 rpm
- Number of Blades: 4
- Microphone Location and Orientation: Five feet off blower axis from blade location. Set 45 degrees from vertical toward blower and perpendicular to blower axis (see Fig. 25).
- Surroundings: Semi-reverberant (see Fig. 25 for details)
- Equipment: General Radio Type 1564A Sound and Vibration Analyzer
  General Radio Type 1521 B Graphic Level Recorder
  General Radio Type 1560-P4 Preamplifier
  General Radio Type 1560-2131 Microphone
  General Radio Type 1562 Sound-Level Calibrator

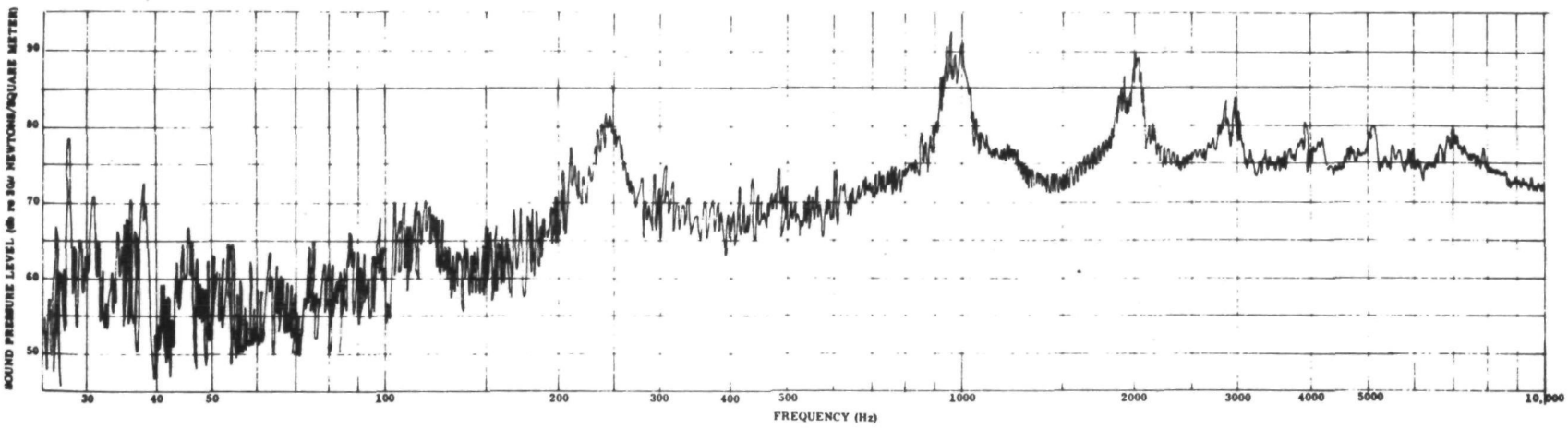

FIGURE 24. SOUND PRESSURE LEVEL VERSUS FREQUENCY FOR BLOWER WITHOUT INLET FLOW STRAIGHTENER

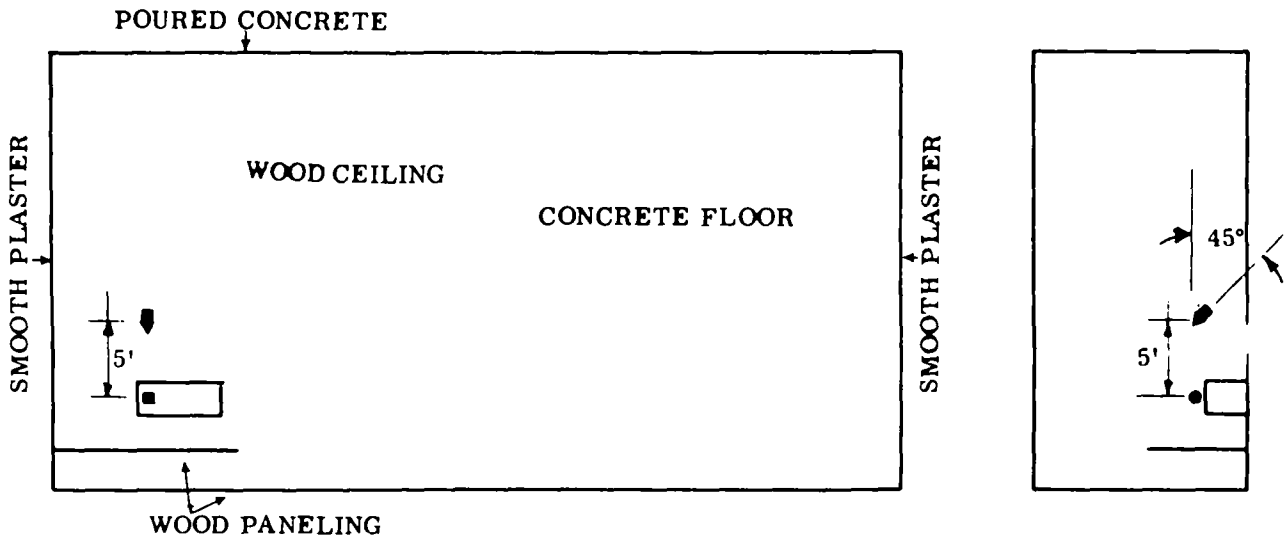

FIGURE 25. NOISE MEASUREMENT ROOM GEOMETRY AND MATERIALS

- Background Noise: Background noise was observed to be more than 10 db below peak levels occurring at 250 cps, 980 cps, 2000 cps, and 3000 cps.

- Background levels are at least 5 db below blower levels at all other frequencies except in the ranges 25-220 cps and 350-400 cps where blower and background levels are equivalent.

An approximation of overall noise level of the blower in a free acoustic field can be made using the following relation:

$$\text{Reduction in Noise Level (db)} = 10 \log_{10} \frac{a_2}{a_1}$$

where a_2 is the new sound absorption coefficient which is one for this case by definition of a free field

a_1 is the room sound-absorption coefficient determined by relative room wall areas multiplied by their respective material absorption coefficients.

If S is the total room wall surface area, then for a predominant level of 980 cps

$$a_1 = \frac{2S}{5} \text{ (Absorption coefficient of concrete)}$$

$$+ \frac{2S}{5} \text{ (Absorption coefficient of wood paneling)}$$

$$+ \frac{S}{5} \text{ (Absorption coefficient of smooth plaster)}$$

$$= S\frac{2}{5}\ (0.0175) + \frac{2}{5}\ (0.06) + \frac{1}{5}\ (0.035)$$

$$= 0.034S$$

Then Reduction in Noise Level is = $10 \log_{10} 1.00/0.034 = 14.7$ db.

This implies that the blower operating in a free field without inlet guide vanes would register approximately 80 db overall sound pressure level assuming the same relative microphone position.

Figure 24 shows four distinct frequency peaks of

1. 92 db at 980 cps (this was also noted as the predominant noise level frequency with vanes.)
2. 90 db at 2000 cps
3. 83 db at 2900 cps
4. 81 db at 245 cps

Blade passage frequency is

$$\frac{14,000 \text{ Rev/Min}}{60 \text{ Sec/Min}}\ 4\ \frac{\text{Cycles}}{\text{Rev}} = 935 \text{ cps}$$

The first three measured peaks have frequencies corresponding to the first, second and third order of blade passage frequencies, respectively. A fourth peak is coincident with the blade support rotational frequency. It can be deduced that bearing noise and or single blade passage frequency is the cause of this peak. The exact cause is not of immediate interest because it is considerably lower than the fundamental and first harmonic peaks caused by blade passage excitations. Appendix A discusses several design approaches that could be incorporated into an optimum fan design that can reduce blade passing frequency tones in an optimum configuration.

6.2.3 Delta-P Fuel Pressure Regulator Calibrations

In order to maintain the desired air-fuel ratio independent of fan voltage, fan or motor efficiency reductions, or blade fouling a delta-P regulator was developed to control fuel pressure directly proportional to the pressure differential across the air metering valve. Figure 1 functionally describes the operation of the valve. In order to obtain as low an operating range as practical a large diameter actuator was used (Fig. 26) to convert the pressure drop ($P_1 - P_2$) across the air metering valve into an effective control force. Development tests on the regulator valve were performed with the fuel metering valve as the flow load component. Supply pressure was provided by the Rankine combustor's system fuel pump. Air for the actuator input was regulated from the shop air system as the main test parameter variable. At a differential actuator input of 1.0, 2.0 and 2.5 inches of H_2O differential, the metering valve was placed in the 100, 50 and 1 percent flow positions. The fuel bypass adjustment was then set to give the best regulation across the range of fuel flows and input air pressures. Throughout the remainder of the test it was locked in position while both air pressure and fuel flow were varied. Regulated fuel pressure was recorded at each of the three flow conditions at every 0.1 inch from 1.0 to 2.5 inches of H_2O input pressure.

Several different configurations of springs and diaphragms were tested. A PVC molded diaphragm and a thin flat rubber diaphragm proved to be the best. A plot (Fig. 27) of the regulated pressure versus actuator input signal for the PVC

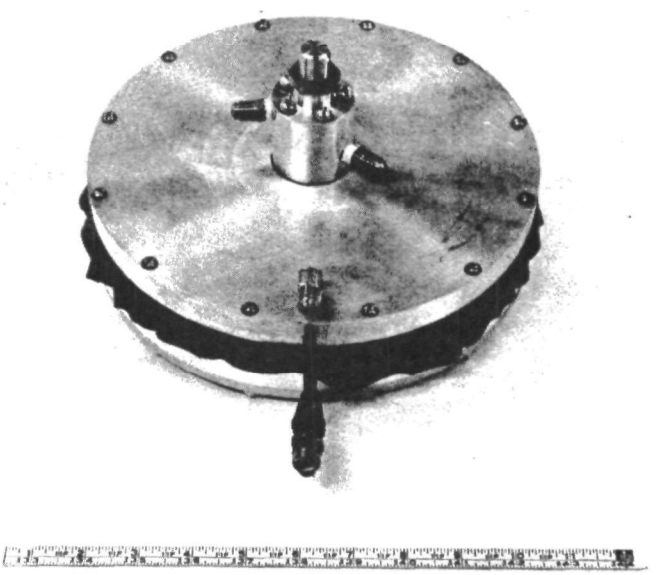

FIGURE 26. FUEL PRESSURE REGULATOR INSTALLED ON $P_1 - P_2$ ACTUATOR

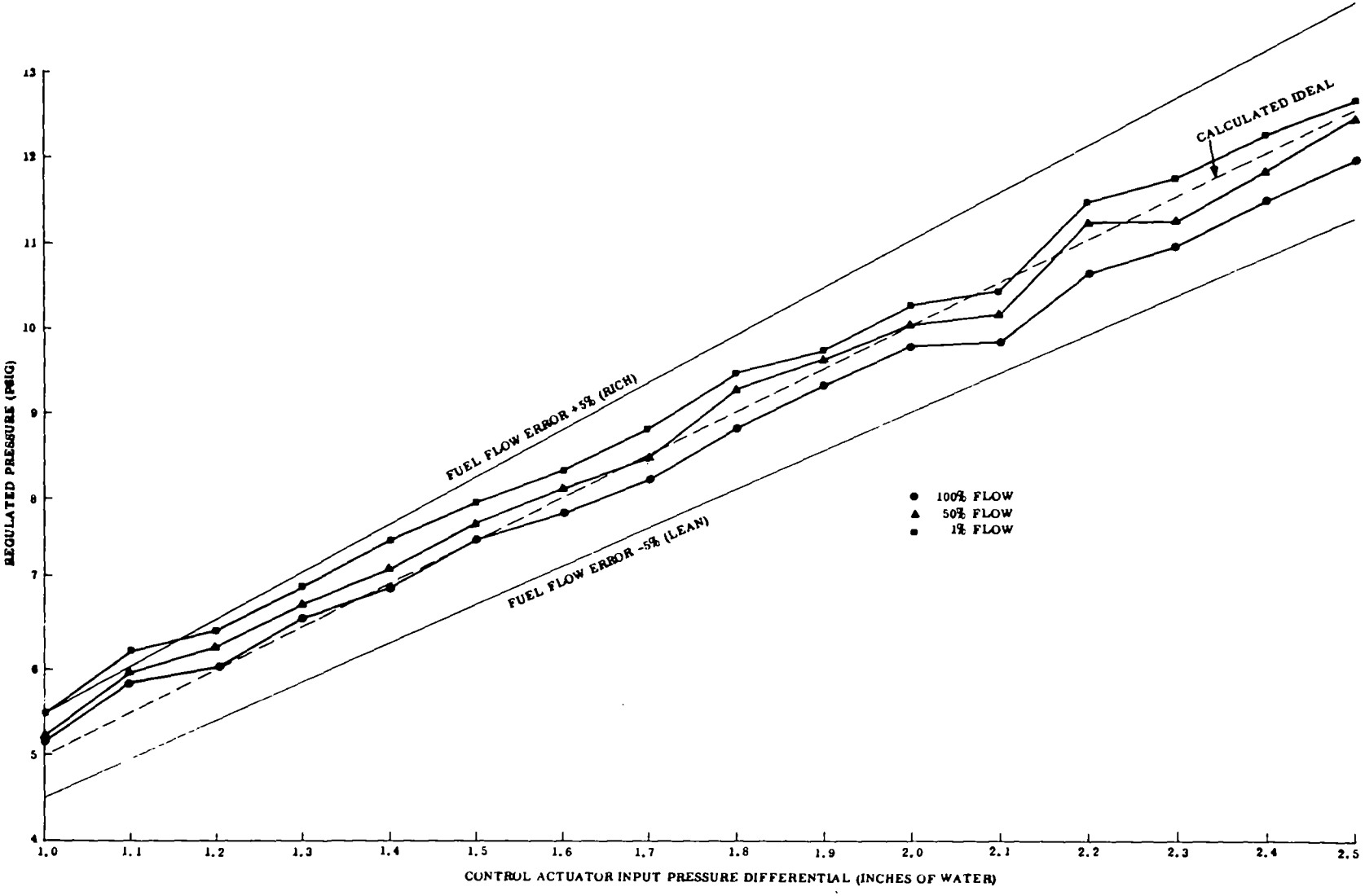

FIGURE 27. FUEL PRESSURE REGULATOR WITH MOLDED 0.012 INCH THICK PVC DIAPHRAGM

diaphragm shows that it has reasonably good performance across the extended operating range. The dashed line plotted in the figure represents exact (zero error) compensation. An upper and lower 5 percent error in fuel flow is also included. Only at the low end of the input pressure range does the regulated pressure output cause a flow error of more than 5 percent (7.5% rich). This diaphragm configuration used 0.012 PVC with a molded convolution between the outside ring seal and the center plate support. It is a rugged diaphragm but has corresponding high stiffness. Irregularities in the convolution and the high stiffness caused the nonlinearities in the performance curve.

A flat diaphragm made of thin resiliant rubber (0.008 inch thick) had virtually zero stiffness. Results of test with this material showed that it regulated pressure accurately enough to hold the flow of fuel within ±4 percent of the ideal across the entire range of input pressures (Fig. 28). Final calibration tests results are given in Table III. Normal operation of the system would be in the range of 1.0 to 2.0 inches (if voltage to the motor is reduced to reduce part load parasitic losses). Within this range the valve regulates pressure accurately enough to hold the flow within ±3 percent of the ideal.

6.3 TRANSIENT RESPONSE EMISSIONS TESTS

6.3.1 Description of Demonstration Combustor System

A fully integrated combustion system was tested for emissions. Figure 29 shows a cross section of the complete system. Air is drawn through the fan and delivered into the air valve chamber. From this chamber the air either is metered into the combustor section through the air metering ports or it is bypassed through the ports located on the outer diameter of the valve housing. Figure 29 is only one of several configurations tested in the fully integrated system emission tests. Most of the tests were performed with a 36-inch long extension between the air valve and fan to provide a better aerodynamic matching between these components.

Figure 30 illustrates the system with the fan mounted inside of the extension. By mounting the fan within the duct it was possible to vary the axial distance between the fan discharge and air valve. Instrumentation, control and a self contained fuel system including tanks were mounted in a mobile test stand for maximum test flexibility (Fig. 30 and 31). All steady state power levels and transient emission tests were performed with the use of the power lever position as the only variable. Regulation of air and fuel flows was automatically maintained by the previously described components integrated with the combustor. Fuel flow rates during a particular test run were determined by prior calibrations of the fuel metering valve and measurement of the pressure differential across the metering ports. Two variable area flow meters were connected through manual valves in series with the flow metering valve. These were used to verify the calibration of the flow metering valve

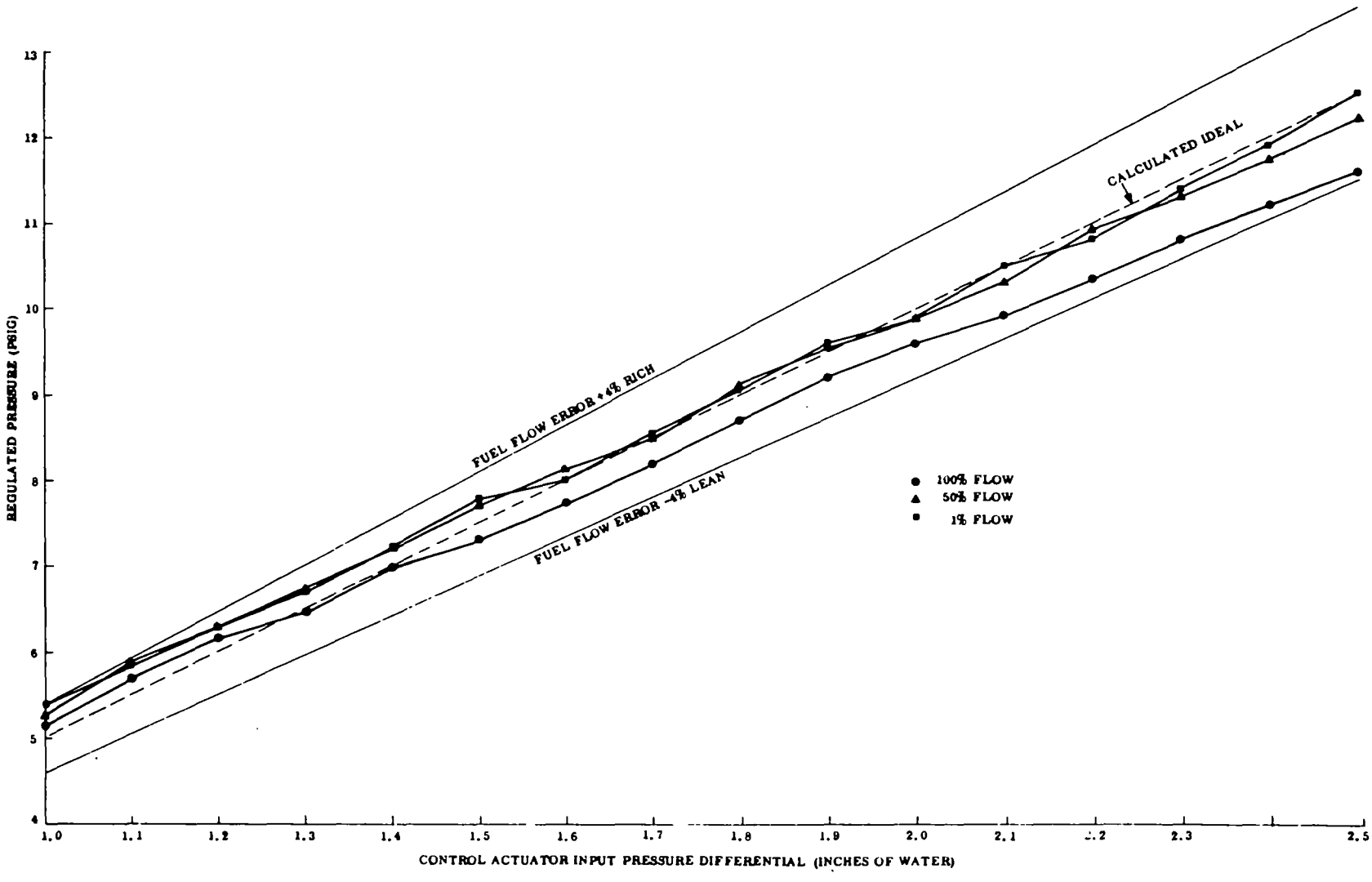

FIGURE 28. FUEL PRESSURE REGULATOR PERFORMANCE WITH 0.008 INCH FLAT RUBBER DIAPHRAGM

TABLE III

PRESSURE REGULATOR CALIBRATION WITH 0.008 INCH FLAT RUBBER DIAPHRAGM

Test Points	Flow Meter Readings (pph) (Uncorrected)	Regulated Fuel Valve Inlet Pressure (psig)	Pump Discharge Press (psig)	Actuator Sensor Input (in. of H_2O)	Regulator Back Pressure (psig)	Valve Stroke (Inches)
1%						
1A	1.0	9.9	10.8	2.0	0.32	0.006
2A	1.0	10.5	11.3	2.1	0.35	
3A	1.05	10.8	11.8	2.2	0.35	
4A	1.1	11.4	12.2	2.3	0.37	
5A	1.1	11.9	12.8	2.4	0.38	
6A	1.2	12.5	13.3	2.5	0.38	
7A	0.9	9.6	10.4	1.9	0.38	
8A	0.8	9.05	10.0	1.8	0.38	
9A	0.7	8.55	9.4	1.7	0.38	
10A	0.7	8.0	9.0	1.6	0.38	
11A	0.7	7.8	8.8	1.5	0.38	
12A	0.7	7.25	8.1	1.4	0.38	
13A	0.7	6.70	7.5	1.3	0.38	
14A	0.6	6.30	7.1	1.2	0.38	
15A	0.6	5.85	6.8	1.1	0.38	
16A	0.6	5.40	6.2	1.0	0.38	
50%						
1B	49.1	9.9	10.8	2.0	0.05	0.866
2B	50.0	10.30	11.1	2.1	0.10	
3B	51.5	10.90	11.8	2.2	0.10	
4B	52.5	11.30	12.2	2.3	0.12	
5B	53.5	11.70	12.6	2.4	1.4	
6B	55.0	12.20	13.1	2.5	1.6	
7B	48.0	9.55	10.4	1.9	0.08	
8B	47.0	9.10	10.0	1.8	0.05	
9B	45.5	8.50	9.4	1.7	0.02	
10B	44.0	8.15	9.0	1.6	0.01	
11B	43.0	7.70	8.6	1.5	0	
12B	41.8	7.20	8.1	1.4	0	
13B	40.10	6.75	7.7	1.3	0	
14B	39.0	6.30	7.1	1.2	0	
15B	37.8	5.90	6.8	1.1	0	
16B	36.0	5.35	6.3	1.0	0	
100%						
1C	96.0	9.60	10.5	0.95	2.0	0.8915
2C	98.0	9.90	10.8	1.00	2.1	
3C	99.5	10.35	11.2	1.05	2.2	
4C	100.2	10.80	11.6	1.10	2.3	
5C	104.0	11.20	12.1	1.15	2.4	
6C	106.2	11.60	12.5	1.20	2.5	
7C	93.5	9.20	10.0	0.92	1.9	
8C	91.0	8.70	9.6	0.88	1.8	
9C	88.0	8.20	9.2	0.80	1.7	
10C	85.5	7.75	8.8	0.75	1.6	
11C	83.2	7.30	8.2	0.70	1.5	
12C	81.0	7.00	7.9	0.65	1.4	
13C	78.0	6.45	7.5	0.60	1.3	
14C	76.0	6.15	7.0	0.55	1.2	
15C	73.5	5.70	6.5	0.50	1.1	
16C	70.2	5.25	6.2	0.45	1.0	

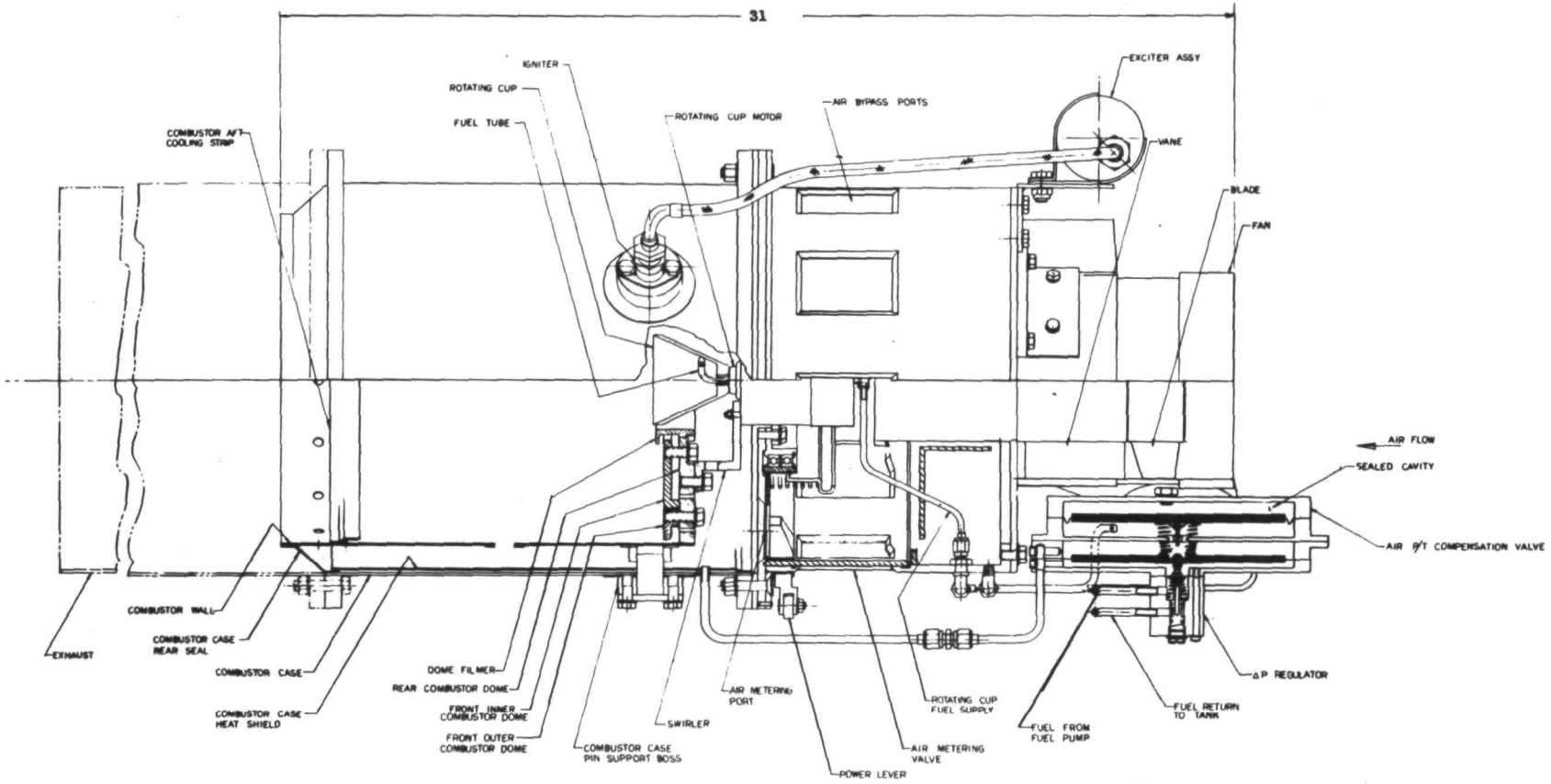

FIGURE 29. DEMONSTRATION SYSTEM

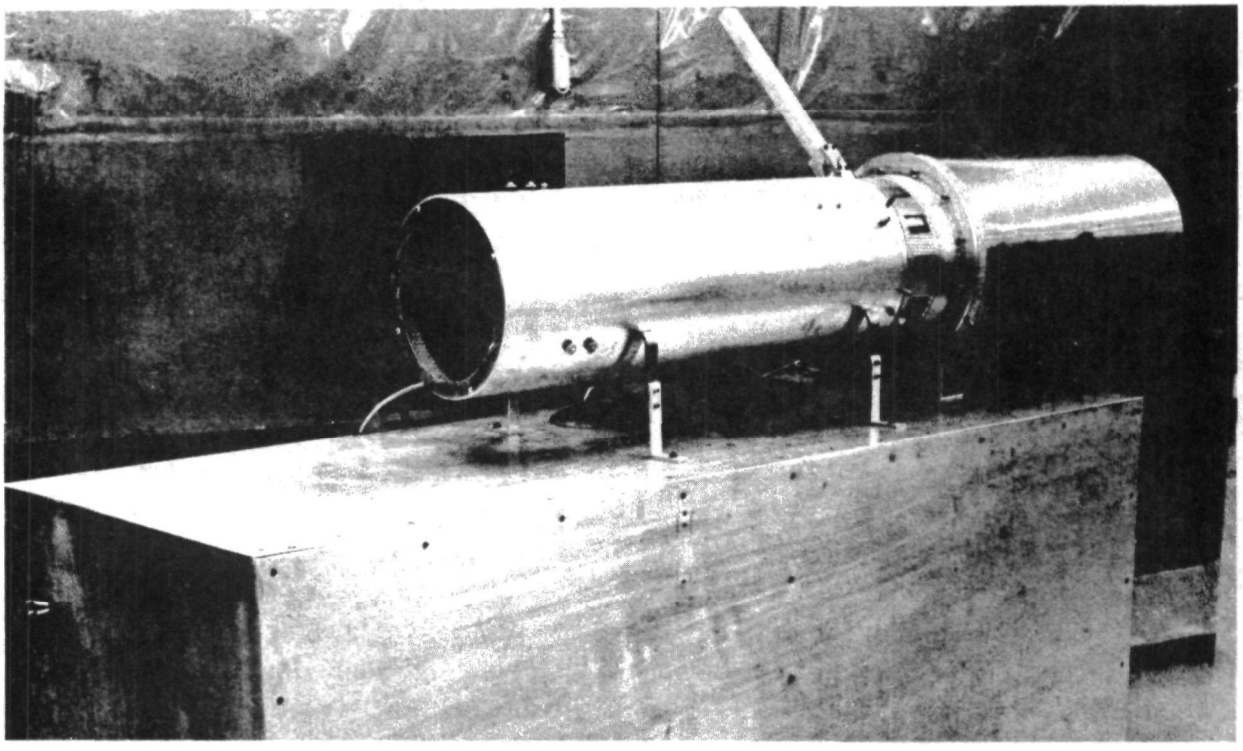

FIGURE 30. DEMONSTRATION SYSTEM WITH LONG MIXING DUCT

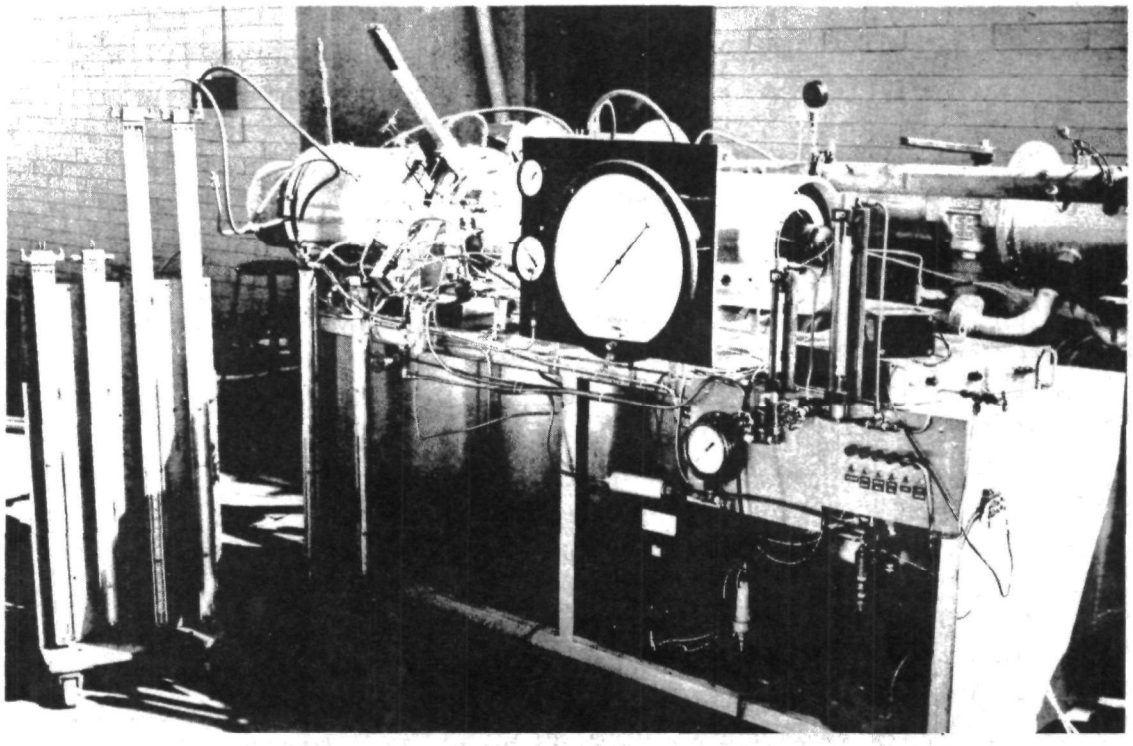

FIGURE 31. INTEGRATED SYSTEM DEMONSTRATION TEST STAND ARRANGEMENT

periodically throughout the test phase. They could not be incorporated in the system continuously since they have a flow sensitive pressure restriction that would modify the fuel pressure regulator's control of air-fuel ratio. Two flow meters are necessary since a 10 to 1 flow ratio is the normal range of these instruments. Fuel delta-P across the metering valve was recorded on both a precision laboratory gauge with divisions of 0.1 psi and an electric transducer displayed on a strip recorder during transient tests. An electric position transducer connected directly to the power lever position recorded stroke or power level directly in percent of full power on a strip recorder. Its basic function was to establish power rate input changes during transients. Air-fuel ratio was obtained by an averaging probe CO_2 measurements in the exhaust and cross checked against combustor air flow calibrations made with standard orifice flow meters.

6.3.2 Startup and Shutdown Transients

The design goal for this demonstration was to be able to start the combustor and to be up to full power in three seconds. Experimental analysis indicated that startup was optimum at the 30 percent power lever position. Figure 32 shows the results of a startup from 30 percent and followed by an immediate power increase to 100 percent in three seconds. In this start the blower was at operating speed prior to ignition excitation and opening of the fuel valve solenoid. Fuel was circulating through the regulator valve and being bypassed to the tank at the time the solenoid valve opens to connect fuel to the rotating cup feed tube. Transient gas emissions were obtained by recording the output of each of the four gas analyzer systems on a strip chart. Response delays of each of the four measurement systems is from 2 to 5 seconds with the relatively short exhaust gas sampling lines used in this test (less than 20 feet). It is not possible to directly plot the emissions in gm per Kgm of fuel since the fuel flow and air flow cannot be exactly established during a transient. Additionally the transient response of present state-of-the-art gas analyzers is not sufficiently fast to provide for exact analysis of a transient load change. However, a reasonably good quantative estimate of transient performance can be made by an analysis of the direct volumetric emission data obtained as a function of time on the Beckman strip chart recorder. Design goal limits are indicated on the exhaust gas concentration scales. These limits are based on calculations that relate the mass emission goals to the volumetric flowrate and the air-fuel ratio as obtained from the CO_2 concentrations. At the startup transient none of the emission levels exceeded the volumetric design goals. Hydrocarbon (measured as C_1) came relatively close to the limit, 20 ppm compared to a limit of 35 ppm. After one minute of operation the system was subjected to decrease power transient from 100 percent to 5 percent in two seconds and then an increase to 100 percent in 2.7 seconds. After another twenty seconds at 100 percent power the combustor was shutdown by closing the systems fuel cutoff solenoid valve. A transient peak of 700 ppm in HC emissions was recorded. Cause of this high peak appears to be a small amount of fuel leaking into the combustor after the initial closing of the solenoid.

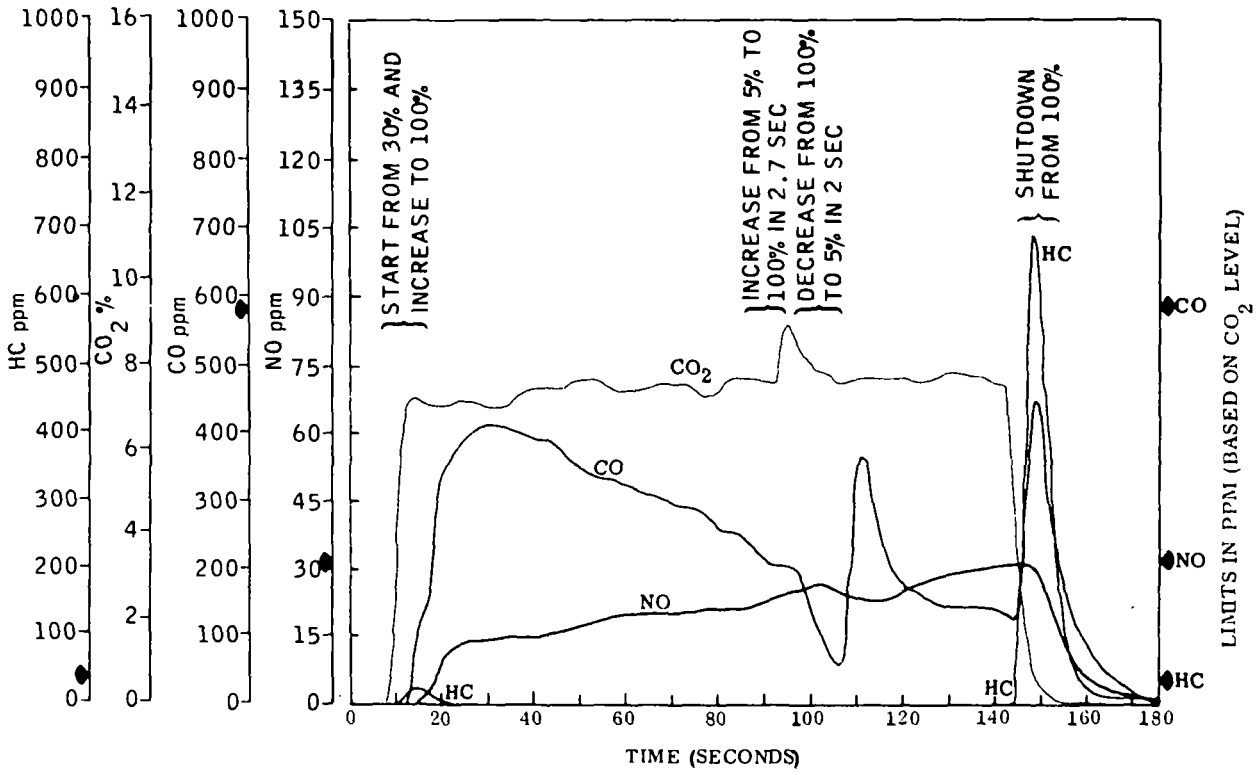

FIGURE 32. STARTUP AND SHUTDOWN EMISSIONS

In the demonstration configuration the solenoid valve was located approximately 12 inches from the rotating cup. In a specially designed installation the shutoff valve could be located directly in the fuel supply tube to eliminate any possibility of after drip. An alternative would be to utilize a solenoid valve with sufficient "negative" displacement to extract a small fuel volume from the fuel supply tube as the valve closes.

6.3.3 Power Level Transient Emissions

A major performance goal of the program was to be able to rapidly modulate power from any one power level to another without severe increases in emissions. A response rate of 50 percent of full power per second was established as a preliminary goal. Table IV lists emission level transients in ppm obtained from strip chart records for power changes. For each transient test the demonstration system's power lever was manually positioned from a high heat release (A) down to a lower heat release (B). At level (B) the fuel flow was stabilized with a dwell period of approximately 0.5 second. Immediately after the dwell the lever was moved back to the initial heat release position of (A). Movement of the lever was controlled in each test to obtain a rate of change of greater than 50 percent per second. Fuel flow corresponding to the lower lever position is listed in the first two columns of Table IV.

TABLE IV

POWER LEVEL TRANSIENT EMISSIONS (COMBUSTOR CONFIGURATION "D")

Transient From A and B to A		Transient Time (sec)			Emissions Measured										
					CO (ppm)			NO (ppm)			HC (ppm)			CO_2 (%)	
A(pph)	B(pph)	t_1	t_2	t_3	Limit	Steady State	Peak	Limit	Steady State	Peak	Limit	Steady State	Peak	Steady State	Peak
109	5	1.70	0.6	1.85	534	45	8	28	42	45	32	14	14	6.5	8.3
109	10	1.40	0.6	1.65	534	45	285	28	46	48	32	13	15	6.5	9.7
109	30	1.70	0.4	0.9	534	40	40	28	49	50	32	15	15	6.65	8.05
109	50	0.7	0.7	0.6	591	15	223	31	43	39	35	13.5	25	7.2	6.3
109	70	0.36	0.46	0.30	534	45	45	28	47	47	32	15	15	6.5	6.65
50	5	0.65	0.7	0.75	591	15	940	31	46	46	35	12.5	23	7.2	9.5
50	20	0.26	0.58	0.23	591	15	30	31	46	46	35	18	18	7.2	7.7
80	30	0.79	0.58	0.6	591	15	60	31	52	52	35	16	16	7.2	8.05

* Combustor Configuration "D"

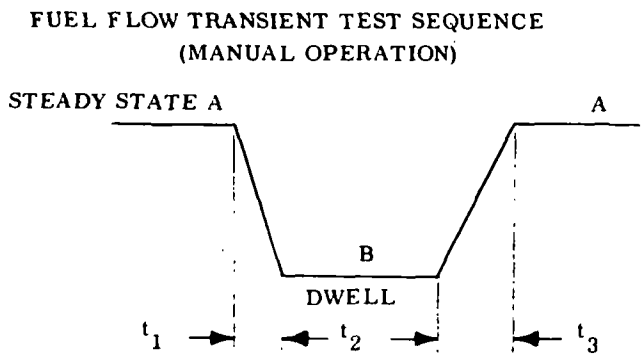

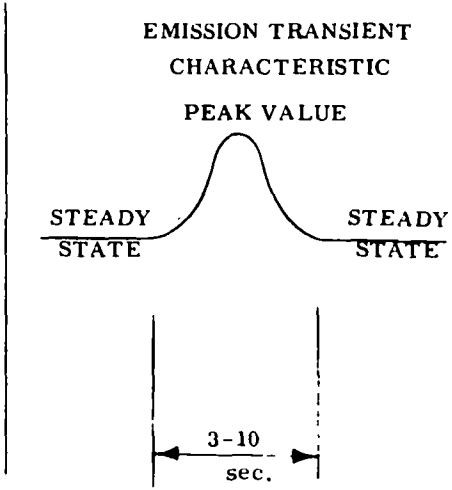

Transient time periods between lever positions is tabulated in the next columns. A comparison between the steady state and peak value of emissions is used to determine the transient performance characteristic of the system. From the results it can be seen that only CO has a characteristic transient peak significantly higher than the steady state emission levels. In two transient tests the HC also exhibited a significant peaking tendency.

NO emission levels showed essentially no deviations from steady state levels during these transient tests. Combustion configuration "D" (see Section 7) was used for transient tests and thus the steady state NO levels were higher than the design goals. However, the basic measured response characteristic of the NO to power level transients is not expected to vary significantly with the lower NO configuration "A". The configuration differences were that "D" had 25 percent more air in the primary zone than "A". "D" also had less heat loss from the flame due to the use of radiation shielding. An analysis of the HC and CO peaks against the design goal limits indicated that only in one test was the limit exceeded. A detailed analysis of this test (50 to 5 pounds per hour) was made by comparing the results strip chart records of the time dependent parameters. Figure 33 compares the high peak emission results with a typical low peak emission tests. In the top graph a high CO peak is recorded well above the limit (indicated by an arrowhead on the scale). A peak in the HC level is relatively high but well within the limit. For comparison a typical response characteristic (Fig. 33B) indicates virtually no HC peak and a CO peak well below its limit. A detail analysis of the lever position versus time (dotted lines) indicates that one major difference between the two tests is rate of change of power. From this data, and other similar traces it appears that the emission peaks on CO and HC increase significantly as the rate of change in lever position (fuel flow) increases. It also appears that the sensitivity to rate change is only during power decrease transients below 30 pounds per hour fuel flow. It appears transient at rates several times the goal of 50 percent per second can be achieved without significant emission peaking at all conditions except decreasing from 30 pounds per hour. The rate of decrease that appears to have caused the high CO peaking was 140 percent per second.

Although well below limits even a rate of 68 percent per second causes significant peaking in CO. It should be noted the HC emissions have virtually no peaks at the same 68 percent per second rate.

In summary, it can be stated that the system has good transient emission characteristics and can meet the emission levels at the transient rates established as goals for interfacing with the vapor generator. However, since some vapor generators may require very high combustor system response (depending upon margin of safety between fluid operating and decomposition temperatures) additional consideration should be given to improvement of the air-fuel ratio control during transients at the low power levels.

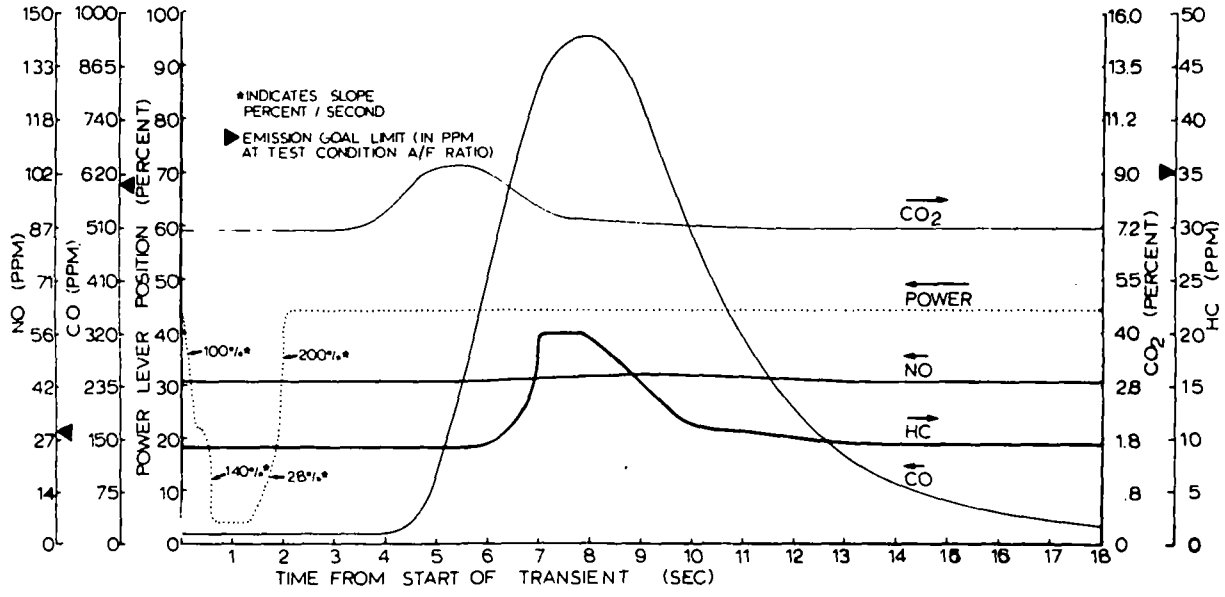

A. HIGH CO AND HC PEAK RESPONSE (POWER LEVER RATE APPROXIMATELY 150%/SEC)

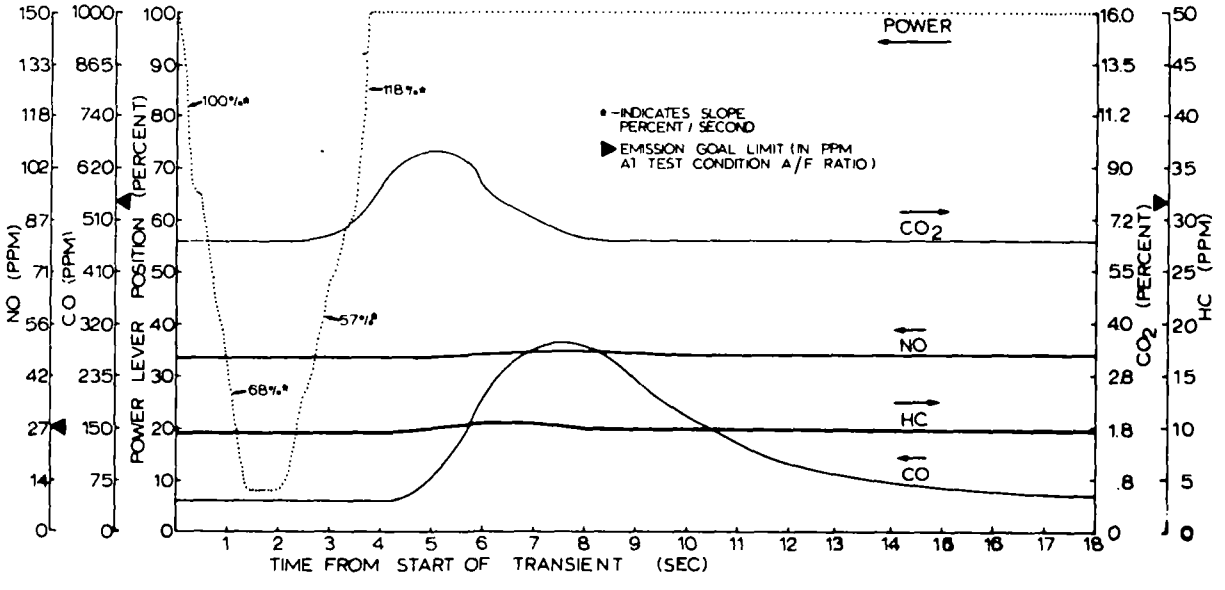

B. TYPICAL CHARACTERISTICS (POWER LEVER RATE APPROXIMATELY 50%/SEC)

FIGURE 33. POWER LEVEL TRANSIENT EMISSIONS (COMBUSTOR CONFIGURATION "D", SEE FIGURE 81)

7

COMBUSTOR DISCUSSION

7.1 REACTION KINETIC STUDY BY COMPUTER MODELLING

7.1.1 Summary

The computer model showed that, given adequate combustion volume, CO and NO emissions can be kept at a low level at high fuel rates. At low fuel flows NO emissions would be unacceptable but could be reduced by introducing heat losses to the vaporizer from the flame.

7.1.2 Emissions Analysis

This section describes the methods used to calculate the emissions from the combustor.

The method used are incorporated into three computer programs:

1. Steady-State Combustion Program (SCP)
2. Chemical Equilibrium Program (ODE)
3. Generalized Kinetics Program (GKP) - Dynamic Science Report No. TR-C70-227-I.

The first calculates the liquid phase heat release profile in terms of the vaporization rate of the liquid droplets. Liquid properties and injection parameters are required input, and the output consists of the vaporization rate of the liquid spray in the combustion field.

The Chemical Equilibrium Program (ODE) is used to calculate initial equilibrium concentrations in species in the primary zone to initiate the kinetics calculations.

The Generalized Kinetics Program is used for calculation of emissions, and solves the one-dimensional nonequilibrium reacting gas flow equations for a pressure or area defined streamtube for any input defined gaseous chemical reactions. Reaction rates are input as an Arrhenius reaction expression and all competing reaction for a

particular species are included. The ability of the program to consider arbitrary mass, momentum, and energy addition, coupled with the steady state combustion program, gives GKP the added capability of handling two phase flow problems (liquid droplet combustion).

The chemical species and the kinetic reaction system are defined by the input of the symbolic species names (N, NO, NO_2, O, etc.) and the reaction set in symbolic form (NO + M = N + O + M), where M is an arbitrary third body (all other species). Program output consists of the fluid dynamic variables (residence time, velocity, temperature, area ratio, and density) and species concentrations as a function of normalized distance. Plotting capability is available for fluid dynamic properties, chemical species concentration, total derivative with respect to distance, partial derivatives of these total derivatives with respect to any other variable and the net production rate of any reaction.

The fluid dynamic and chemical relaxation equations are integrated numerically using an implicit procedure developed by Dynamic Science personnel. The advantage of the implicit technique is that it allows chemical systems near equilibrium to be analyzed in a practical manner. This is important in emission analysis as the thermodynamic properties of the reacting mixture are controlled by the near equilibrium concentrations of the major species.

The program was developed for the kinetic analysis of rocket engines, and was selected by the Interagency Chemical Rocket Propulsion Group as the reference program for the Aerospace industry. It has been modified to analyze generalized chemical flow problems rather than the more limited rocket nozzle analysis.

The flow chart in Figure 34 gives a brief description of the input and output of GKP.

7.1.3 Initial Calculation

The initial effort involved setting up the Steady-State Spray Combustion Program to provide the liquid heat release rate profile. Figure 35 shows the resulting calculation of the evaporation rate for Jet A fuel injected into a 200 feet per second air stream at low velocity (5 feet per second velocity component along the air stream). Initial mass median drop size was estimated as 50 micron and a relatively low standard deviation of the spray (nearly uniform size distribution) was used as these are the characteristics of the rotating cup atomizer being employed. (200 Feet per second being the air stream velocity that will occur at full heat release in the preliminary combustor design.)

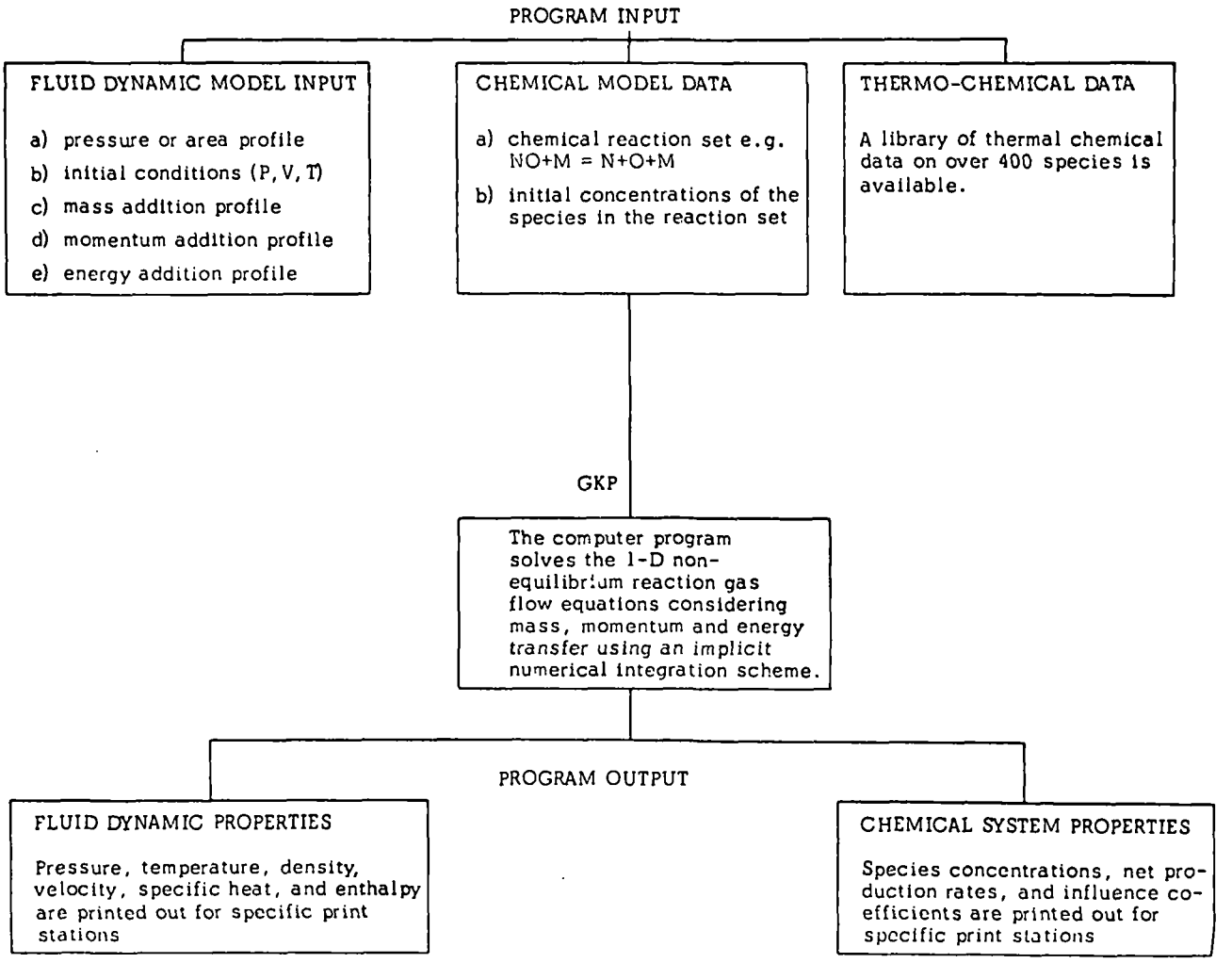

FIGURE 34. FLOWCHART, GENERALIZED KINETICS PROGRAM

From Figure 35, it is seen that vaporization is nearly completed two inches from the injection point. Also shown are vaporization histories for three of the typical drop groups comprising the spray. This short lifetime of the liquid at the full heat release condition of the combustor provides the logical basis to initiate the emission calculations based on gas-gas equilibrium. Droplet lifetimes at lower heat release rates are shown in Figure 36.

To provide a comparison base between the non-equilibrium emission estimates calculated using the kinetics program and those expected at chemical equilibrium, a matrix of air-fuel ratios was run. Figure 37 shows the calculated flame temperatures and Figure 38 shows equilibrium concentrations of carbon monoxide and nitric oxide (defined as CO and NO, respectively). A second series of runs on the equilibrium program was run with NO suppressed (program did not consider NO species) to provide start conditions for the non-equilibrium kinetics calculations. Kinetics runs were

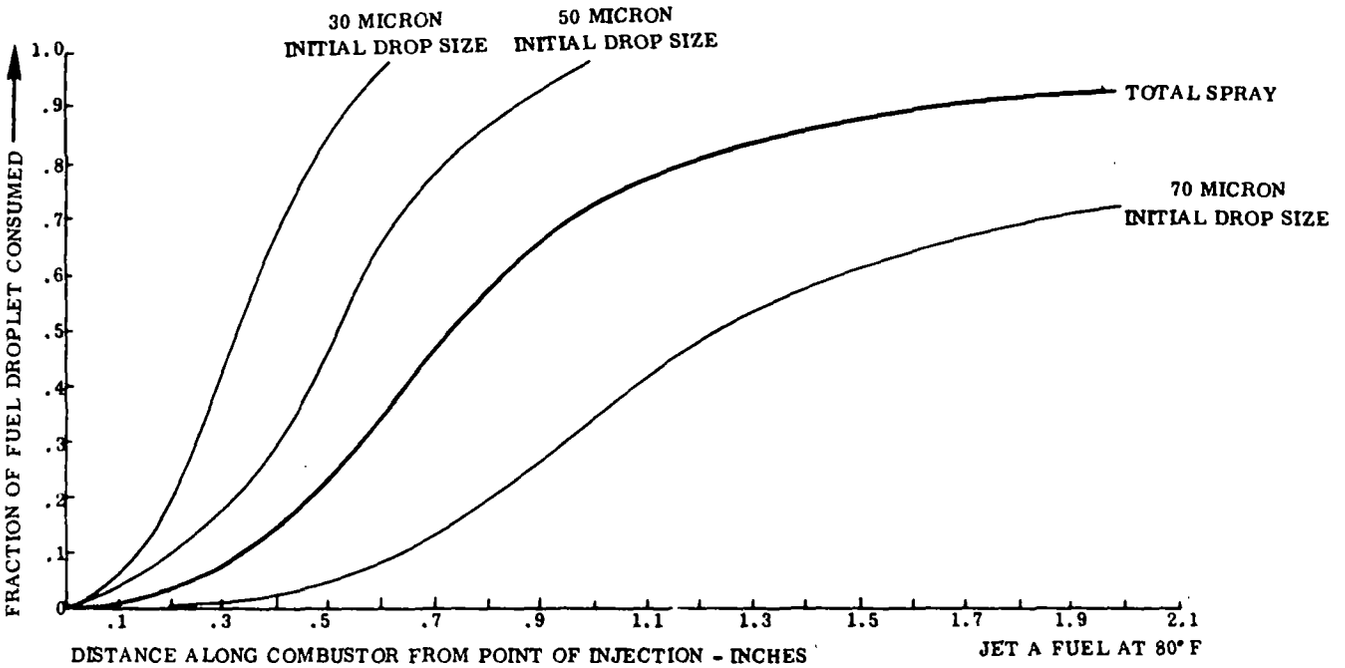

FIGURE 35. FUEL DROPLET LIFETIME AT MAXIMUM HEAT RELEASE RATE (2×10^6 BTU/HR)

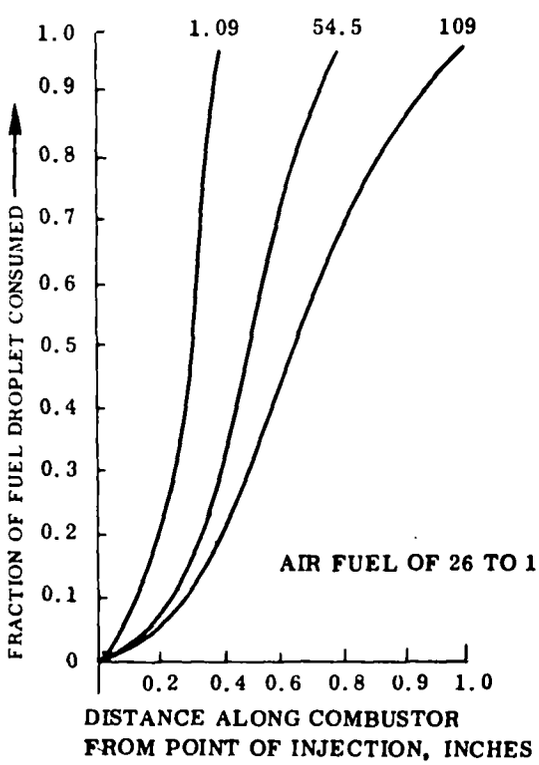

FIGURE 36. FUEL DROPLET LIFETIME, 50 MICRON DROP SIZE, AT 109, 45.5, AND 1.09 LB/HR OF FUEL

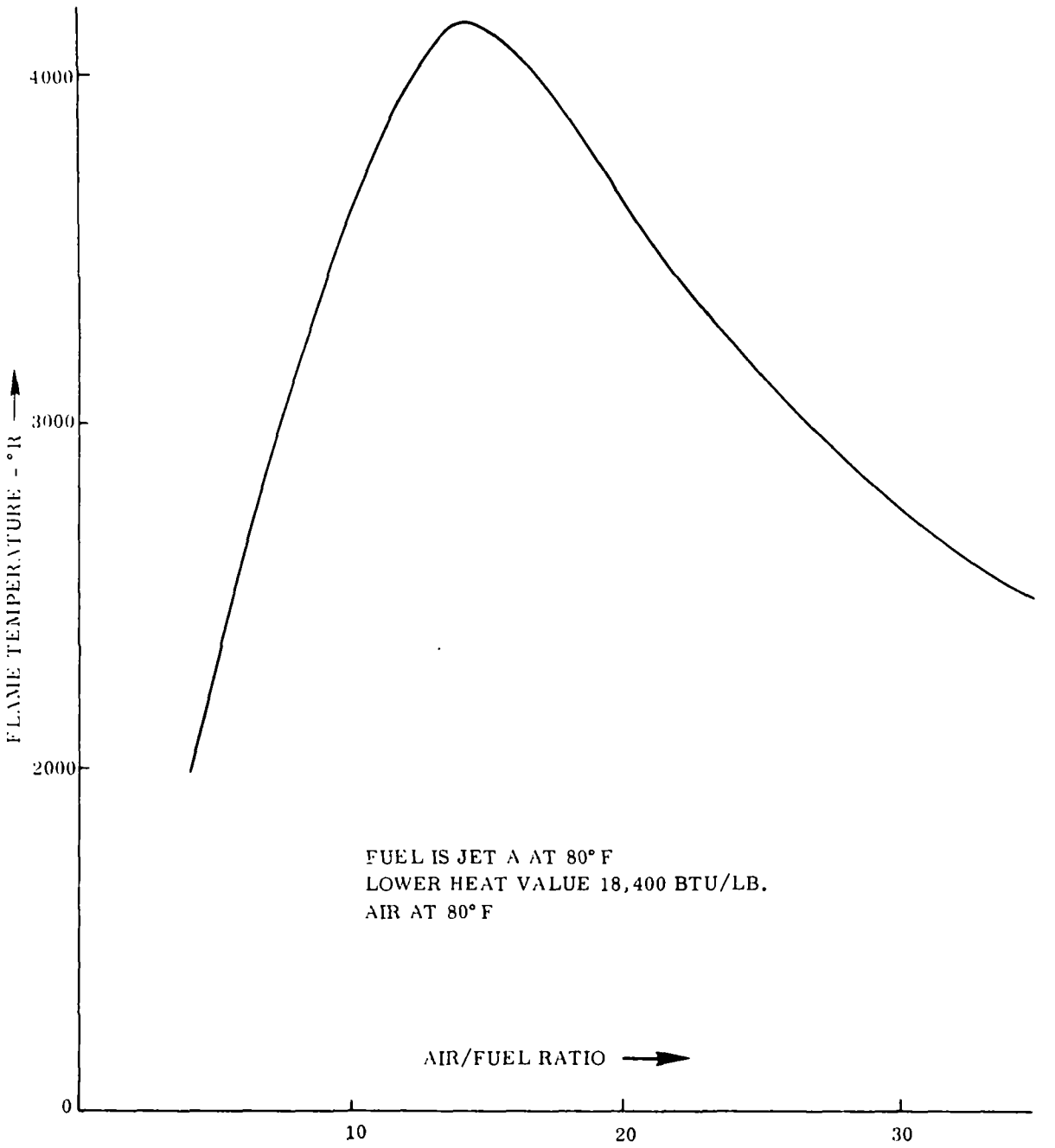

FIGURE 37. EQUILIBRIUM FLAME TEMPERATURE AS A FUNCTION OF AIR/FUEL RATIO

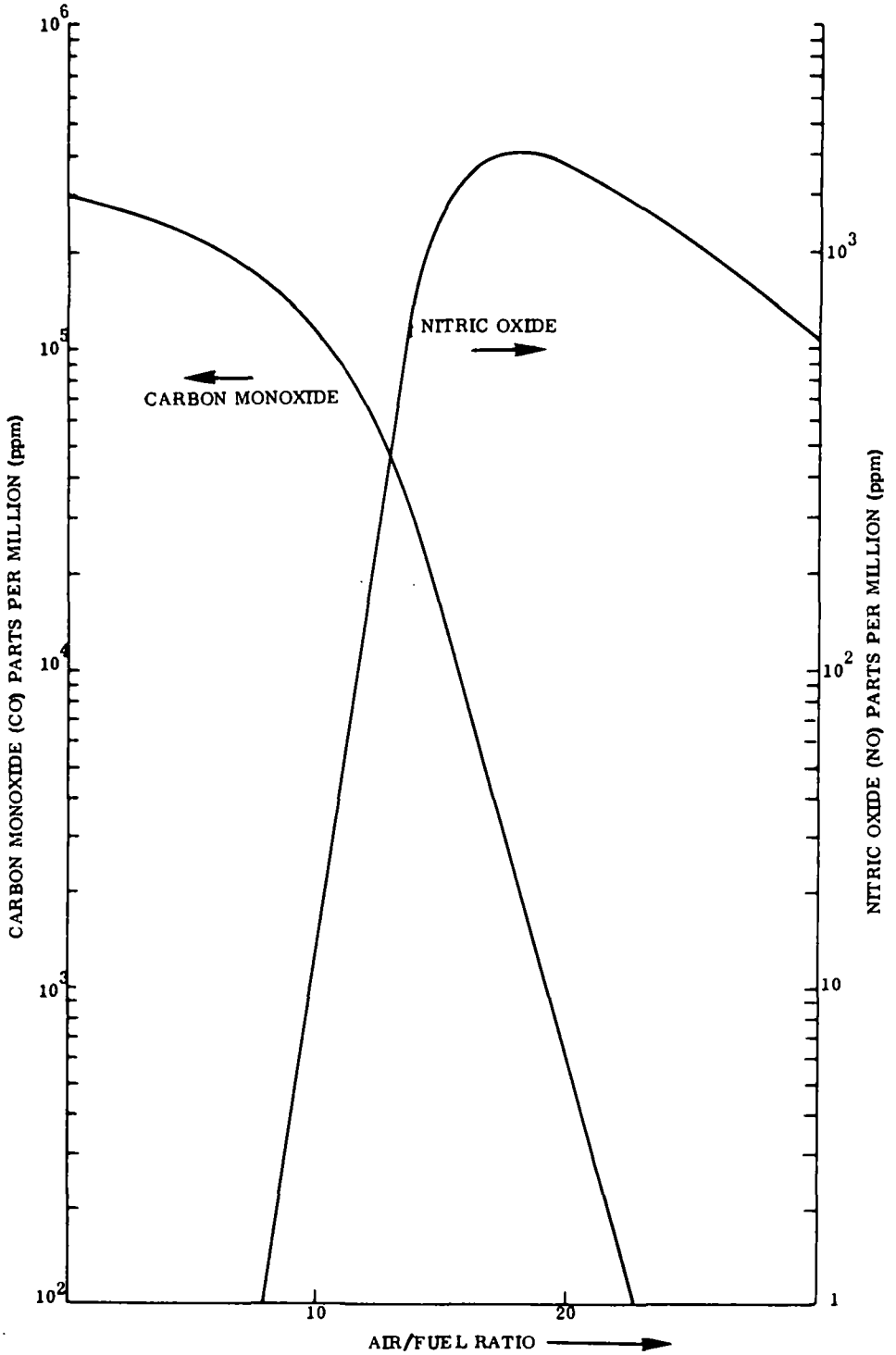

FIGURE 38. EQUILIBRIUM CONCENTRATIONS BY VOLUME OF CARBON MONOXIDE AND NITRIC OXIDE AS A FUNCTION OF AIR/ FUEL RATIO

A/F = 4.0	Mole Fraction	A/F = 6.5	Mole Fraction	A/F = 9.2	Mole Fraction
N2	.463957	N2	.538731	N2	0.621527
O2	1.18E-24	O2	2.46E-13	O2	5.45E-8
H2O	.000124	H2O	.052206	H2O	.114005
H2	.227118	H2	.165783	H2	.079833
OH	4.78E-14	OH	5.57E-8	OH	0.000034
O	4.12E-21	O	1.84E-12	O	8.7E-8
H	1.78E-8	H	.000007	H	.000274
ARGON	.005950	ARGON	.006907	ARGON	.007968
NO	0.	NO	0.	NO	0.
N	8.24E-20	N	3.92E-14	N	2.39E-10
NO2	0.0	NO2	6.51E-18	NO2	2.8E-12
CO2	.000128	CO2	0.021520	CO2	.044272
CO	.249527	CO	.194841	CO	.132084
C	0.	C	0.	C	0.
N2O	0.0	N2O	5.18E-14	N2O	1.35E-10
NH3	.000021	NH3	.000004	NH3	4.1E-7
CH4	0.052821				

FIGURE 39. PRIMARY EQUILIBRIUM COMPOSITION

initiated with zero initial NO as the time to vaporize liquid was calculated as small compared with NO formation time. Also, the primary flame zone is fuel-rich and little NO is formed even at equilibrium (infinite dwell time) for a fuel-rich system. Figure 39 shows the equilibrium start conditions used for primary zones at air-fuel of 4.0, 6.5, and 9.2. The equilibrium results are for a kerosene type fuel ($C_{10}H_{22}$ molecular weight used) with heating value of 18,400 BTU/lb and thus are not general results. Other fuels must be examined on an individual basis.

The third area of initial calculations involved gathering input data for the kinetics program. The program starts a kinetic chemistry calculation at a prescribed input chemistry (calculated from equilibrium) representative of the primary zone. Mass, momentum, and energy are then inputs to the primary zone at prescribed rates based on mixing processes occurring within the combustor. The basic input then con-

sists of tables of these quantities as a function of distance through the combustor. At constant pressure the gas dynamic relations within the program then calculate the residence time (velocity) as a function of these quantities, i.e., residence time is not a constant throughout the combustor. Addition rate tables used for analysis of the combustor configurations will be presented in the following section.

The kinetic reaction mechanism used for emission estimates is shown in Figure 40. The low molecular weight hydrocarbon reactions were necessitated by the addition of the methane species at an air-fuel of 4 (see Fig. 39).

7.1.4 Combustor Design by Computer Modelling

The preliminary combustor design used is based on typical criteria used in the design of gas turbine combustors modified to limit the peak temperatures in the flame (Fig. 41). This has been shown by the reaction studies to reduce the formation of nitric oxide. The control of flame temperature is achieved by control of the amount, position, mode and speed of air injection into the combustor.

The combustor is divided into three zones as follows:

1. A primary flame zone consisting of about one-third of the combustor volume and lying immediately downstream of the point of fuel injection. This is where ignition and combustion commences.

2. A secondary flame zone consisting of about one-third of the combustor volume and lying immediately downstream of the primary flame zone. In this region, most of the combustion reactions approach completion.

3. A tertiary flame zone consisting of the remaining combustor volume and lying immediately downstream of the secondary flame zone. In this region, air is added and mixed with the combustion products to bring them to a safe level of temperature for use in the engine boiler.

   Air is injected into these three regions either as high velocity jets or as low velocity films flowing along the combustor walls. The later films serve in the office of a control on wall temperature by minimizing the amount of hot combustion productions that can impinge on the walls of the combustor.

To calculate emissions, a knowledge of the method of air injection and mixing in the combustor is required. Two different methods of air injection were devised and designated as designs A and B (ref. Fig. 41 and 45, respectively). Small modifications in the methods of air injection were done with both designs and the resultant emissions estimated.

```
REACTIONS
 N2    = N + N ,          A=1.0E18,  N=1.0,  B=0.0,    ODK PAGE 7-6
 O2    = O + O ,          A=1.9E16,  N=0.5,  B=0.0,    ODK PAGE 7-6
 H2    = H + H ,          A=7.5E18,  N=1.0,  B=0.0,    ODK PAGE 7-6
 OH = H + O,           A=3.6E+18,  N=1.0,  B= 0.,                          14
 H2O   = H + OH,          A=1.17E17, N=0.0,  B=0.0,    LEEDS 2  NOV 68, P-31
 NO2   = O + NO,          A=1.6E15,  N=0.0,  B=-1.79,  TR-A69-103 P-17, JAN 69
 N2O   = O + N2,          A= 1.0E18, N=1.0, B=0.0,
 CO2 = CO + O,       A= 5.1E+15, N=0.,  B=3.58,                          16
 CO = C + O ,  A=3.0E16, N=0.5, B=0.0.                    ODK- P-7-6
 CH4 = CH3 + H ,    A= 3.0E16,  N= 0.5,  B=0.0,           1D-2P PROG, P 7-49
 CH3 = CH2 + H ,    A= 3.0E16,  N= 0.5,  B=0.0,           1D-2P PROG, P 7-49
 CH2 = CH  + H ,    A= 3.0E16,  N= 0.5,  B=0.0,           1D-2P PROG, P 7-49
 CH  = C   + H ,    A= 3.0E16,  N= 0.5,  B=0.0,           1D-2P PROG, P 7-49
END TBR REAX
```

```
 CO2 + H  = CO + OH  ,  A= 5.6E11, N=0.0,  B=1.080,  LEEDS 1  MAY 68, P-4
 CO  +  CO  =  CO2  +  C      ,  A=2.11E16,  N= 1.0,   B=0.0, 1D-2P PROG 7-50, 33
 H2  +  O2  =  OH   + OH      ,  A=2.70E16,  N= 1.0,   B=53., 1D-2P PROG 7-51, 43
 OH + H   = H2 + O   ,  A= 1.74E13,N=0.0,  B= 9.45,  LEEDS 2  NOV 68, P-1
 H2O + H  = OH + H2  ,  A= 2.19E13,N=0.0,  B= 5.15,  LEEDS 2  NOV 68, P-9
 OH +  O  = H + O2   ,  A= 2.0E14, N=0.0,  B=17.0,   TR-A69-103 P-21, JAN 69
 H2O + O  = OH + OH  ,  A= 5.75E12,N=0.0,  B=0.78,   LEEDS 2  NOV 68, P-20
 NO + O = O2 + N    ,     A=1.8E8,  N=-1.5,B=5.94,   TR-A69-103  P-18, JAN 69
 N2 + O = NO + N    ,     A=1.3E13, N=0.0, B=0.0,    TR-A69-103  P-18, JAN 69
 NO + O2= NO2+ O    ,     A=1.8E13, N=0.0, B=1.05,   TR-A69-103  P-18, JAN 69
 N2 + O2 = N2O + O ,   A= 3.0E+13,  N= 0.0, B= 26.8,                28  50
 CO + O2 = CO2 + O,  A=1.9E+13, N=0., B=54.15,                          163
 CO + H =  C + OH,   A=1.2E+14,  N=0., B= 25.83,                        103
 CO + N =  C + NO,   A=1.2E+16,  N=1.0, B=0.,                           108
 CO + O = C + O2,    A= 2.4E+13, N=0., B=1.987,                         107
 CO + H2 = CH +OH ,    A= 3.E+13, N=0., B=0.,                           42
 CO + H = CH +O ,      A= 3.E+13, N=0., B=0.,                           43
 C    +  H2   =  CH    + H       ,  A=5.30E11,   N= .5,   B=2.24,1D-2P PROG 7-51, 49
 C    +  H2O  =  CH    + OH      ,  A=1.05E11,   N= .5,   B=2.24,1D-2P PROG 7-51, 50
 C    +  OH   =  CH    + O       ,  A=5.3E11,    N= .5,   B=2.24,1D-2P PROG 7-51, 54
 CO   +  OH   =  CH    + O2      ,  A=1.75E10,   N= .5,   B=28.2,1D-2P PROG 7-51, 59
 CH3 + H2 = CH4 + H, A= 1.5E+14, N=0., B=14,                            174
 C    +  CH3  =  CH    + CH2     ,  A=1.05E11,   N= .5,   B=2.24,1D-2P PROG 7-52, 63
 C    +  CH2  =  CH    + CH      ,  A=1.05E11,   N= .5,   B=2.24,1D-2P PROG 7-52, 64
 CH4  +  C    =  CH3   + CH      ,  A=1.05E11,   N= .5,   B=2.24,1D-2P PROG 7-52, 66
 CH3  +  CH   =  CH2   + CH2     ,  A=1.05E11,   N= .5,   B=2.74,1D-2P PROG 7-52, 69
 CH4  +  CH   =  CH3   + CH2     ,  A=1.05E11,   N= .5,   B=2.74,1D-2P PROG 7-52, 70
 CH3  +  CH3  =  CH2   + CH4     ,  A=1.05E11,   N= .5,   B=2.82,1D-2P PROG 7-52, 71
 H2   +  CH   =  CH2   + H       ,  A=1.05E11,   N= .5,   B=2.74,1D-2P PROG 7-52, 80
 H    +  CH3  =  CH2   + H2      ,  A=1.05E11,   N= .5,   B=2.88,1D-2P PROG 7-52, 81
 H2O  +  CH   =  CH2   + OH      ,  A=1.05E11,   N= .5,   B=2.74,1D-2P PROG 7-53, 86
 H2O  +  CH2  =  CH3   + OH      ,  A=1.05E11,   N= .5,   B=3.19,1D-2P PROG 7-53, 88
 OH   +  CH   =  CH2   + O       ,  A=1.05E11,   N= .5,   B=2.74,1D-2P PROG 7-53,100
 O    +  CH3  =  CH2   + OH      ,  A=1.05E11,   N= .5,   B=2.83,1D-2P PROG 7-53,101
 OH + CH3 = CH4 + O, A= 1.E+13, N=0., B= 7.3,                           172
 CH3 + H2O = CH4 + OH, A= 5.E+14, N=0., B=9.9,                          176
LAST CARD
```

FIGURE 40. REACTION SET

Design A, Configuration No. 1 (Fig. 41b)

Twenty-five percent of the total air required for combustion is injected over the rotating cup and mixes instantaneously with the fuel ejected from the lip of the cup. Another twenty-five percent of the total air is injected as film cooling along the combustor wall. The remaining air is injected at the juncture of the primary and secondary flame zones. The assumed rates of mixing of the various quantities of air is shown in Figure 41a, the resultant air-fuel ratios, gas temperatures and emissions are shown in Figures 41d, e and f, respectively, for the maximum heat release rate of 2×10^6 BTU/hr and an exhaust temperature of 2500° F.

The results show carbon monoxide on the high side but low values of nitric oxide.

Design A, Configuration No. 2 (Fig. 42b)

Identical arrangment of air admission as in Configuration No. 1, but with modifications to the method of the air injection at the juncture of the primary and secondary flame zones so that half this air recirculates into the primary zone rather than, as before, into the secondary zone.

The rates of mixing of the air, resultant air-fuel ratios, gas temperatures and emissions are shown in Figures 42 c, d, e and f, respectively.

The results again show carbon monoxide on the high side and also a considerable increase in nitric oxide. The large increase in nitric oxide is caused by the higher primary zone flame temperature which results from the recirculation into it of additional air.

Therefore, for minimum nitric oxide, the recirculation of air must be minimized and the primary flame zone maintained with minimum air. Some increase in secondary flame zone volume must be provided to minimize carbon monoxide.

Design A, Configuration No. 3 (Fig. 43b)

The large quantity of wall cooling used in Configurations 1 and 2, while providing low wall temperatures and hence long combustor life, will tend to reduce effective combustor volume due to quenching of the flame reaction at the cool wall. The quantity of film cooling was therefore drastically reduced as it appears that combustor volume was low.

The results show that emissions are very similar to, but slightly higher than, the results obtained with Configuration No. 1, and have low nitric oxide with high carbon monoxide.

Design A, Configuration No. 4 (Fig. 44b)

Identical arrangement as in Configuration No. 3, but with modifications to the method of air injection at the juncture of the primary and secondary flame zones so that half this air recirculates into the primary zone rather than into the secondary zone, as was in Configuration No. 3.

Again, as with Configuration No. 2, a large increase in nitrix oxide but small change in carbon monoxide is achieved.

The analysis gives results which would not, in practice, be expected; i.e., the increased wall temperatures would provide a larger effective volume in Configurations 3 and 4 and reduce carbon monoxide. Therefore, testing of these configurations is needed for better understanding of the processes at work.

Design B, Configuration No. 1 (Fig. 45b)

Modifications were made to the design of the combustor as in Figure 45b, and air admissions as in Figure 45c used. The essential difference between Design B and A is that a much slower rate of mixing of the air admitted at the juncture of the primary and secondary zones is used in Design B.

Calculations at full heat release were made of the flame temperature and resultant emissions of carbon monoxide and nitric oxide are as shown in Figures 45c and f.

In comparison with Design A, Configuration No. 1, a large increase in nitric oxide occurs, though within required values. Some increase in carbon monoxide also occurs.

The prime reason for the increased nitric oxide lies in the reduction of the rate of admission of the secondary air. This permits combustion to proceed at higher temperatures for a longer period of time than compared to previous configurations. Increased admission of secondary air and earlier injection of tertiary air would serve to reduce both NO and CO considerably.

Because the combustor has to operate at any heat release rate from 100 percent to 1 percent, calculations of temperature and emissions were made at heat releases of 50 percent and 1 percent also. These results are shown superimposed on the results for 100 percent heat release in Figures 45e and f.

A very large increase in NO emissions occurs as heat release is reduced; such values lying outside specification limits. The reason for this is the large increase

in time spent at high temperature when combustor heat output is reduced as likewise, more time is available for complete reaction to carbon dioxide to occur.

Design B, Configuration No. 2 (Fig. 46b)

Identical arrangement of air admission as in Configuration No. 1 but with modifications to the method of the air injection at the juncture of the primary and secondary flame zones so that 100 percent of this air recirculates into the primary zone rather than, as above, into the secondary zone.

As before, the rates of mixing of the air, resultant air-fuel ratios, gas temperatures, and emissions were computed and are shown in Figure 46c, d, e, and f, respectively, for 100 percent heat release and also for 50 percent and 1 percent of full heat release.

The results are similar to those obtained with Design B, Configuration No. 1, save that some increase in nitric oxide occurs. This is due to the increased time at high temperature caused by introduction of additional air into the primary zone by recirculation from the secondary zone. A similar result was obtained with Design A, Configuration No. 2, and for the same reason.

Heat Losses

At low levels of heat release, it is expected that substantial reductions in flame temperature could occur due to the large masses of cool metals surrounding the flame. This heat loss would depend considerably on the design and location of the boiler. Calculations were done of the effects of small heat losses on the emissions from Design B in both Configuration No. 1 and 2.

A substantial reduction in volume of nitric oxide emissions is obtained with only small heat losses, reference Figures 47 and 48 with both configurations. Effects on carbon monoxide formation are small.

As nitric oxide emissions are still excessive at low heat release rates, it is necessary for considerable reductions in flame temperature to be made.

Conclusions

Emissions of nitric oxide are, at low heat releases, considerably outside required limits and well within limits at high heat releases. Carbon monoxide is well within limits at low heat releases, and marginally in limit at high heat releases. Vaporizer (boiler) design could have a major effect on emissions as heat losses from the flame can be high.

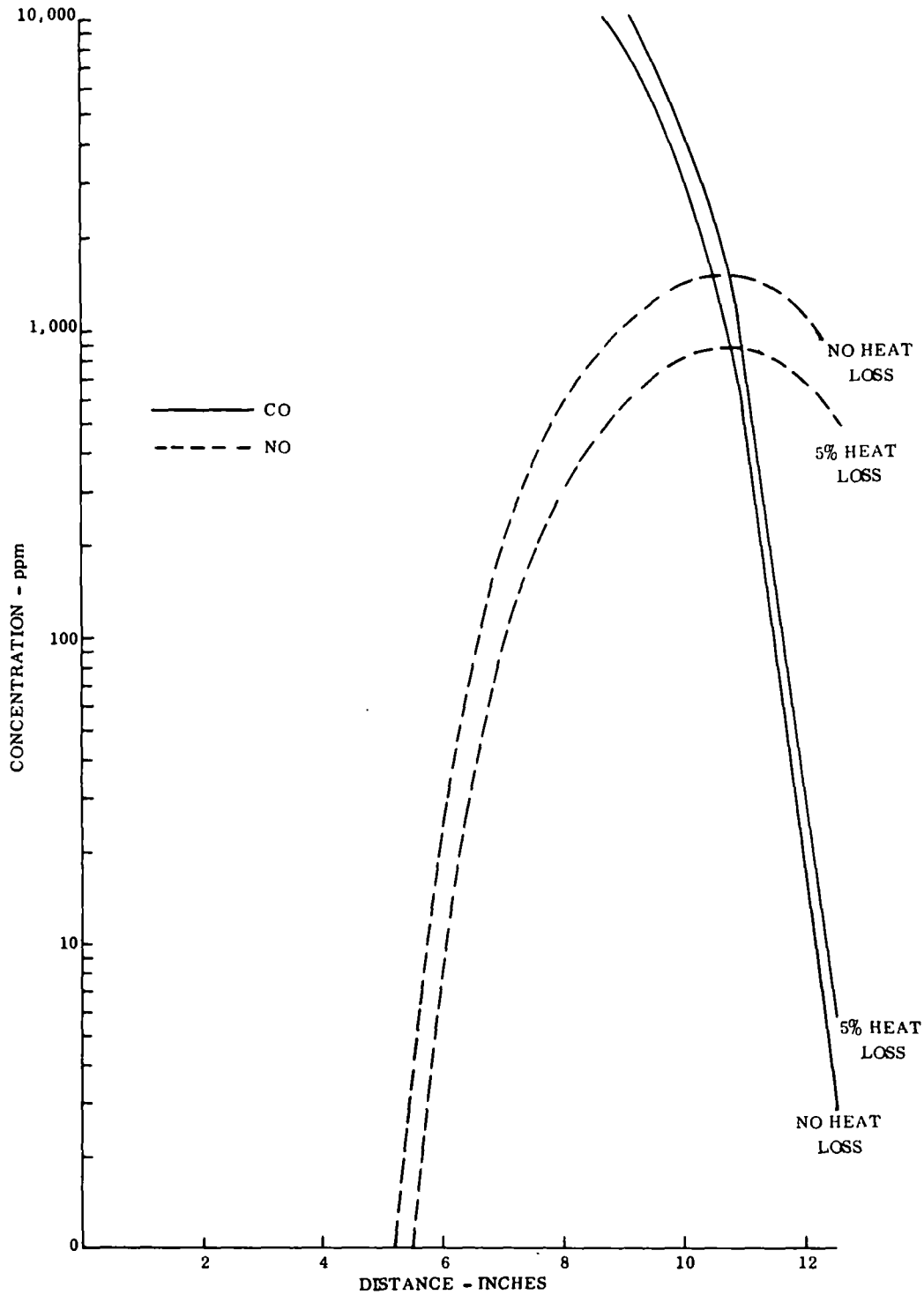

FIGURE 47. EMISSIONS AT ONE PERCENT HEAT RELEASE WITH AND WITHOUT A FIVE PERCENT HEAT LOSS FOR DESIGN A, CONFIGURATION NO. 1

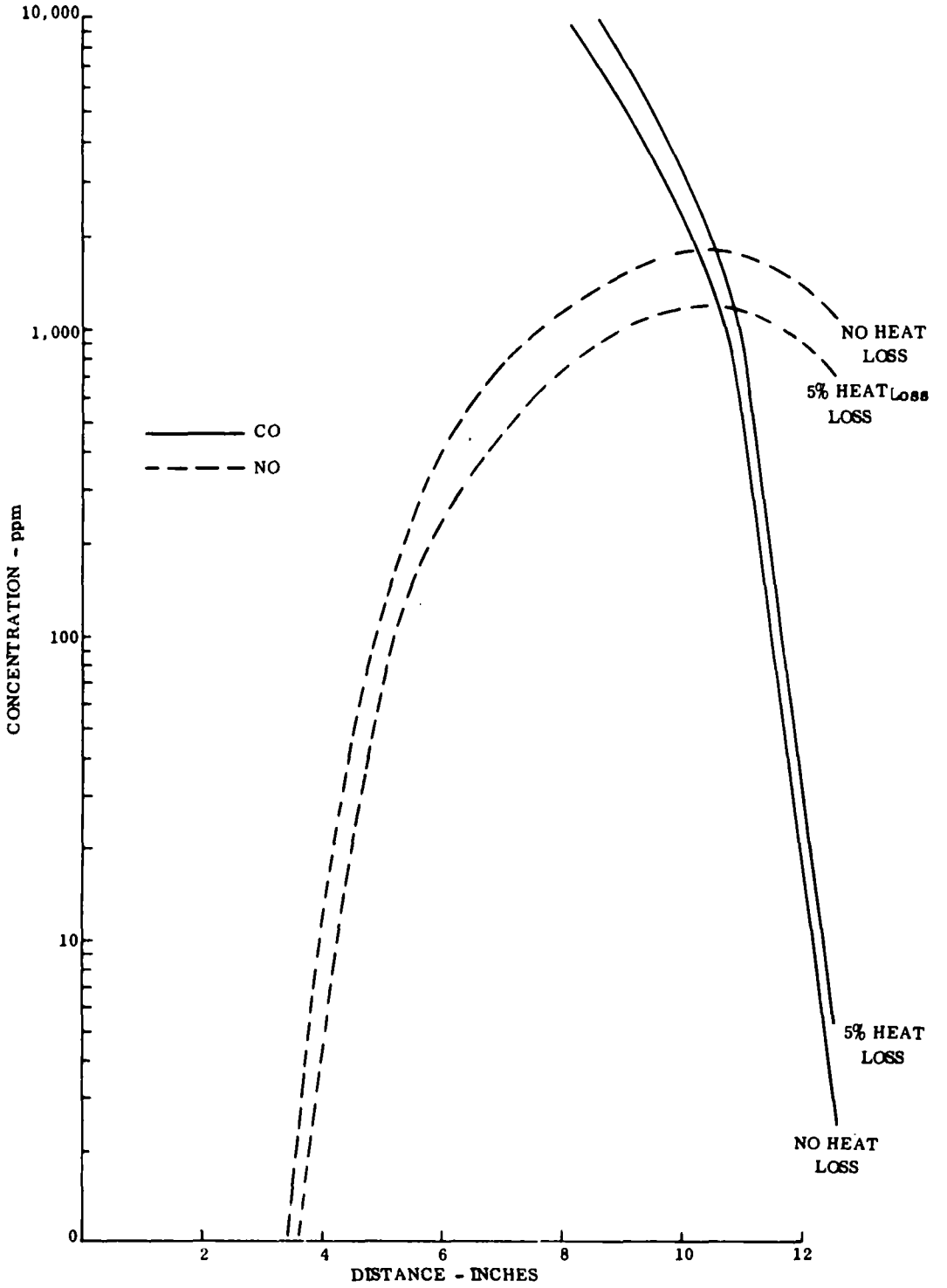

FIGURE 48. EMISSION AT ONE PERCENT HEAT RELEASE WITH AND WITHOUT A FIVE PERCENT HEAT LOSS FOR DESIGN A, CONFIGURATION NO. 2

Discussion

Results show that for minimum emission of nitric oxide, the rate of admission of air must be carefully controlled. In the primary zone, the flame must be kept rich, with minimum air; and in the secondary zone excess air must be added as rapidly as possible. If this can be done over the entire operating range of the combustor from 1 percent to 100 percent heat release, then the formation of nitric oxide can be eliminated almost completely, especially if heat losses to the vaporizer can be used to limit flame temperature. Carbon monoxide should not present a problem with such an arrangement of air admission, save perhaps at or near maximum heat release. If this is so, an increase in combustor volume may be required to hold emissions within limits. By providing sufficient volume, the carbon monoxide formation would be reduced to an extremely low level. Heat losses to the vaporizer would, however, tend to raise CO emissions.

In essence, the distriction of CO and the formation of NO is a process that is controlled by the mixing residence times and heat losses of the reaction gas within the combustor. The mixing process can be controlled by hardware configuration and it is possible, therefore, to design a combustor that will minimize both NO and CO emissions over a wide range of turndown and operating conditions.

7.2 COMBUSTOR AND TEST RIG DESIGN

7.2.1 Combustor Design

A combustor was designed and fabricated. These parts are shown in Figures 29, 49, 50, 51, 52, and 53. The distribuiion of the air admission into the combustor was set up initially per Design B, Configuration No. 1.

The heart of the system is the rotating cup fuel injector which makes the 100 to 1 turndown ratio possible. The rotating cup has the following advantages:

- Essentially no fuel pressure. This allows the use of a small low pressure fuel pump and avoids fuel contamination because there are no small fuel metering orifices.
- Degree of atomization is not dependent on fuel flow or viscosity.
- Minimum cost. The cup and its drive motor are inexpensive as is its auxiliary equipment (fuel pump and ignition).
- Is a proven design. It has been used for many years in combustors.

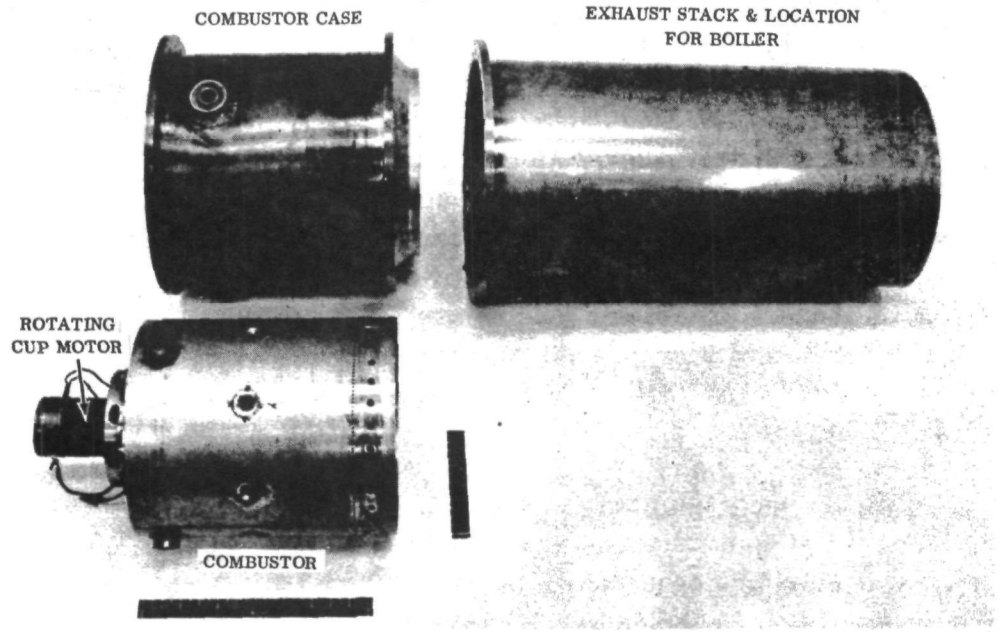

FIGURE 49. SIDE VIEW OF ROTATING CUP COMBUSTOR ASSEMBLY

- Controlled spray - the angle is predictable and hence ignition reliability is high.

- No power requirements. For test flexibility the cup is separately driven. In practice it would be mounted onto the fan motor shaft and the additional power required would be negligible.

A weight breakdown for the experimental and production versions of the combustor assembly, together with the materials used is shown below.

Current Weight Pounds		Production Version Weight Pounds
28.78	Combustor	6.0
38.00	Combustor Case	4.75
0.69	Fuel Injector Cup	0.23
3.00	Injector Drive Motor	*
4.28	Combustor Swirler and Dome Assembly	1.25
1.25	Support Pins and Ignitor	0.75
76.00	Total Weight	12.78

* Integrated with fan motor.

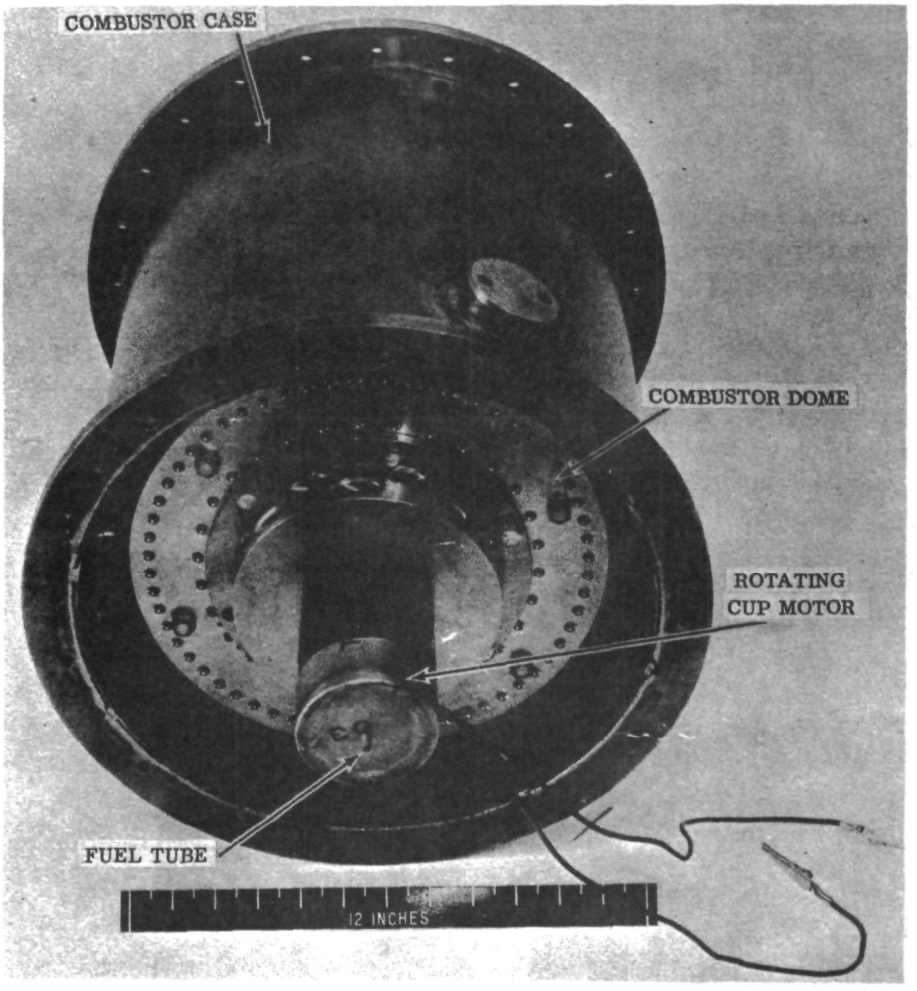

FIGURE 50. FRONT VIEW OF ROTATING CUP COMBUSTOR AND CASE

Combustor materials are:

Combustor Case and Flanges	Mild Steel (0.062 in. gauge)
Combustor Liner	Hastelloy X (0.062 in. gauge)
Combustor Swirler and Dome Assembly	321 Stainless Steel
Fuel Injector Cup	Mild Steel
Support Pins	Mild Steel

In practice, tests indicate that all materials used could be low cost mild steel or cast iron save for the liner which would be a 300 series stainless steel.

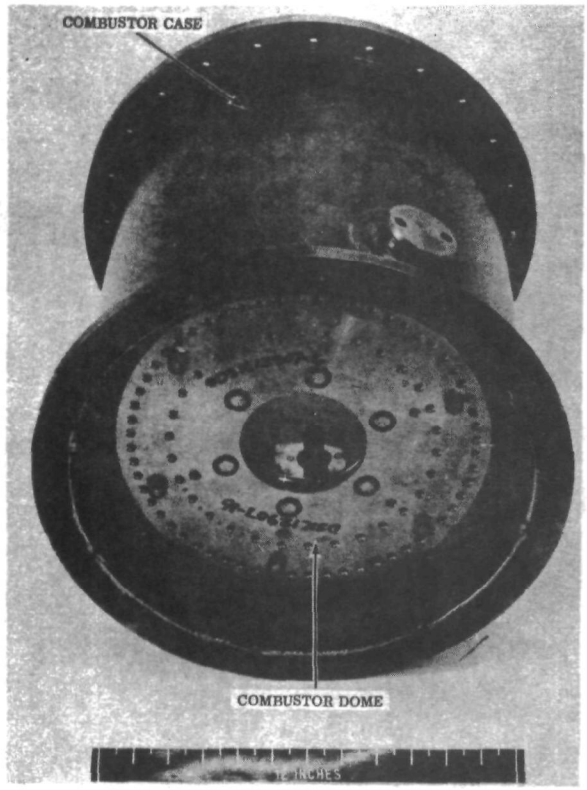

FIGURE 51.

FRONT VIEW OF ROTATING CUP COMBUSTOR AND CASE WITH ROTATING CUP REMOVED

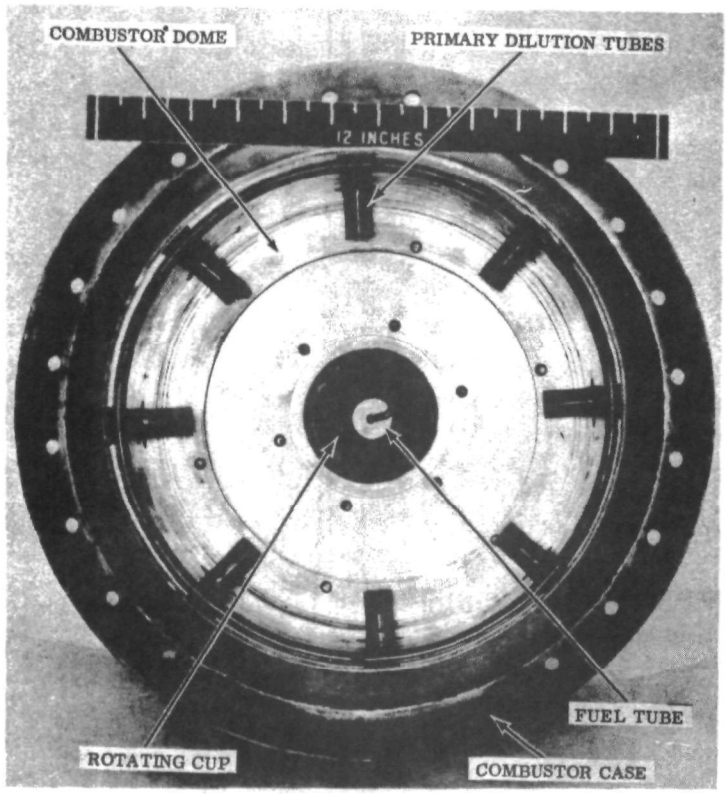

FIGURE 52.

REAR VIEW OF ROTATING CUP COMBUSTOR AND CASE

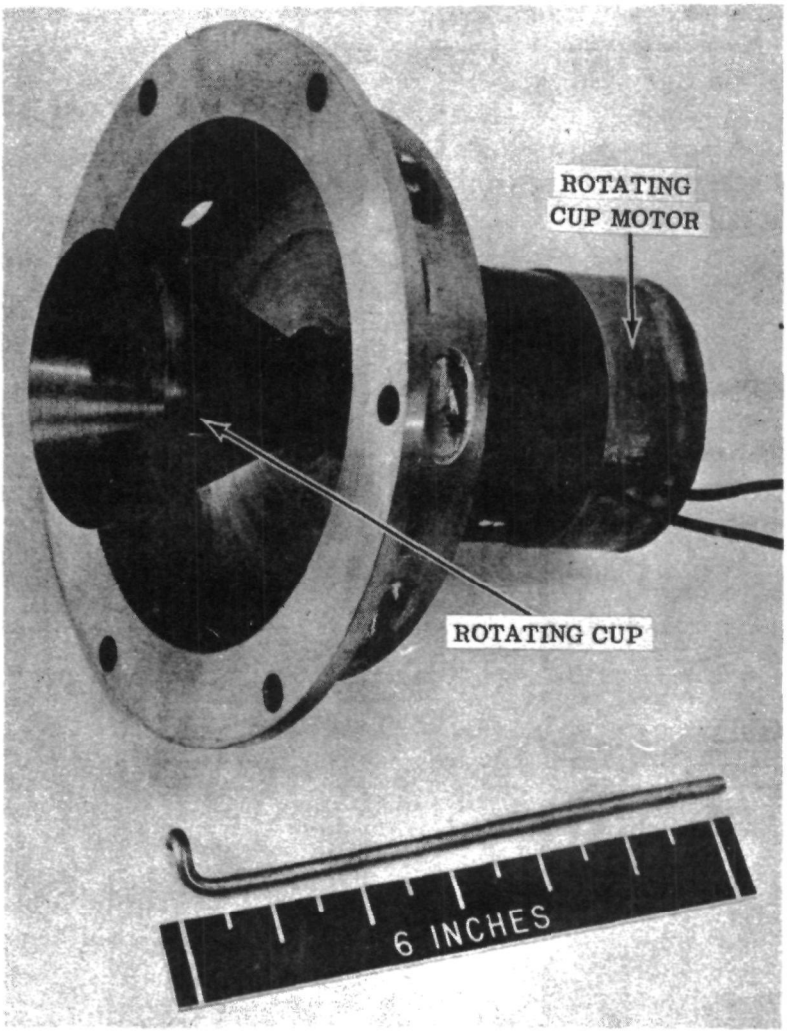

FIGURE 53. ROTATING CUP AND MOTOR ASSEMBLY

7.2.2 Combustor Test Rig Design

Air Supplies

Prior to tests with a fan and air metering valve, tests were done with a slave air supplied by a remote air compressor. The very wide range of fuel flows to be investigated required a corresponding wide range of air flows. For tests to have significance, the air flow must be measured accurately. This requires metering orifices having pressure losses far in excess of the capability of the chosen fan and therefore air to the combustor had to be provided from a higher pressure source. This air was supplied from a centrifugal compressor that supplied air, via a system of metering orifices, through a ten inch diameter pipe, directly mounted onto the combustor case, Figure 54 and 56. This air was manually controlled to any required flow by means of a throttling valve. Throughout the test, the air supply was

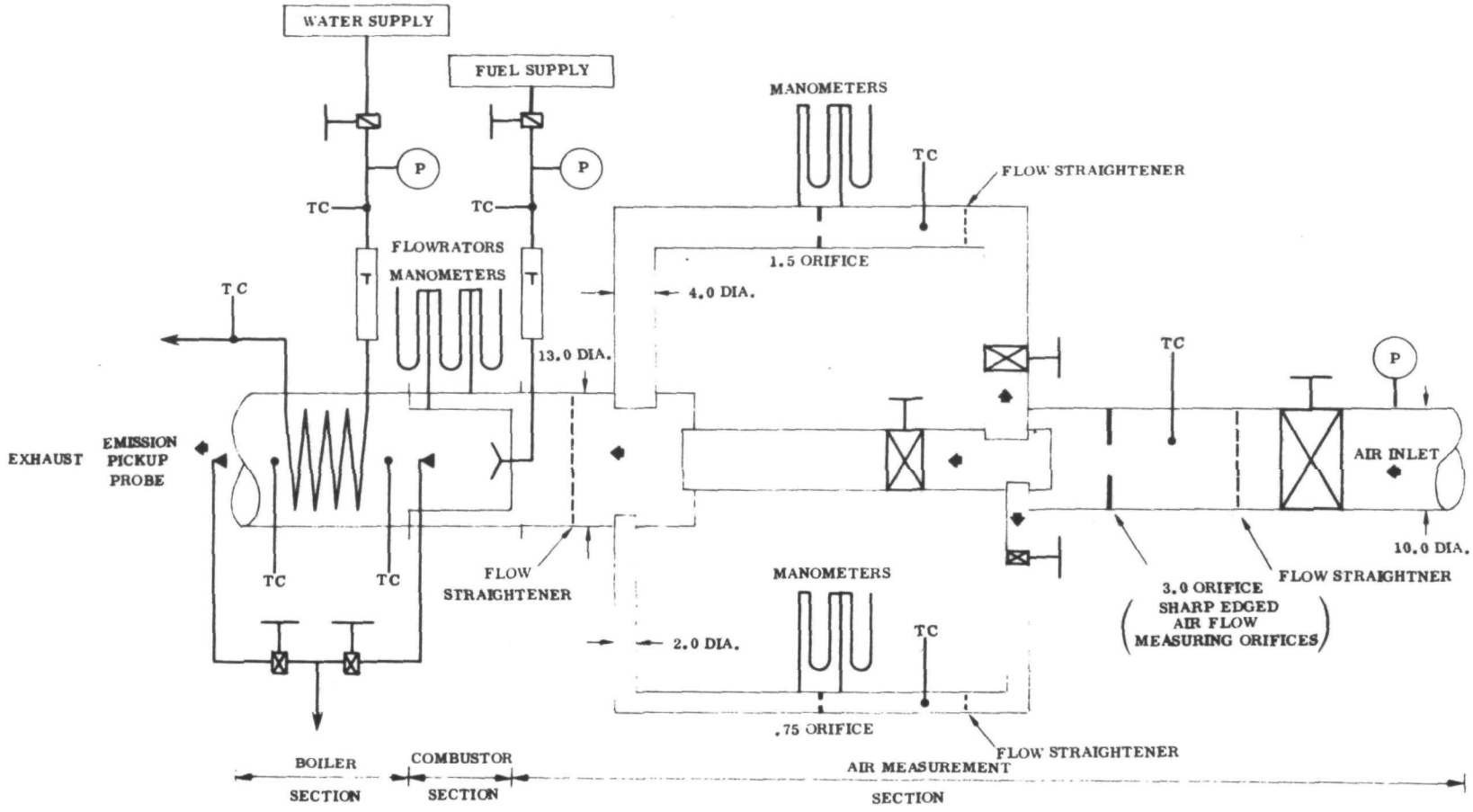

FIGURE 54. SCHEMATIC OF COMBUSTOR TEST RIG

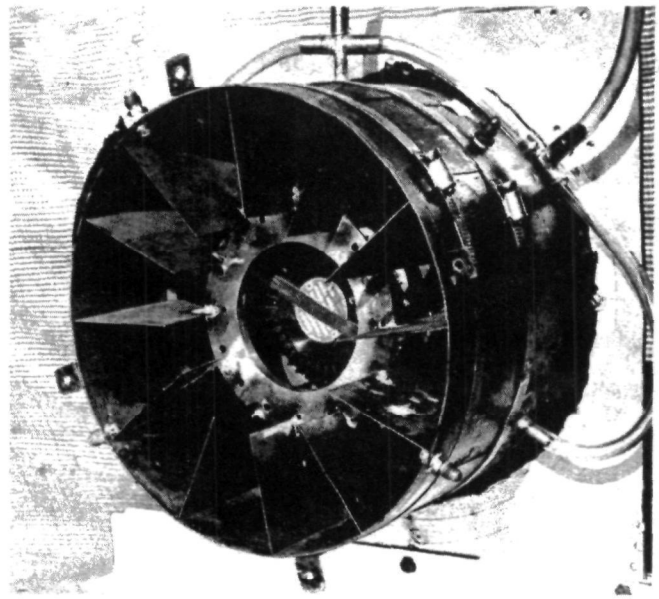

FIGURE 55. REAR VIEW OF FAN AND CONTROL VALVE ASSEMBLY SHOWING ANTI-SWIRL PLATES INSTALLED

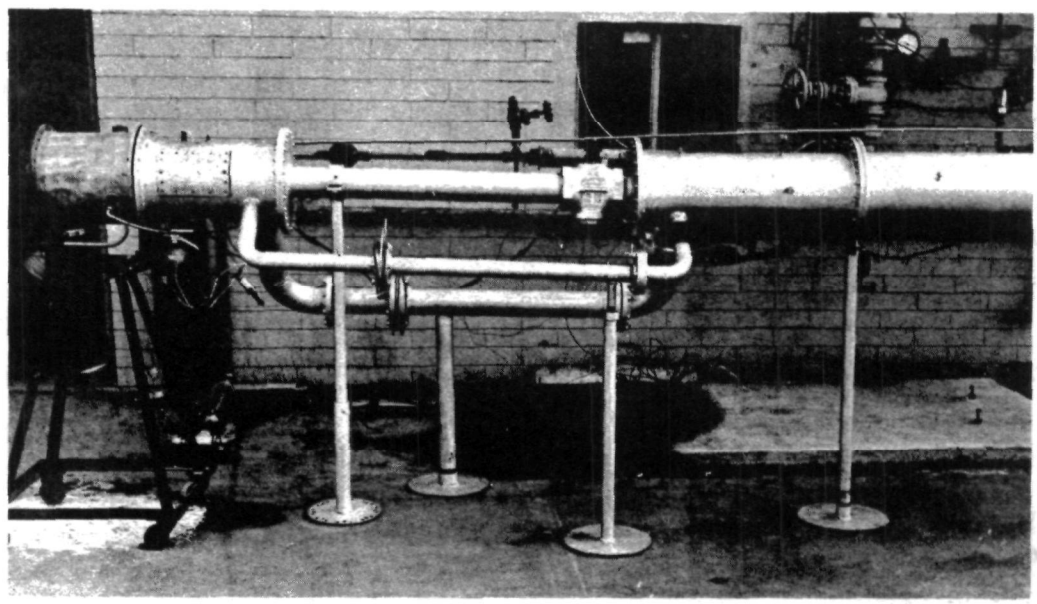

FIGURE 56. COMBUSTOR RIG SHOWING ARRANGEMENT OF AIR METERING ORIFICES

maintained at levels of flow, temperature, and pressure appropriate to the fan capabilities (2830 lb/hr, 80° F, and 12 inches water), but is capable of a much larger range, with up to 7000 pounds per hour of flow, at temperatures from -40° F to +1200° F and pressures to 250 psig.

There is an aerodynamic influence on the combustor caused by the particular method of control of the air from the fan to the combustor. Air is passed through a metering valve consisting of twelve variable area openings into the combustor at a velocity of 95.5 feet per second as dictated by the pressure drop across this area (Fig. 55). Because of the interaction of the aerodynamics of the fan and the air bypassed overboard, and because of the turning losses in the metering chamber, this air has a profile of velocity in both circumferential and radial directions, and a tangential velocity component that varies considerably over the operating range of the combustor.

At maximum fuel flow, the air exiting from the metering valve into the combustor annulus, is accelerated and passes into the combustor at a velocity of 195 feet per second. At this flow, the effects of radial and swirl velocity profiles on combustor air distribution are assumed negligible. However, at minimum fuel flow the air velocities into the combustor are small at 1.95 feet per second, and as the same 95.5 feet per second velocity is maintained at the control area, the effects of velocity profiles could be considerable. It is not possible to simulate such aerodynamic influences except by use of the fan and this, of course, destroys the object of the test rig. Therefore, final combustor development must be carried out with the fan. In order to minimize differences between fan and rig aerodynamics, the combustor was designed such as to minimize the effects of entry velocity variations. On the rig, any velocity profiles from the upstream metering section are eliminated by means of a flow straightener.

7.2.3 Instrumentation

Flow Measurements - Air

Air flow is measured by means of any of three orifice runs that are mounted in parallel upstream of the combustor (Fig. 56 and 54). Because of the wide range of air flows, three different orifices of 3/4, 1-1/2, and 3 inches diameter are used. Each orifice is sized for optimum Reynolds number at air flows corresponding to respective fuel flows midway in the ranges of 109 to 22.8, 22.8 to 4.77, and 4.77 to 1 pounds per hour. The orifices are sharp edged, with corner pressure taps, and have upstream flow straighteners to minimize aerodynamic influence on the metering section from the upstream on-off valves. These valves are manually operated so that air flow can be diverted to the metering orifice appropriate to the air flow being used. Because of the cumbersome nature of this instrumentation, it is not possible to simulate, except approximately, the transients that will in practice occur as fuel flow is varied.

Flow Measurements - Fuel

Fuel flow is measured by three Fisher-Porter flow meters mounted in-series and covering a range of flows from 0.2 to 200 pounds per hour. The flow meters are calibrated against a master flow meter which is also used to calibrate the flow meters used in tests on the fuel metering valve. This minimizes the possibility of cumulative errors.

Temperature - Measurement

A Solar design and fabricated Pt-Rh thermocouple (Fig. 57 and 58) was used to measure combustor outlet temperatures. Triple radiation shielding is provided to a 0.04 inch diameter bare bead Pt-10%Rh versus Pt thermocouple. Three concentric Pt-Rh radiation tubes are arranged to reduce radiation losses to low levels in this unit. High convective heat inputs (to offset radiation heat losses) are provided by a high velocity aspiration system that draws the combustor discharge across the thermocouple bead. Good results were obtained at temperatures up to 3030° F and velocities of 0.6 Mach number. The thermocouple could be mounted in forty different locations to provide an accurate description of both circumferential and radial temperature profiles at the exit of the combustor as shown in Figure 59.

Pressure Measurement

Pressure measurements are taken by means of Bourdon gauges, water and mercury manometers. All critical pressures are duplicated to minimize errors. Because at fuel flows much below 20 pounds per hour, the air flow is so small as to cause negligible combustor pressure loss, it is not possible nor is it very meaningful to accurately record the actual loss at such flows. Fuel pressure is not measured, it can be considered with negligible error, as being at the prevailing combustor pressure and which is, without a vaporizer, ambient pressure.

Fuel Supplies

Fuel is supplied to the combustor via the flow meters at a pressure slightly in excess of the combustor pressure and is throttled to the required level by means of a needle valve. The standard fuel used in the tests is JP-5. Such a fuel has a more precisely controlled specification than the fuels required to be used (#1 Diesel, Jet A, and kerosene), and has combustion characteristics typical but slightly worse than these fuels (i.e., is likely to have slightly higher CO and H/C emissions), Appendix B. Other fuels available and briefly used are JP-4 and #2 Diesel, and which represent fuels having combustor characteristics outside the best and worst likely limits expected of the specific fuels.

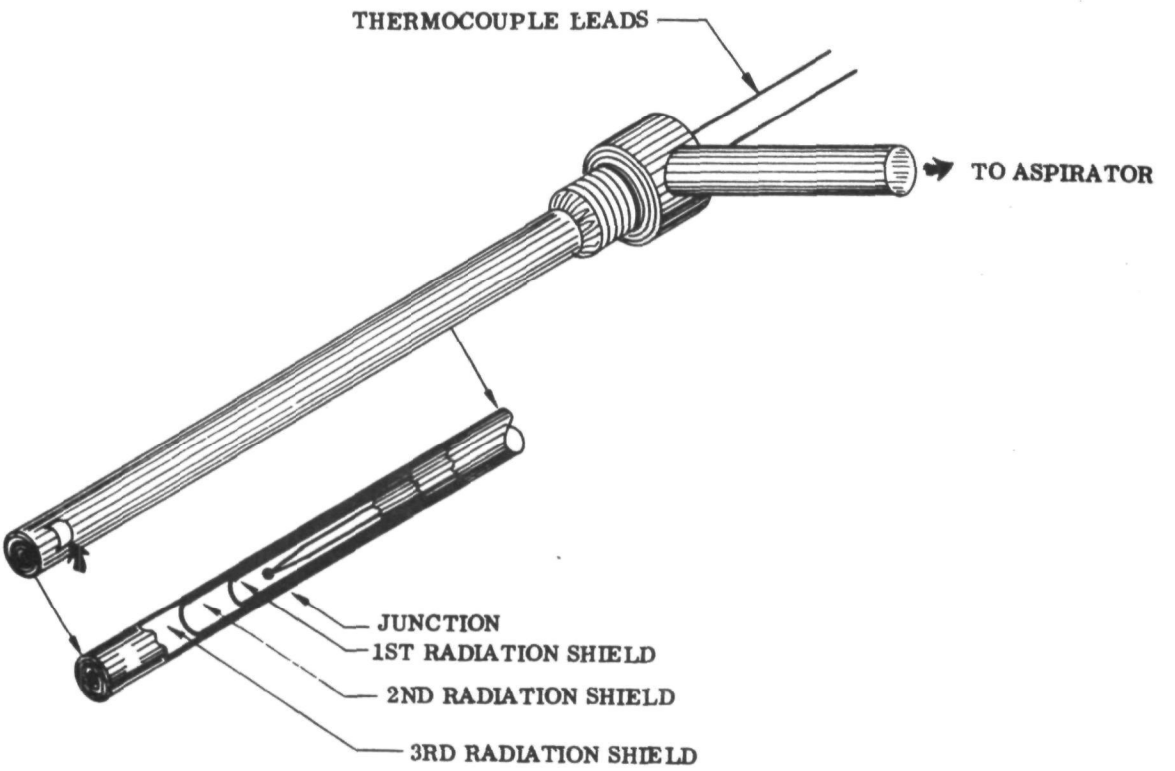

FIGURE 57. END VIEW - HIGH TEMPERATURE PROBE WITH TRIPLE RADIATION SHIELD AND HIGH VELOCITY ASPIRATION SYSTEM

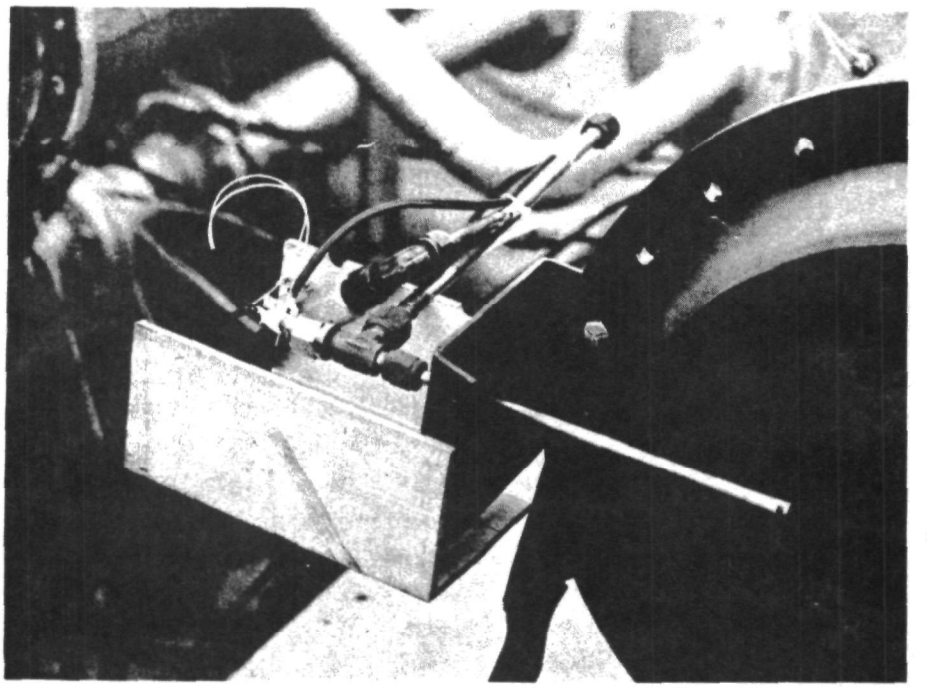

FIGURE 58. INSTALLATION OF A HIGH TEMPERATURE THERMOCOUPLE

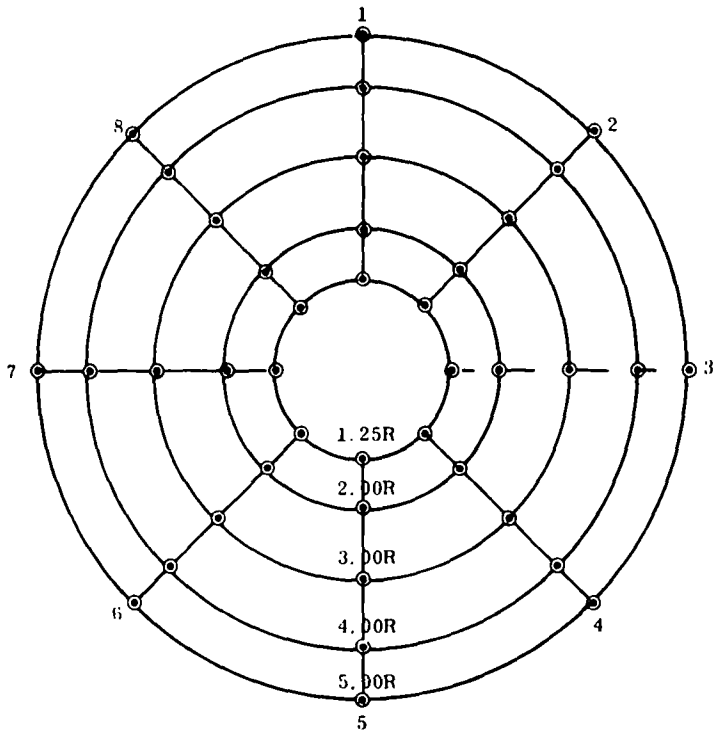

FIGURE 59. CIRCUMFERENTIAL AND RADIAL POSITIONS OF THERMOCOUPLE AT THE EXIT OF THE COMBUSTOR

Emissions are powerfully influenced by air-fuel ratio which is influenced by, among other things, fuel volatility. Therefore, a range of volatilities was deemed necessary in the tests in order to obtain as much understanding as possible of the processes involved in emissions (especially emissions of NO_2)

Emission Sampling Probes

Various types of sampling probes were investigated and the final type used is as shown in Figure 60. The probes consisted of 29 pickup points located at points of equal area across the combustor to provide a representative average sample.

In the case of CO, NO and CO_2 the probe was cooled to room temperature by means of an air cooling jacket so as to ensure no further reactions inside the probes and to allow removal of water vapors.

A separate probe, of identical design, was used to sample for unburnt hydrocarbons. To ensure no reactions inside the probe, but also to prevent condensation, the probe was cooled to a temperature of 350 to 375° F. The entire HC sampling line connecting the probe to the FID was electrically heated to 350 to 375° F for the same reason.

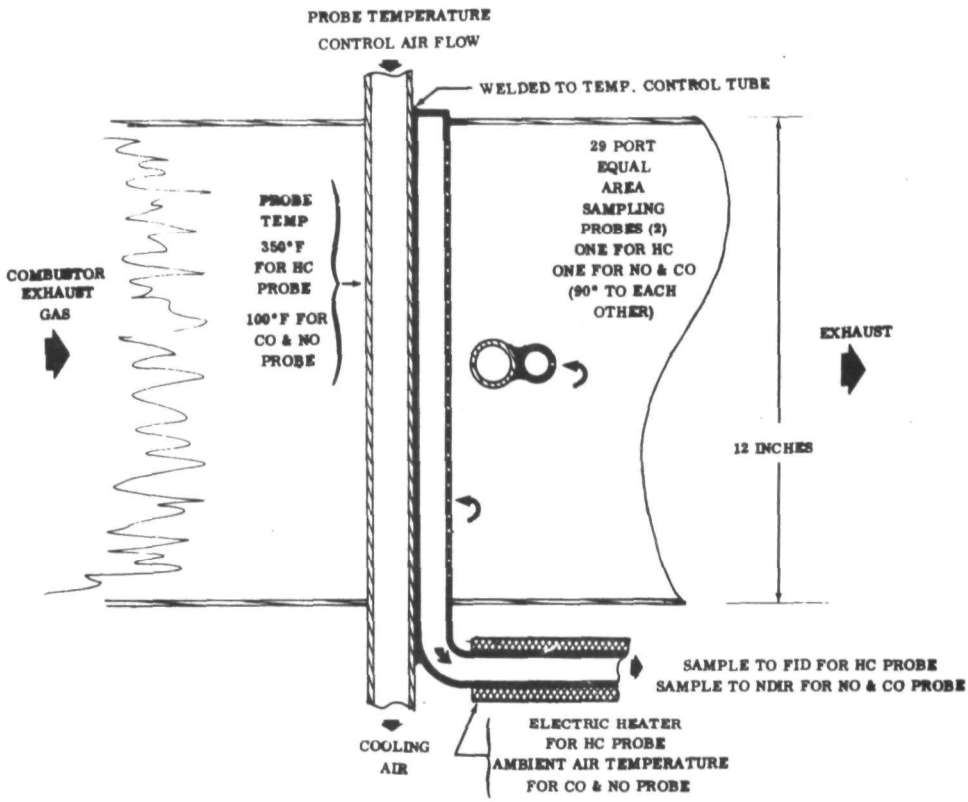

FIGURE 60. SCHEMATIC OF EMISSION PICKUP PROBE

7.3 COMBUSTOR DEVELOPMENT

7.3.1 Summary

Initial combustor development was done on a rig without use of a fan and metering valve and emissions were at reasonable levels. Tests with a fan and metering valve required more development to get acceptable emissions. When a vaporizer was installed at the combustor exit emissions levels increased to unacceptable levels and indicates some radiation shielding may be necessary to get acceptable emissions.

7.3.2 Preliminary Combustor Rig Tests

The combustor was run over a range of fuel flows from 5 to 109 lb/hr using JP-5 fuel, and with the air-fuel ratio maintained at various values between 22 and 30. From these results it was possible to find the optimum air-fuel at any fuel flow for minimum emissions. This optimum air-fuel is shown in Figure 61. It can be seen that only at maximum fuel flow is the design value of 26 air-fuels achieved. With reducing fuel flows a small reduction in air-fuel is required. However, at values of fuel flow less than about 50 lb/hr a considerable excess of air is required to obtain an acceptable flame.

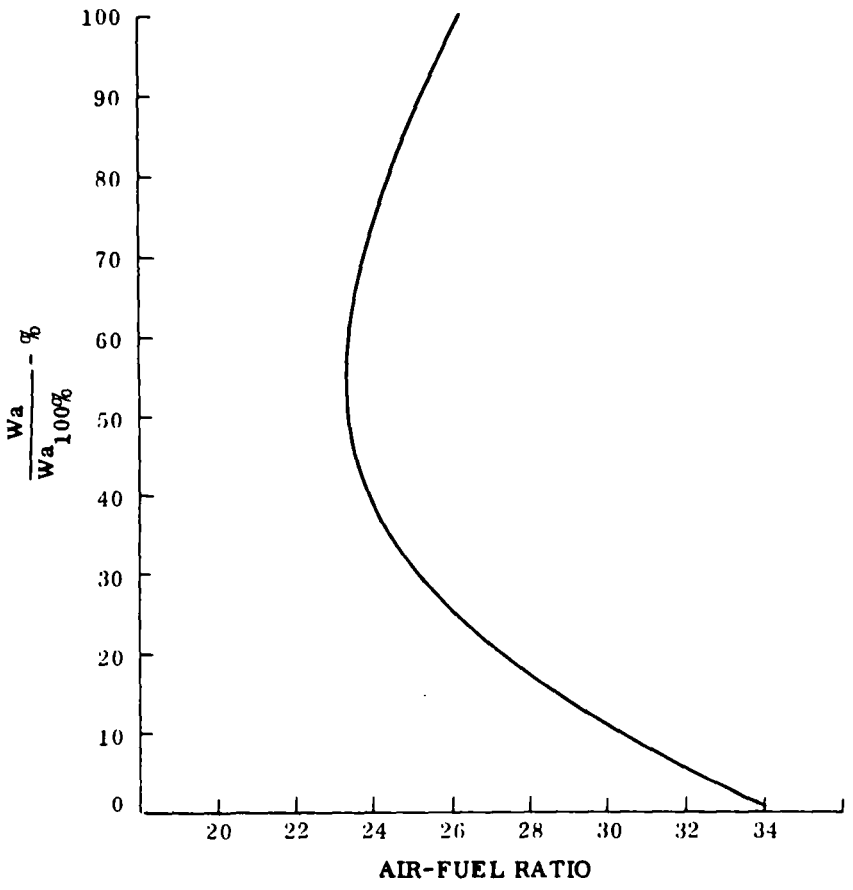

FIGURE 61. AIR-FUEL RATIO FOR MINIMUM EMISSIONS AS A FUNCTION OF COMBUSTOR AIR FLOW

The actual emissions resulting from maintenance of this optimum air-fuel relationship with fuel flow are shown in Figure 62 and 63 together with the increased emissions resulting from a 10 percent error in air-fuel (it is not to be expected that control of air-fuel can, in practice, be maintained much closer than this).

7.3.3 Combustor Pressure Loss Reduction

Up to this date, combustor pressure loss had been 12.7 inches H_2O. It was necessary to reduce it to 8 inches H_2O in order to keep the power consumption of the fan within reasonable limits. This was done and there was a considerable increase in flame length and emissions, notably hydrocarbons and carbon monoxide. Changes to the hole pattern of the combustor were made though the original staging of air-fuel ratios within the primary, secondary, and tertiary flame zones was maintained.

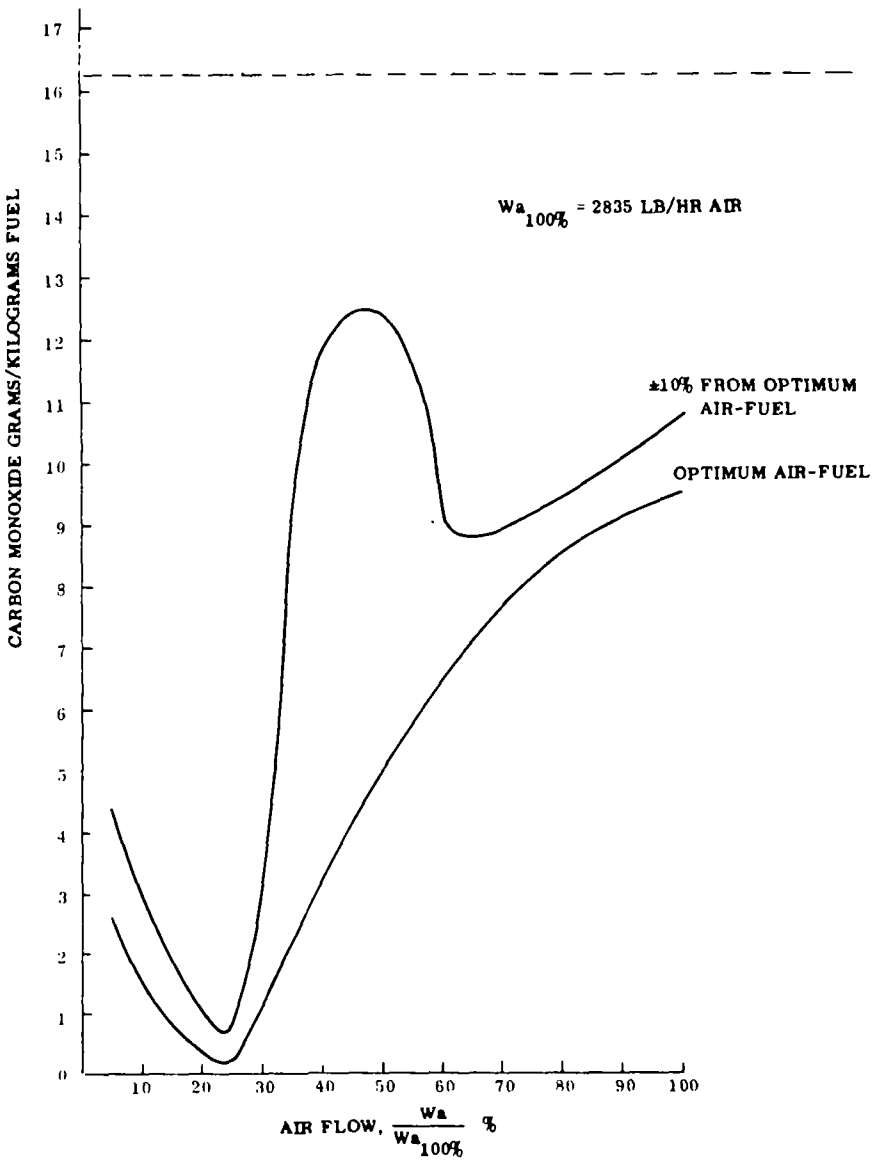

FIGURE 62. EMISSIONS OF CARBON MONOXIDE AS A FUNCTION OF COMBUSTOR AIR FLOW, AT OPTIMUM AIR FUEL FOR MINIMUM EMISSIONS AND ALSO WITH A ±10% DEVIATION OF AIR FUEL FROM OPTIMUM

The effect of reduced pressure drop was that penetration of air into the flame was reduced. Consequently, the poor mixing of air and fuel resulted in lean and rich pockets that caused lengthening flame due to, in both instances, a reduction in the rate of combustion.

Modifications were made to the hole size and pattern to improve mixing with beneficial results, though it was not possible to reduce flame length to the values

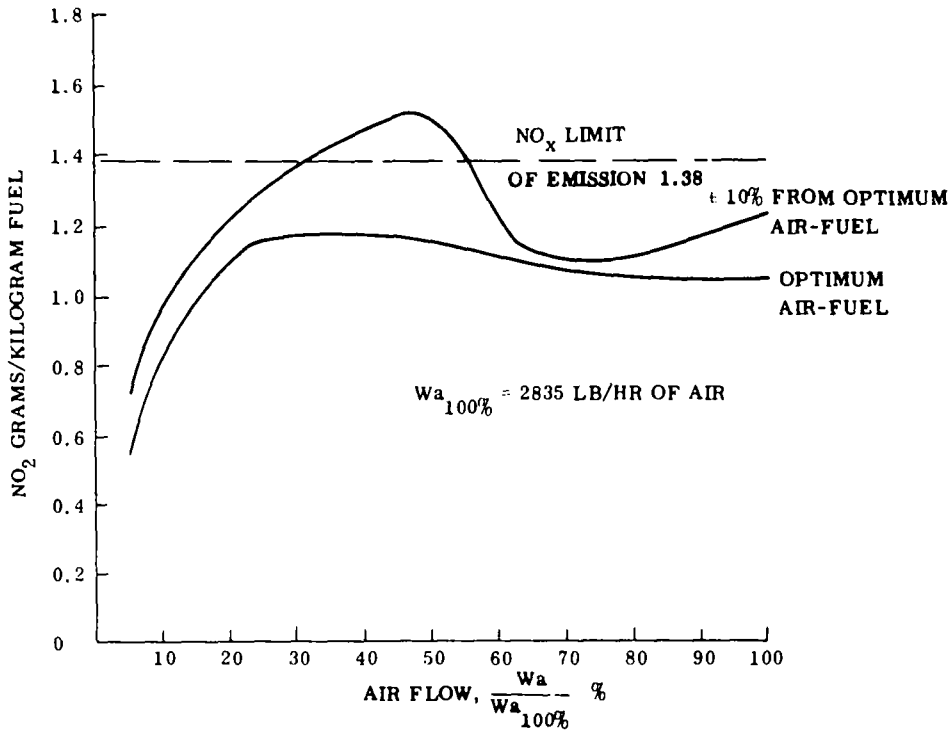

FIGURE 63. EMISSIONS OF NO_2 AS A FUNCTION OF COMBUSTOR AIR FLOW, AT OPTIMUM AIR-FUEL FOR MINIMUM EMISSIONS AND ALSO WITH A ±10% DEVIATION OF AIR-FUEL FROM OPTIMUM

recorded with the high loss combustor. Results are shown in Figures 64. By maintenance of an air-fuel of 22, it was possible to achieve the required goals in emissions. Small errors in air-fuel would, however, result in emissions outside limits.

In general, the results are in agreement with theory. Figure 64a shows the time dependence of NO formation as with decreasing fuel flow (inversely proportional to combustion time), emissions increase.

Figure 64b shows the time dependence of CO formation in that increasing fuel flows result in increased emissions of CO. Minimum emissions are achieved with reduced air-fuels as a result of increased reaction rate of the higher temperatures. It would appear that an optimum combustor, operating at the design point of 26 air-fuels, would have NO emissions considerably below limits but would require increased combustor length to reduce CO.

Figure 64c is more difficult to interpret as large variations in hydrocarbon emissions are seen. This might be explained by the high background emissions and below which it is possible to maintain the flame when air-fuel is optimum.

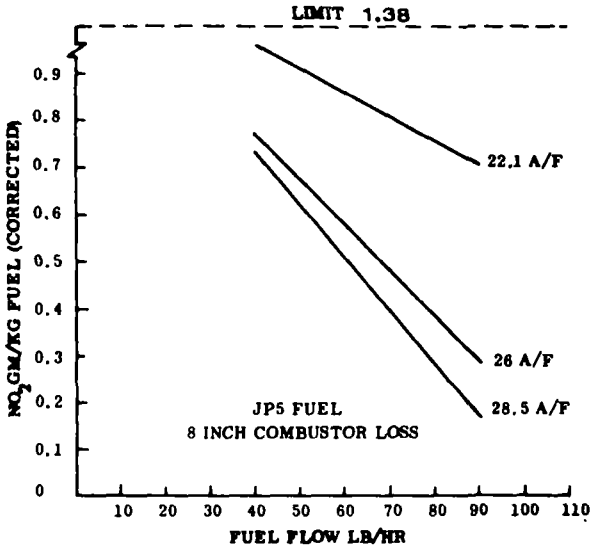

A. NO_2
REDUCED PRESSURE LOSS

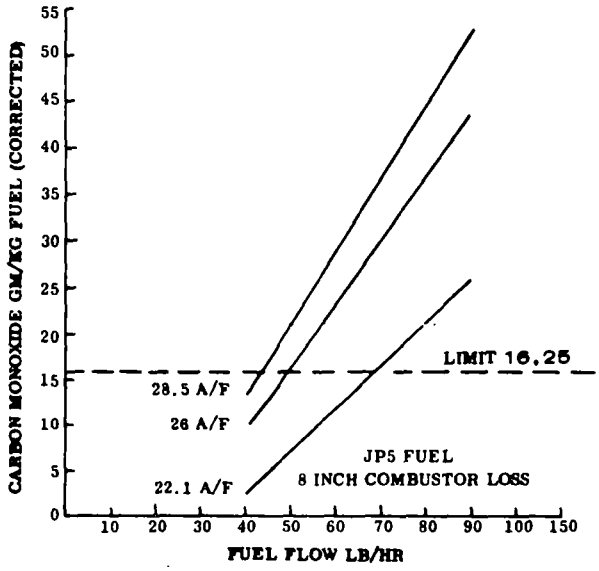

B. CARBON MONOXIDE

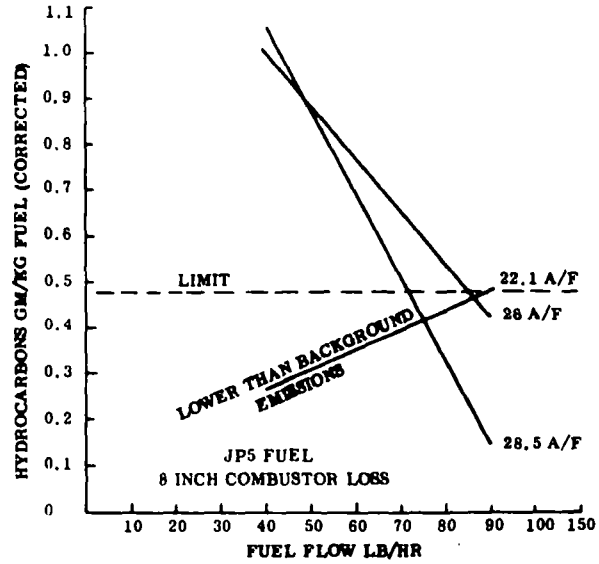

C. HYDROCARBONS

FIGURE 64. EFFECT OF FUEL FLOW ON EMISSIONS AT DIFFERING AIR-FUEL RATIOS USING RIG AIR SUPPLIES

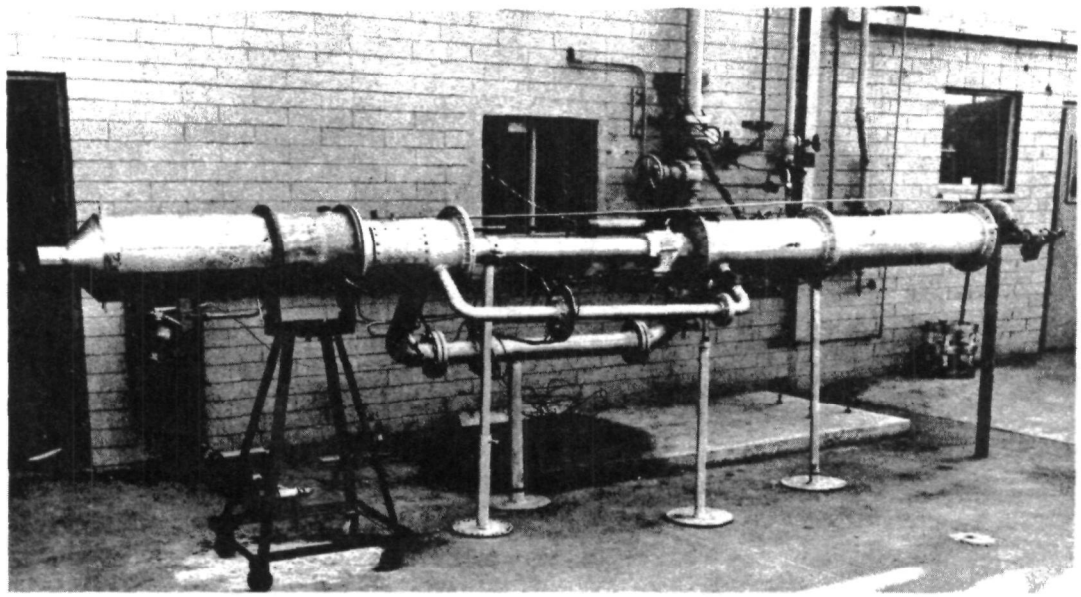

FIGURE 65. COMBUSTOR RIG WITH VAPORIZER INSTALLED

7.3.4 Simulated Vaporizer Tests

A vaporizer was designed to simulate an actual installation and assembled onto the end of the combustor (Fig. 65). The vaporizer consisted of 250 feet of 0.7 inch inside diameter stainless tube. In order to obtain sufficient heat transfer it was necessary to use a gas side pressure drop of 1.75 inch of water. It was not therefore possible to use with the fan because of the increased pressure losses.

Emission measurements, Figure 66, showed a considerably reduction in flame performance. Unburned hydrocarbon emissions increased by up to fifty times, carbon monoxide increased slightly and NO_2 emissions decreased about fifty percent.

This flame performance is not acceptable and is a direct result of the heat losses from the flame to the vaporizer caused, principally, by flame radiation.

Therefore, because of the major influence of the vaporizer on flame performance, it is essential to develop the combustor as an integrated unit with the vaporizer.

It is noteworthy that nitrogen oxide emissions were reduced due to heat losses, as is to be expected. This would allow a control on nitrogen oxide emissions somewhat independent of air-fuel ratio provide sufficient volume was provided as to allow reaction of hydrocarbons and carbon monoxide. By shielding the vaporizer from the flame, the emissions as previously reported could be maintained.

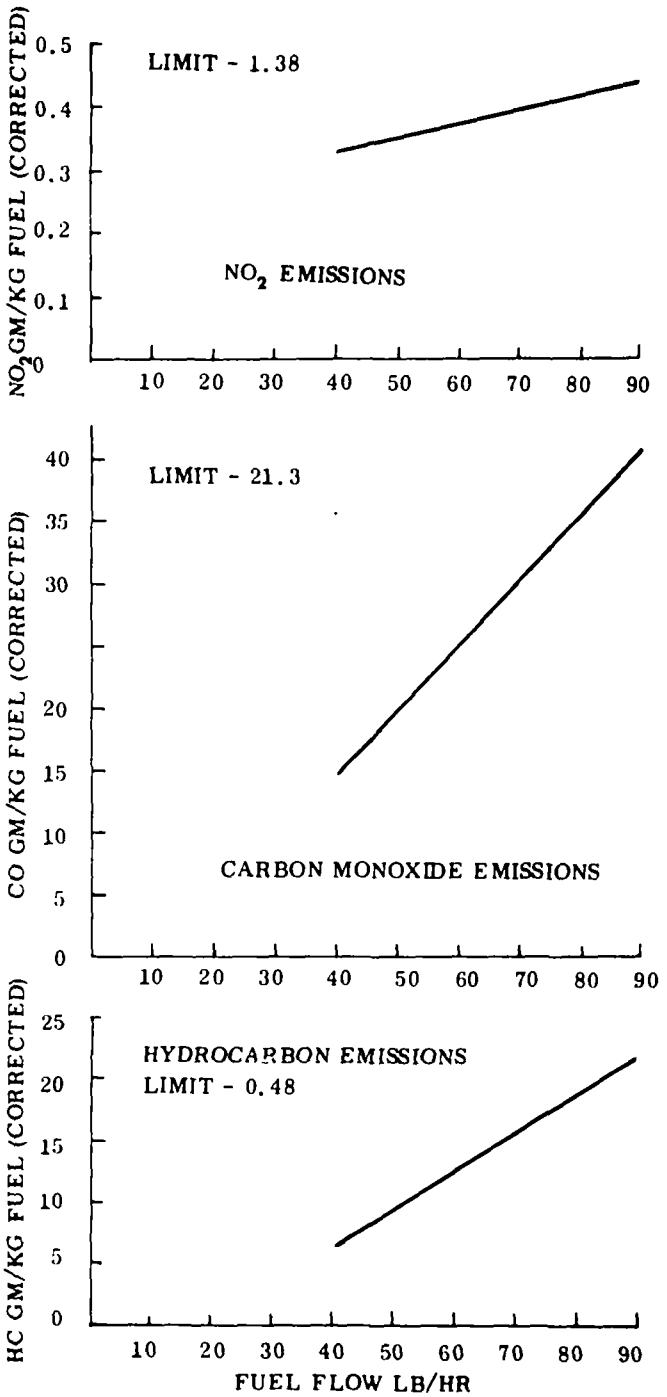

FIGURE 66. EFFECT OF VARYING FUEL FLOW ON EMISSIONS WHEN AIR-FUEL IS MAINTAINED AT A CONSTANT VALUE (26/1) AND USING A RIG AIR SUPPLY AND BOILER

The low levels of nitrogen oxides that have been reported in domestic furnaces are probably as a result of radiation heat losses. Heat losses can be readily controlled in such an installation because of the single fueling rate used. However, modulation of heat rate requires on-off control of fuel which results in unacceptable warm-up emissions of carbon monoxide and hydrocarbons.

7.3.5 Combustor Tests With Fan

The object of reducing combustor pressure loss was to permit testing with a fan whose power requirement was within the limits set as a goal for parasitic power. The combustor and fan were therefore assembled together, with the air metering valve, for further combustor tests (Fig. 29). The fuel and air metering valves were, however, manually operated.

Tests were done over a wide range of operating conditions varying from 109 to 5 lb/hr. It was obvious that considerable differences in flame performance from that seen using the test rig air supplies. Two effects were seen.

1. At high fuel flows considerable circumferential variations in air flow occurred. Consequently, large differences, circumferentially, in flame length resulted. Emissions were high, especially of hydrocarbons and temperature distribution was unacceptable.

2. At low fuel flows the flame appeared uniform but air-fuels in the various zones were different from those occurring on the combustor test rig.

The circumferential air maldistributions were investigated by flow tests. The basic check was to coat the flow surfaces with oil and then inject talcum into the fan. These checks indicated that the flow was unstable, resulting in separations in air at different circumferential locations. The nature of such flow differences are shown schematically in Figure 67a and b.

The only method of effectively controlling such air maldistributions without use of excessive pressure loss or combustor volume is to design the fan and combustor as an integral unit with low flow velocities and the minimum of diffusion, as in Figure 67c. As the location of the vaporizer can also have an effect on aerodynamics, it also must be integrated into the aerodynamic design.

The axial air maldistributions are explained by the presence of swirl in the fan. The swirl angle was too low to measure, but the tangential velocity component was high in relationship to the combustion velocities. The resultant swirl caused large axial and radial variations in the hole discharge coefficients.

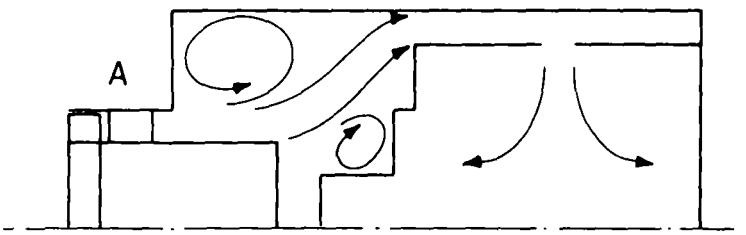

LATE SEPARATION OF AIR RESULTING IN HIGH VELOCITY AIR ENTERING COMBUSTOR CAUSING A COLD SPOT.

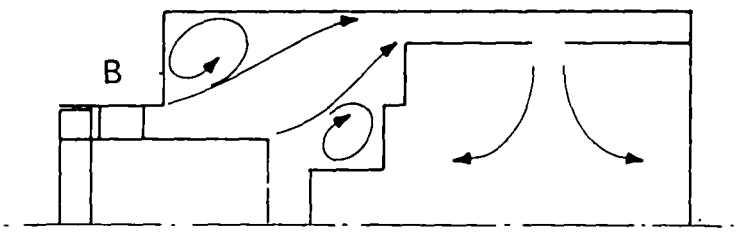

EARLY SEPARATION OF AIR RESULTING IN LOW VELOCITY AIR ENTERING COMBUSTOR CAUSING A HOT SPOT.

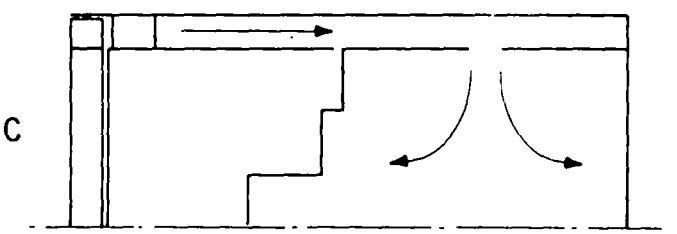

PREVENT SEPARATION BY USING A LARGER FAN OF LOWER VELOCITY THAT DOES NOT REQUIRE DIFFUSION.

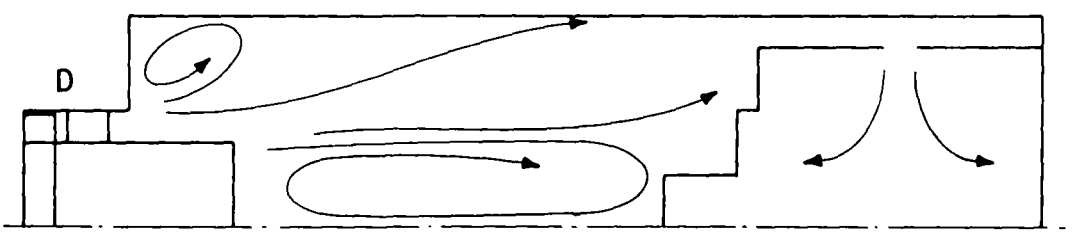

CURRENT SOLUTION IS TO INTERPOSE ALONG MIXING DUCT BETWEEN FAN AND COMBUSTOR TO ALLOW WAKES TO DISSIPATE TO A LOWER VELOCITY.

FIGURE 67. AIR MALDISTRIBUTIONS DUE TO UNSTABLE DIFFUSION

To control such a phenomena means design of a fan with low air velocities and with a minimum of swirl. It is an advantage in this respect to run the fan at low speeds when fuel flows are low, and to have the highest possible combustor pressure loss. Metering plate pressure loss should be kept low.

An optimum fan design was not feasible at this stage involving, as it did, unknowns in vaporizer configuration, cost, and time outside the program scope. Therefore, as a temporary expedient, a large mixing duct, 36 inches in length, was placed between the fan and combustor, Figure 67d. An immediate and radical improvement in flame performance was noted though it was still apparent at the low fuel flows that all air swirl had not been eliminated.

Temperature Traverses

It is essential that rig and fan tests duplicate each other. Otherwise, any demonstration of a working package by use of a rig becomes worthless. Experience indicates that at least half the problems of emission control lies in proper design of a fan and its associated fuel and air control system. Such a system of control, covering as it does an extreme range of flow variations, is considerably beyond current state-of-the-art. A means of checking simulation precisely and in a simple manner is by temperature traverses of both rig and fan package. Ordinarily, at the flame temperatures involved (up to 3200° F), thermocouples are inaccurate and have a very short life. The alternate approach of emission traverses is time consuming, laborious, and expensive. Solar has developed a high temperature thermocouple that has a long life and is accurate (to 1%) at the temperatures involved. Thus a simple tool is available that enables precise definition of aerodynamic simulation and hence combustion reactions by comparing temperature profiles on the rig and actual hardware.

A thermocouple was therefore installed for such a traverse. Traversing was done by locating the thermocouple in forty different locations as shown in Figure 59 and the results and conclusions noted as follows.

Figures 68 and 69 show the average radial profile at combustor exit at a fuel flow of 88 lb/hr when using rig air and fan air supplies, respectively. A comparison of the radial profiles is shown in Figure 70.

It is apparent that good repeatability in radial profile is achieved, indicative of good simulation, aerodynamically (and hence of combustion reactions), between rig and fan. Allowing for the small difference in air flow between the two tests, the difference in temperatures recorded is one percent, and so the traverses can be assumed accurate and representative. The large difference in temperature that exists between the center and outside of the combustor is as a result of inadequate mixing of fuel and air. Consequently, there exists large radial variations in air-fuel.

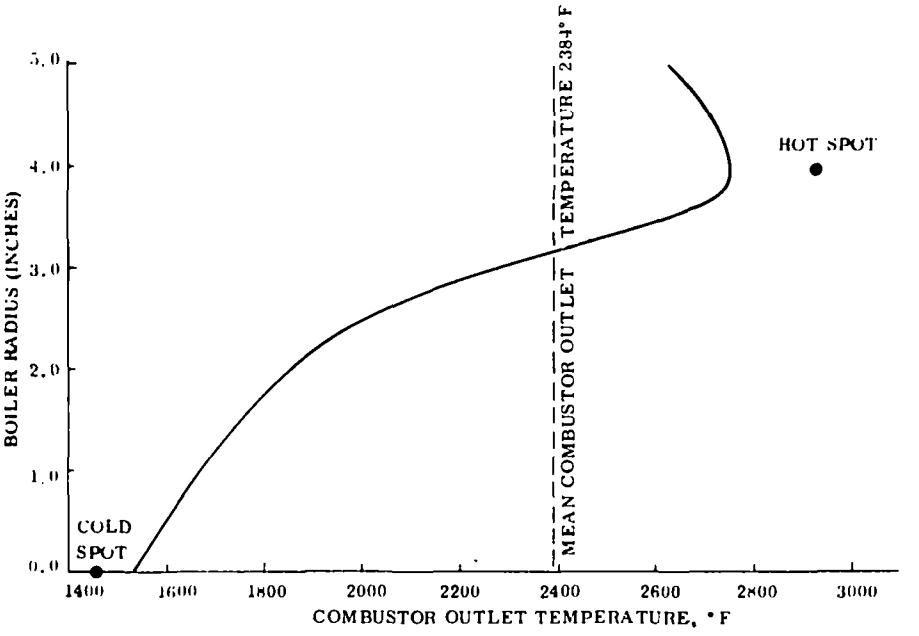

AVERAGE TEMPERATURE	2384° F	TEMPERATURE SPREAD	1462° F
HOT SPOT TEMPERATURE	2920° F	FUEL FLOW	88 LB/HR
COLD SPOT TEMPERATURE	1458° F	COMBUSTOR PRESSURE LOSS	5.7 INCHES WATER

FIGURE 68. AVERAGE RADIAL PROFILE OF TEMPERATURE OUT OF COMBUSTOR USING RIG AIR SUPPLY

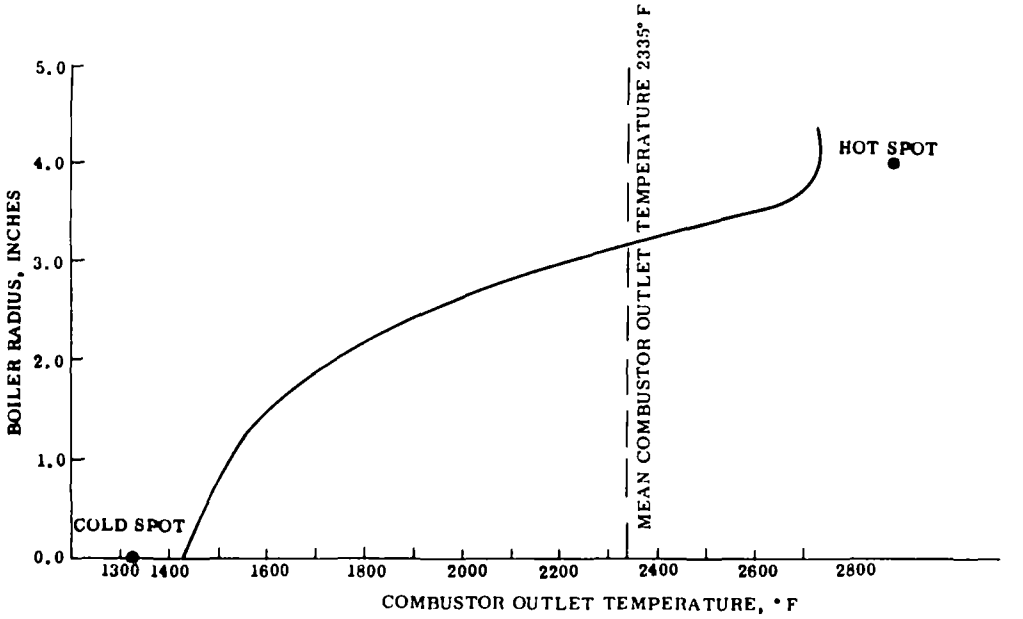

AVERAGE TEMPERATURE	2335° F	TEMPERATURE SPREAD	1565° F
HOT SPOT TEMPERATURE	2380° F	FUEL FLOW	88 LB/HR
COLD SPOT TEMPERATURE	1315° F	COMBUSTOR PRESSURE LOSS	5.8 INCHES WATER

FIGURE 69. AVERAGE RADIAL PROFILE OF TEMPERATURE OUT OF COMBUSTOR USING FAN AIR SUPPLY

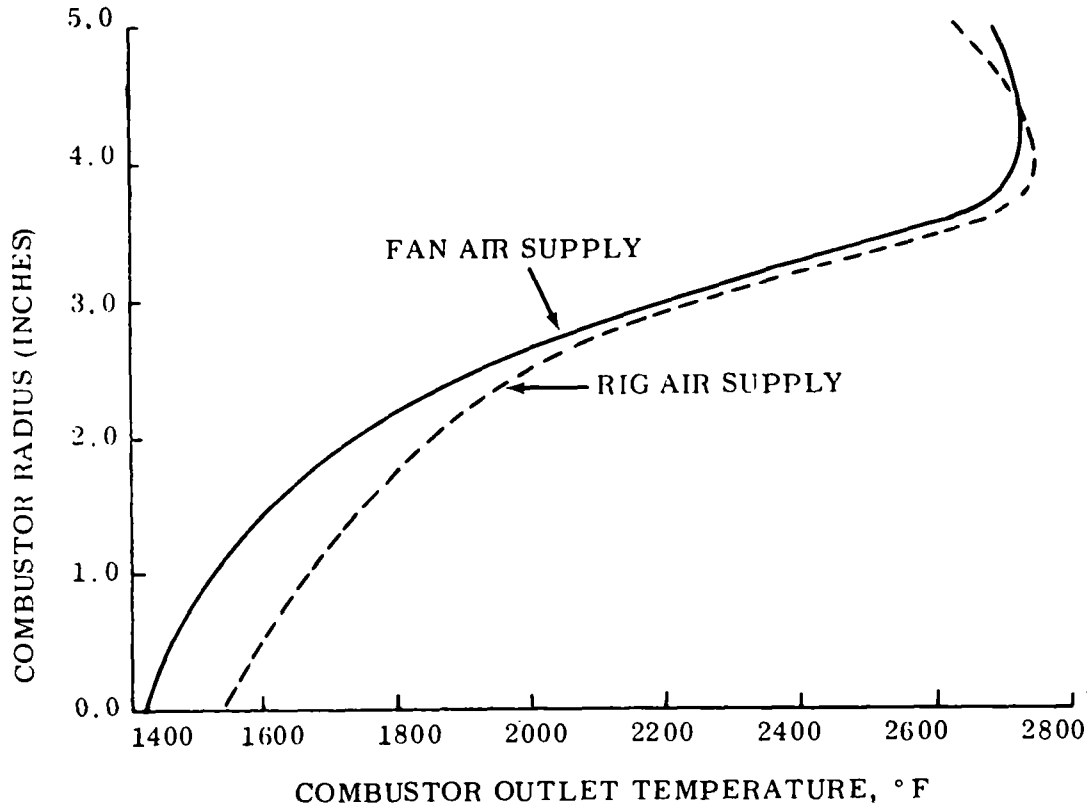

FIGURE 70. REPEATABILITY OF RADIAL PROFILE OF TEMPERATURE OUT OF COMBUSTOR USING BOTH FAN AND RIG AIR SUPPLIES

Theoretically, either a lean or rich mixture will cause an increase in emissions and so there's some room for considerable improvements to be made.

In addition to the radial variations in temperature (and air-fuel) noted, it is seen from Figures 71 and 72 that circumferential variations in radial profile exist. This is shown more clearly in Figures 73 and 74 which show the circumferential temperature distributions at various radial position for rig and fan air systems, respectively.

The variations in temperature distribution between rig and fan are significant, indicating reasonable, but not exact, aerodynamic simulation. The major source of temperature maldistributions lies, however, in inadequate mixing that, as shown above, is simulated exactly on rig and fan systems.

Radial traverses were then done at differing fuel flows, holding air-fuel constant, Figure 75. Changes in profile occurred, indicative of changes in mixing as a function of fuel flow. In general, however, the basic characteristics of cold center, hot wall profile was maintained over a wide range of conditions.

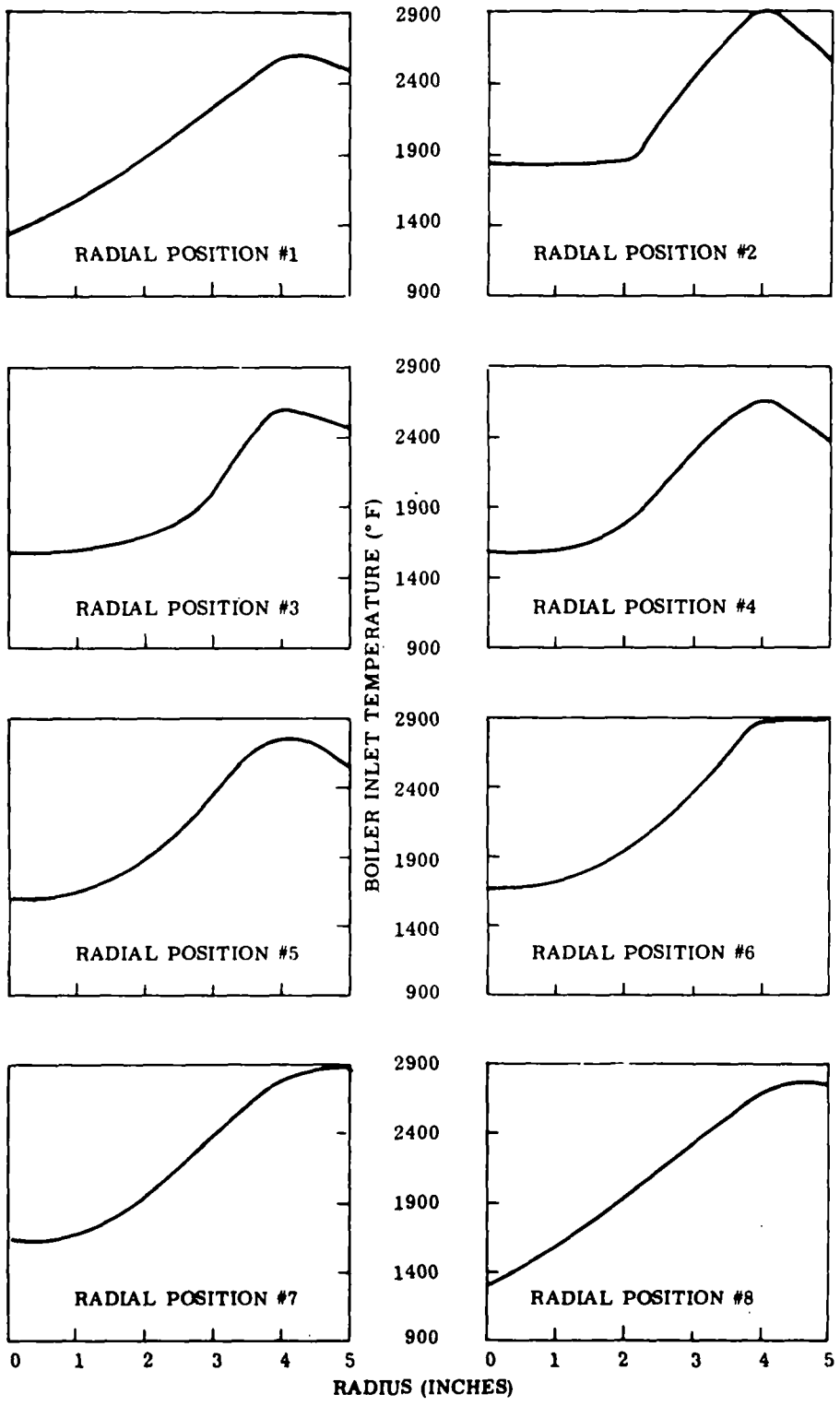

FUEL FLOW 88 LB/HR COMBUSTOR PRESSURE DROP 5.7 INCH WATER

FIGURE 71. RADIAL PROFILE OF TEMPERATURE OUT OF COMBUSTOR AT SEVERAL DIFFERENT CIRCUMFERENTIAL LOCATIONS AND USING THE RIG AIR SUPPLY

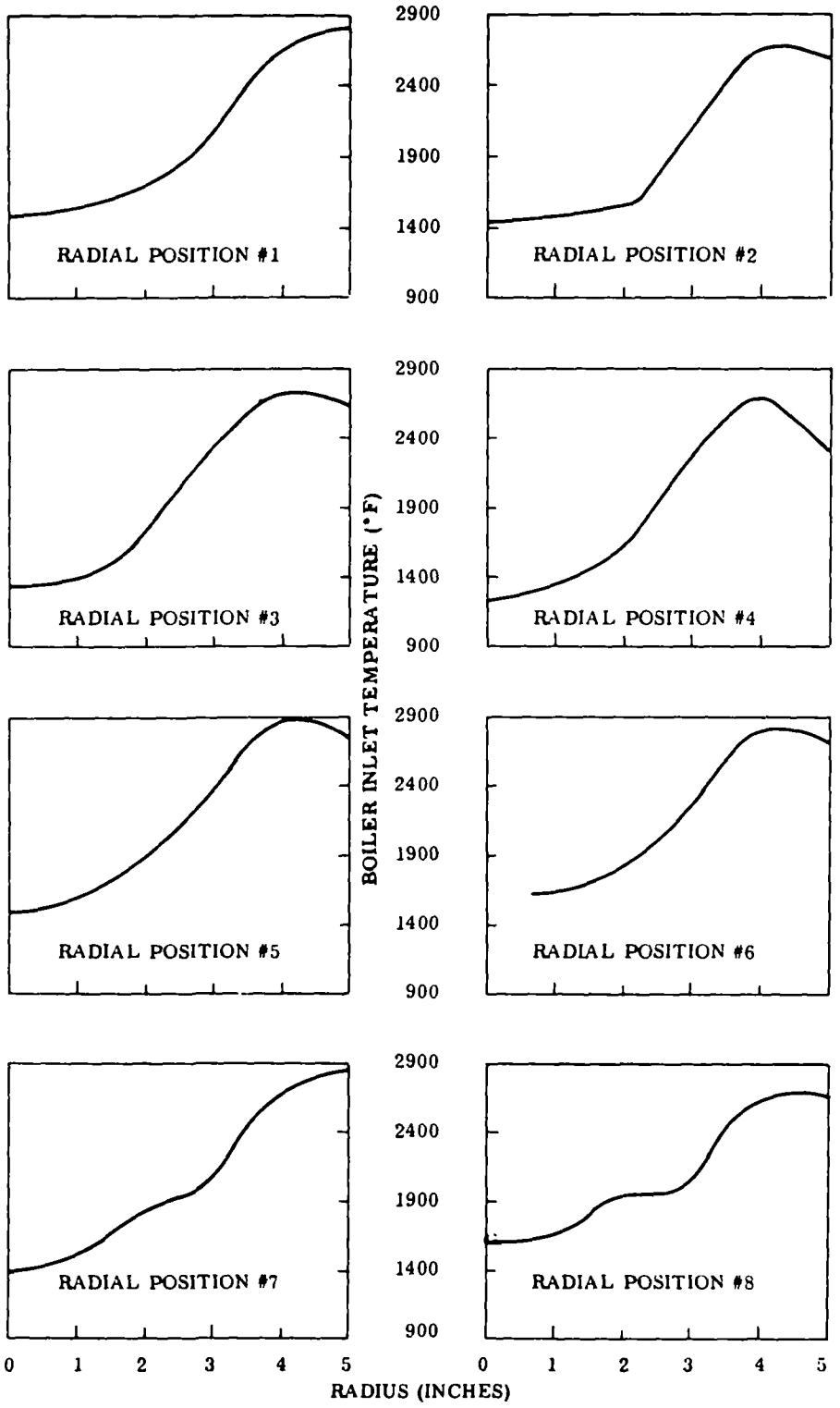

FUEL FLOW 88 LB/HR COMBUSTOR PRESSURE DROP 5.8 INCH WATER

FIGURE 72. RADIAL PROFILE OF TEMPERATURE OUT OF THE COMBUSTOR AT SEVERAL DIFFERENT CIRCUMFERENTIAL LOCATIONS AND USING THE FAN AIR SUPPLY

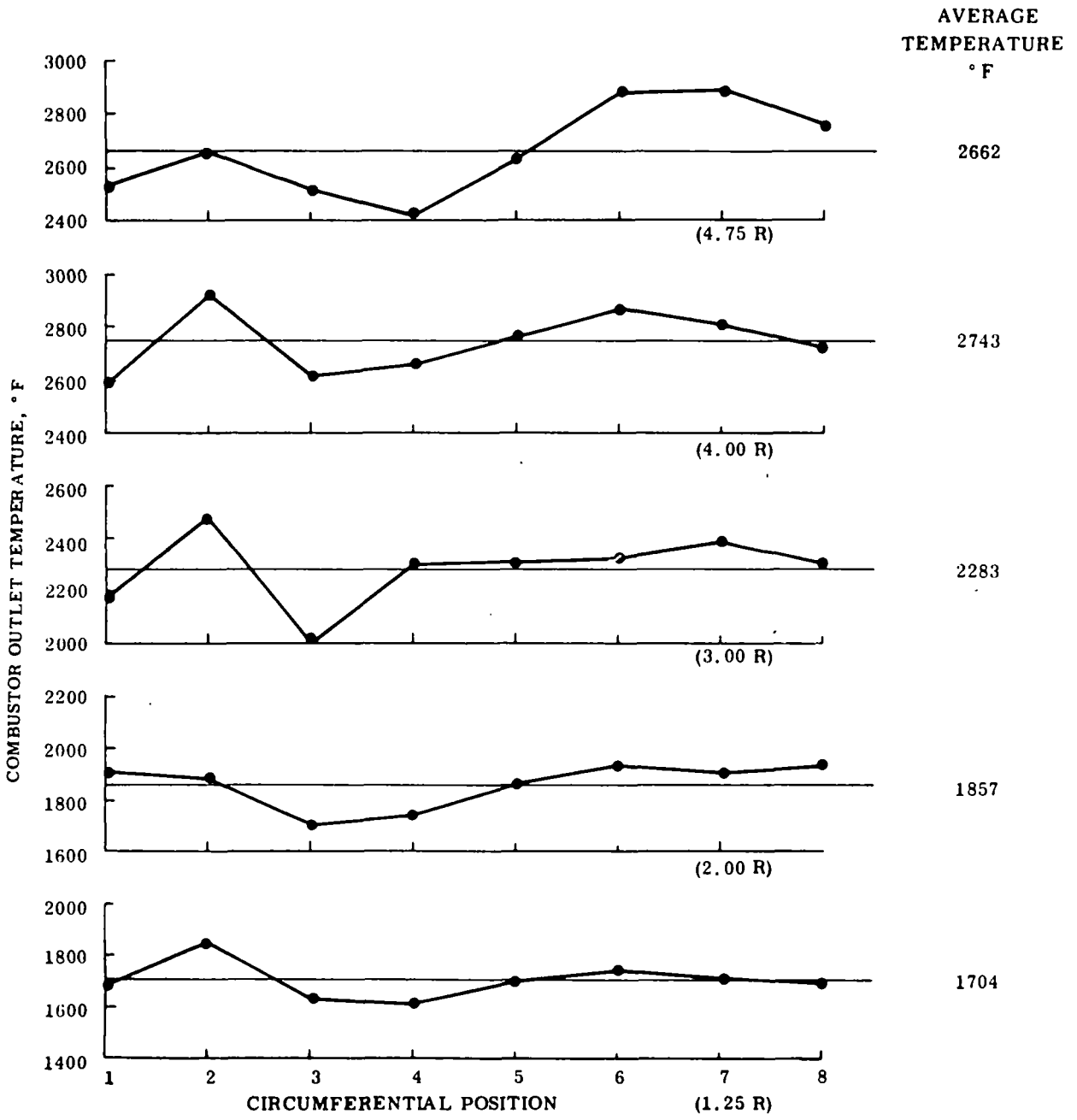

FUEL FLOW, 88 LB/HR
COMBUSTOR PRESSURE LOSS, 5.7 INCHES WATER
AVERAGE TEMPERATURE, 2384 °F

HOT SPOT TEMPERATURE, 2920° F
COLD SPOT TEMPERATURE, 1458° F

FIGURE 73. CIRCUMFERENTIAL VARIATION OF COMBUSTOR OUTLET TEMPERATURE AT DIFFERENT RADII USING RIG AIR SUPPLIES

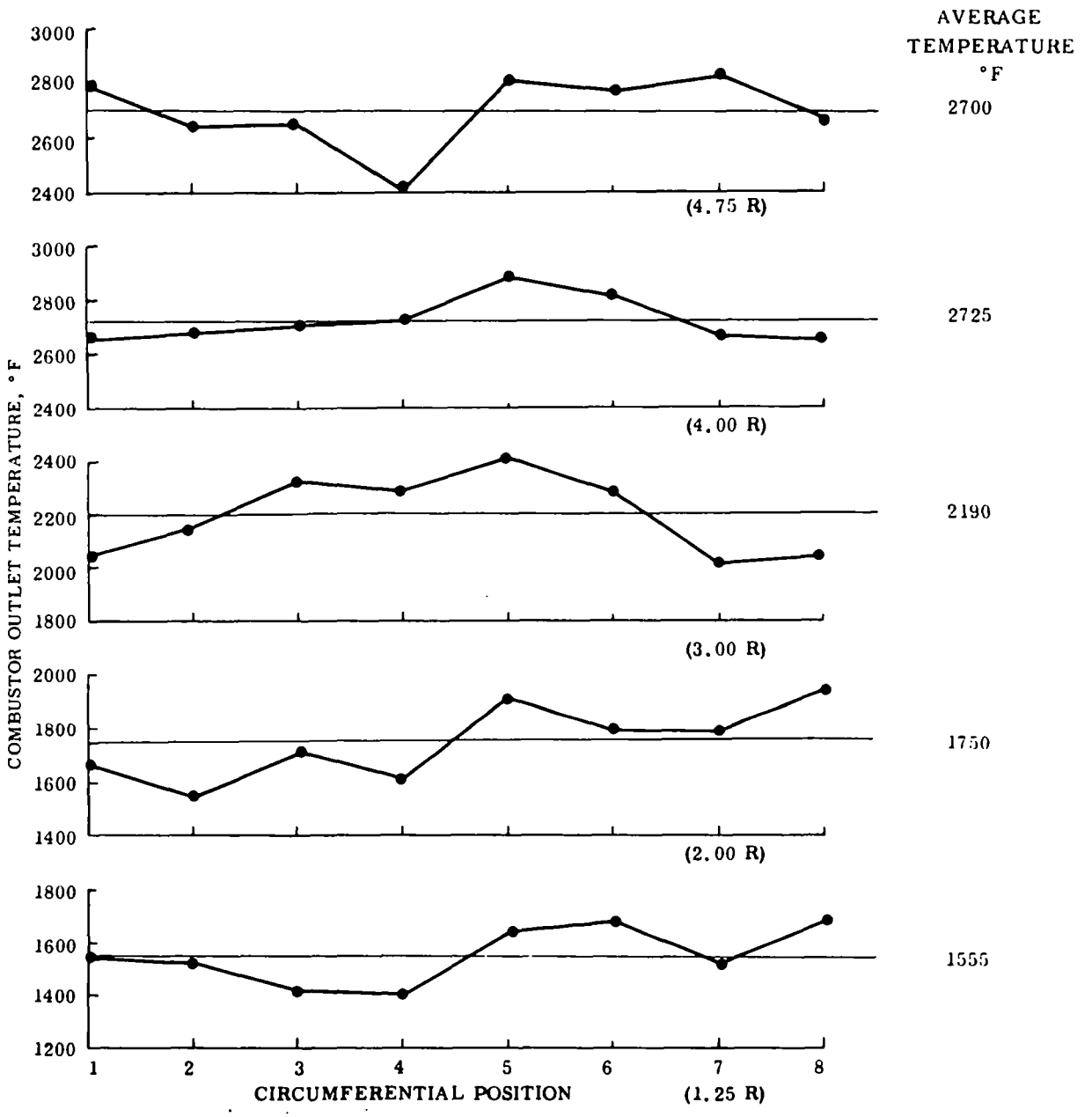

FUEL FLOW, 88 LB/HR
COMBUSTOR PRESSURE LOSS, 5.8 INCH WATER
AVERAGE TEMPERATURE, 2335°F

HOT SPOT TEMPERATURE, 2880°F
COLD SPOT TEMPERATURE, 1315°F

FIGURE 74. CIRCUMFERENTIAL VARIATION OF COMBUSTOR OUTLET TEMPERATURE AT DIFFERENT RADII USING FAN AIR SUPPLY

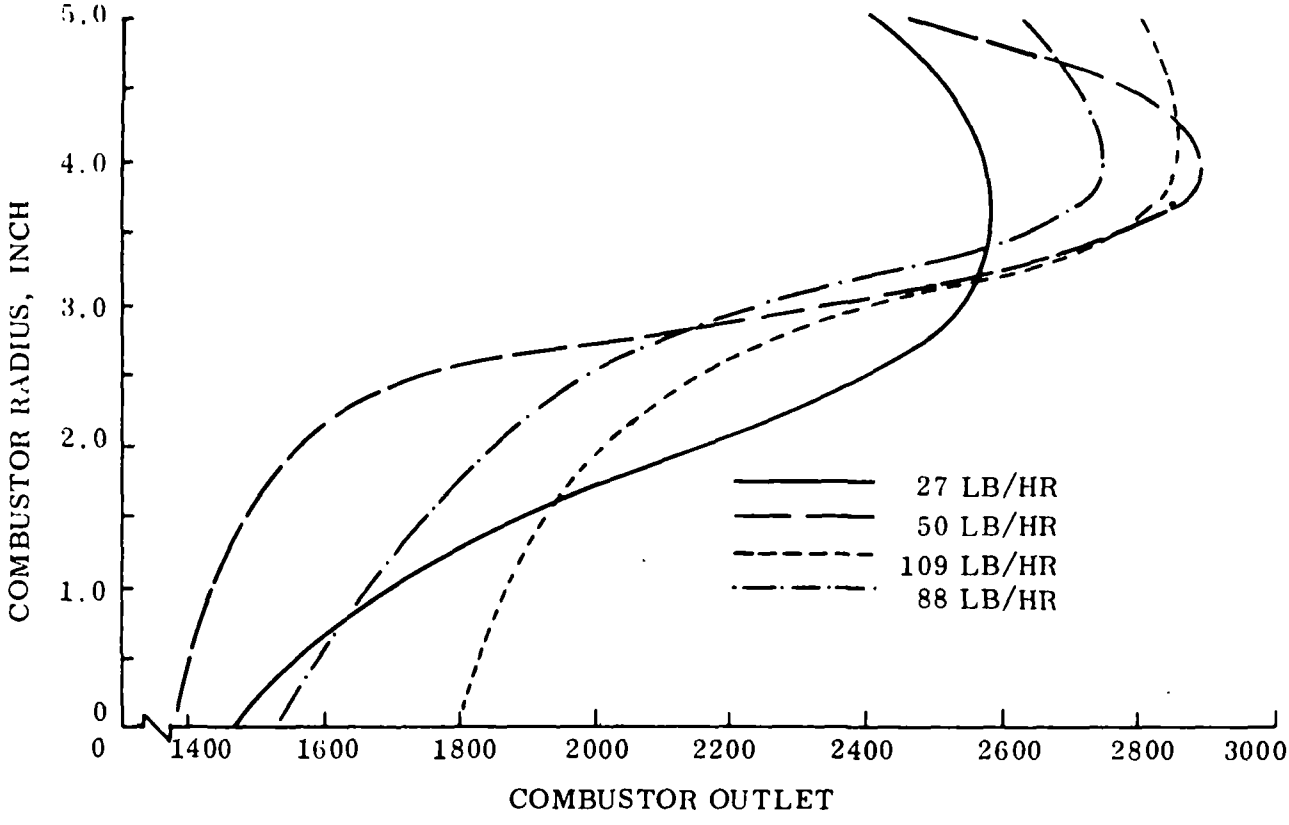

Fuel Flow Lb/Hr	Combustor Loss Inch Water	Temperature Spread ° F
27	0.515	1130
50	2.05	1510
88	5.7	1210
109	8.4	1060

FIGURE 75. RADIAL PROFILE AT VARIOUS FUEL FLOWS, USING RIG AIR SUPPLY

7.3.6 Final Combustor Tests

Because of the large radial temperature profile adjustments were made in the position and number of dilution holes. Considerable modifications to the shape of the radial profile could be made and the final result is shown in Figure 76. A reduction in radial profile spread from about 1300° F to 850° F was made. In practice, by more extensive experimentation, it should be possible to obtain a flat temperature profile, especially if vaporizer inlet temperature requirements can be kept low.

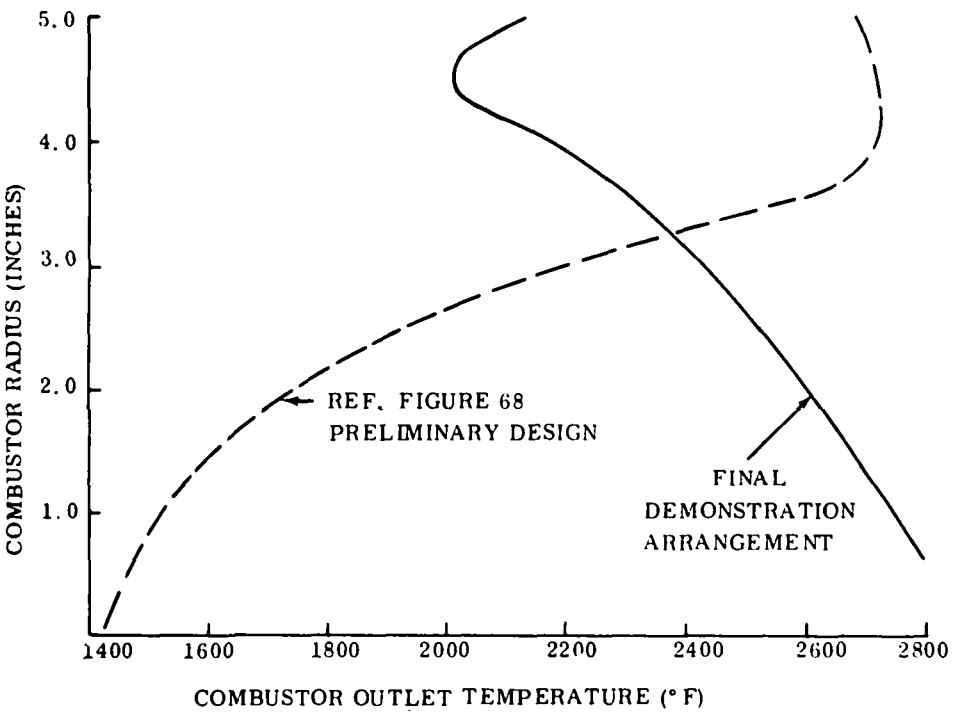

FIGURE 76. RADIAL PROFILE OF TEMPERATURE (FINAL DEMONSTRATION COMPARED TO PRELIMINARY)

Based on previous emission tests the fuel and air metering valves were adjusted to provide for as optimum as possible air-fuel ratio. The resultant combustor outlet temperature as a function of fuel flow is shown in Figure 77. Because the dilution air represents about 20 percent of the total air flow through the combustor this temperature could be increased by a similar amount (to about 3000° F maximum) by its deletion from the combustor. Conversely the temperature could be reduced by any amount by addition of more dilution air. Theoretically either addition or subtraction of dilution should not affect emissions. However, if temperatures of 3000° F are required to minimize vaporizer size, temperature distributions will be dependent on mixing in the flame zone and there would be no excess dilution air available for final trim of the radial profile.

Emission tests were then run and the results are shown in Figures 78, 79, and 80, and also in Figure 81.

All emissions were substantially below the required limits except for carbon monoxide which, at the one pound an hour fuel flow, was above limits. This was caused by excessive air addition (Fig. 77) and, by small modifications to the fuel and air controls it should be possible to achieve the required emission goals.

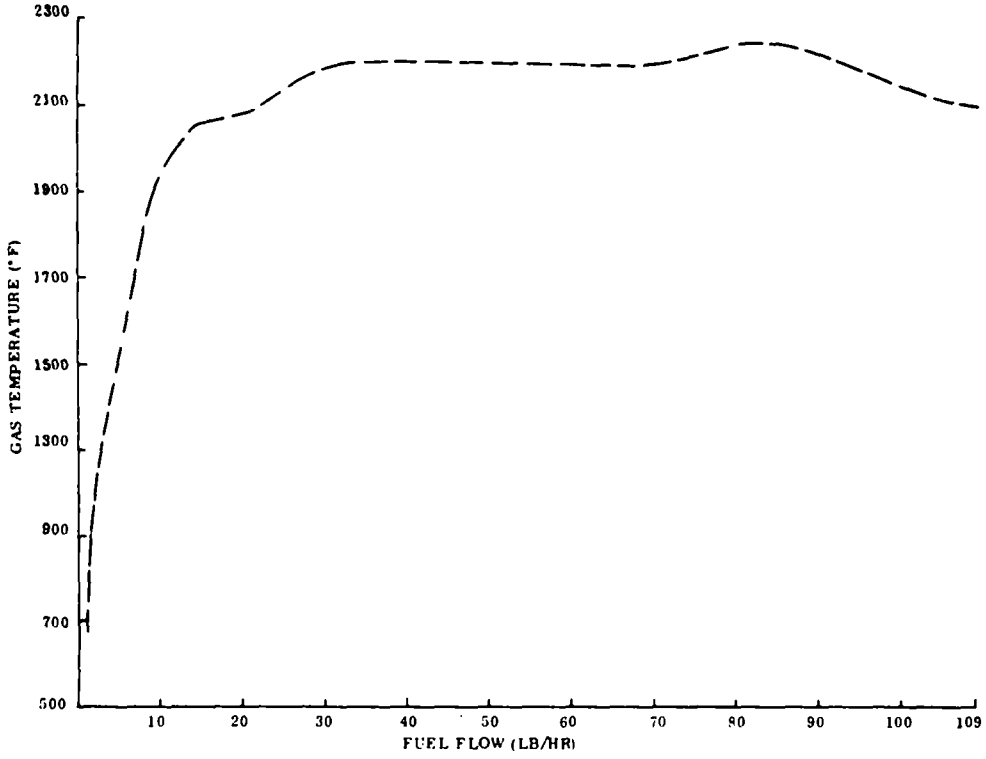

FIGURE 77. FINAL AIR-FUEL CONTROL SYSTEM. DISCHARGE TEMPERATURE VARIATION WITH FUEL FLOW

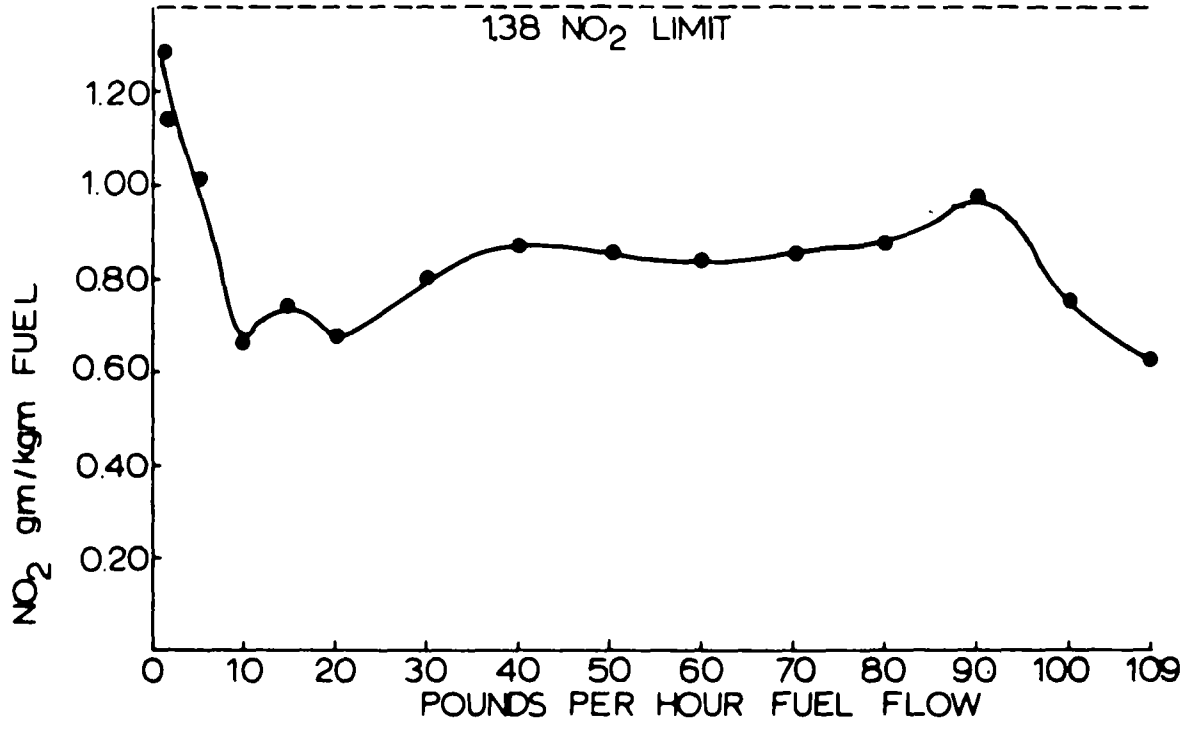

FIGURE 78. EMISSION OF NO_2 AS A FUNCTION OF FUEL FLOW

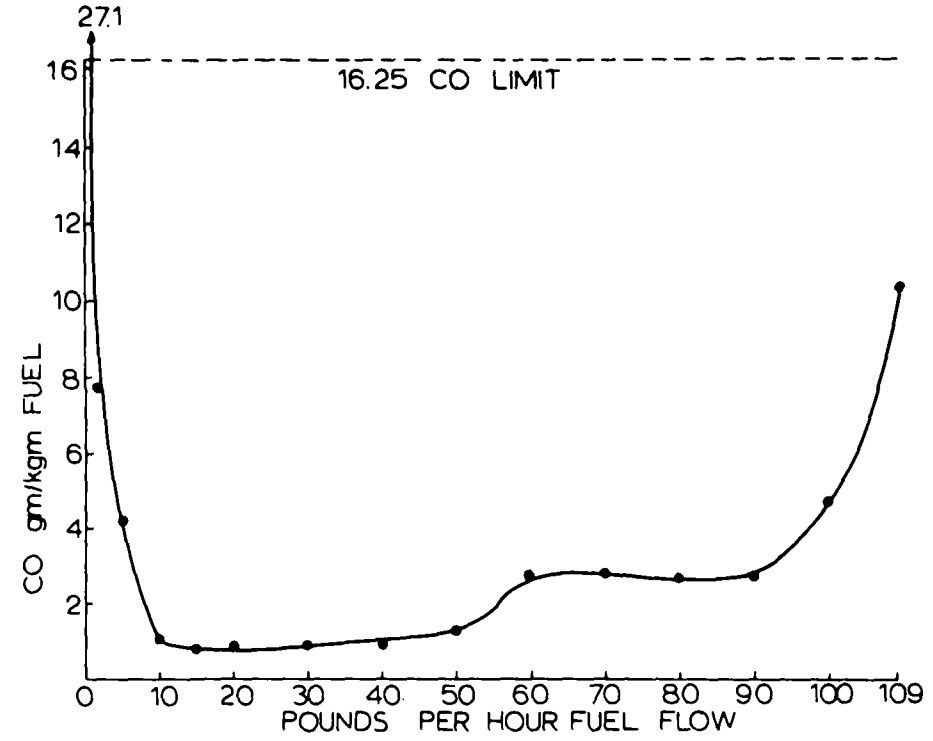

FIGURE 79. EMISSIONS OF CO AS A FUNCTION OF FUEL FLOW (TEST A)

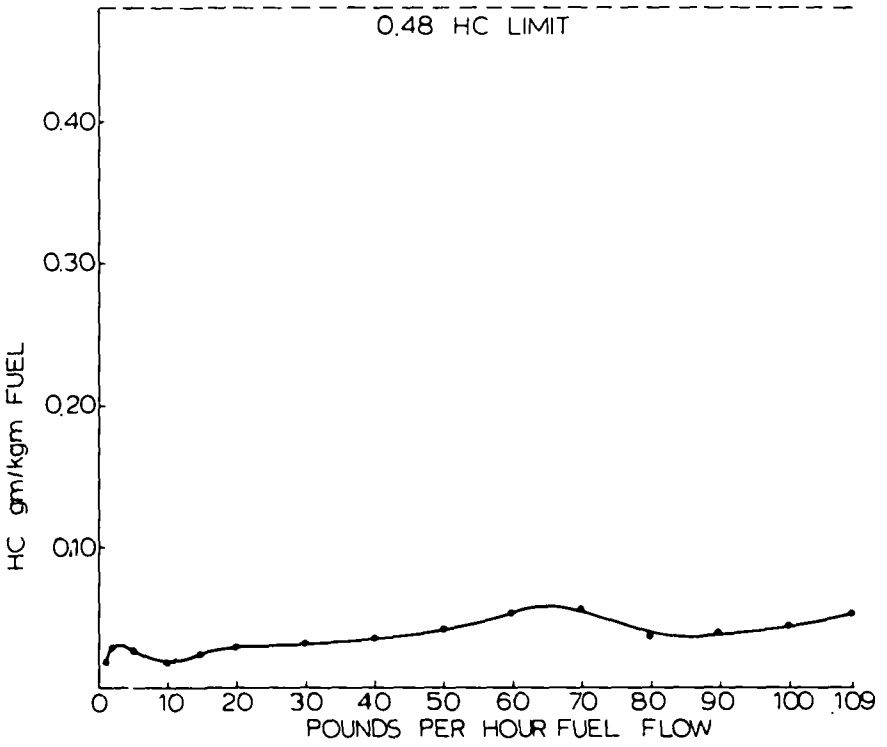

FIGURE 80. EMISSIONS OF HC AS A FUNCTION OF FUEL FLOW (TEST A)

		EMISSIONS AS A FUNCTION OF FUEL FLOW IN GM/KGM															
Fuel Flow pph →		109	100	90	80	70	60	50	40	30	20	15	10	5	2	1	Fuel
Test A	CO	10.4	4.74	2.74	2.69	2.80	2.75	1.34	0.99	0.91	0.86	0.79	1.07	4.33	7.80	27.10	JP 5
	HC	0.053	0.044	0.039	0.036	0.055	0.054	0.042	0.036	0.032	0.029	0.025	0.019	0.026	0.030	0.191	
	*NO_2	0.616	0.754	0.978	0.872	0.851	0.835	0.854	0.874	0.795	0.672	0.734	0.661	1.105	1.140	1.300	
Test B	CO	6.17	5.94	7.29	3.82	2.54	1.79	1.21	1.02	0.09	0.10	0.09	0.10	0.14	0.21	3.04	JP 5
	HC	0.400	0.364	0.250	0.241	0.241	0.234	0.234	0.233	0.248	0.263	0.253	0.261	0.308	0.362	0.283	
	NO_2	1.818	2.100	1.921	1.840	1.928	1.912	1.913	1.910	1.840	2.010	1.836	1.808	2.350	2.910	2.650	
Test C	CO	1.41	1.13	1.07	0.55	0.14	0.07	0.07	0.07	0.00	0.08	0.09	0.10	0.20	0.27	0.48	JP 4
	HC	0.168	0.089	0.129	0.056	0.044	0.029	0.014	0.014	0.014	0.000	0.000	0.000	0.000	0.000	0.000	
	NO_2	1.452	1.542	1.528	1.560	0.430	0.330	1.196	1.065	1.060	1.093	1.158	1.118	1.208	1.468	1.970	
(HC not adjusted for background)	HC	0.322	0.239	0.272	0.197	0.191	0.172	0.158	0.156	0.157	0.123	0.112	0.116	0.184	0.218	0.330	
Test D	CO	2.88	2.60	0.69	0.13	0.00	0.00	0.00	0.00	0.00	0.00	0.00	0.00	0.93	5.81	3.66	JP 5
	HC	0.053	0.048	0.048	0.055	0.060	0.055	0.059	0.062	0.055	0.061	0.063	0.070	0.110	0.202	0.252	
	NO_2	1.702	1.530	1.930	1.702	1.708	1.640	1.540	1.511	1.388	1.351	1.270	1.172	1.831	1.108	1.430	

Test A - Standard configuration, JP 5 fuel maximum heat losses to ambient.
Test B - As with Test A but with minimum possible heat losses to ambient.
Test C - Primary flame zone leaned out 25%, JP 4 fuel, minimum possible heat losses.
Test D - As with Test C but with JP 5 fuel.

* Measured as NO and Reported NO_2 (Appendix D)

FIGURE 81. EMISSIONS AT VARIOUS FUEL FLOWS, WITH DIFFERENT FUELS AND AT TWO AIR-FUEL RATIOS, WITH AND WITHOUT HEAT LOSSES

These tests were done by taking emission samples immediately aft of the combustor exit. Heat losses were substantial, especially at low fuel flows, and would approximate to the heat losses that would occur if a vaporizer had been installed at this emission sampling point.

A long mixing duct was installed aft of the combustor, of ten inches length. This hot duct reduced the view and hence radient losses of the flame to ambient. The resultant emissions are shown in Figure 81 Test B. There was a substantial increase (approximately double) in NO_2 emissions and a reduction in CO emissions as would be expected. The HC emissions increased and this latter phenomena was unexpected and unexplainable. Further investigations are warranted.

Keeping the same overall air-fuel as previously, modifications were made to the primary flame zone such as to increase its air-fuel by 25 percent. The radiation shielding was retained and the results shown in Figure 81, Test D. The results were a very substantial reduction in CO and HC emissions such that, for most of the operational range that would ordinarily be used in city driving, these emissions are negligibly small. Emissions of NO_2 reduced slightly, and thus indicates that a more optimum arrangement of air-fuels in the various zones of combustion exists which could further reduce emissions.

Maintaining the same lean primary flame zone and radiation shielding the test was repeated using JP-4 and the results are in Figure 81, Test C. Changes in emissions were noted, of a small amount. At some fuel flows emissions were higher, at other flows, less than when JP-5 fuel was used, but in general, emissions with

JP-4 were slightly less than with JP-5. Also shown are the HC emissions not corrected for background. (At the test site background HC emissions were high due to the proximity of the municipal airport.) The HC emission levels recorded indicate that the combustion process serves to lower these emissions to less than background.

The results indicate that emissions can be kept below the goals set, but that the design of the vaporizer must be carefully integrated with the combustor in order to avoid excessive heat loss and resultant high emissions.

7.3.7 Combustor Noise

Certain operating conditions of combined Rankine Cycle fan and combustor result in an acoustic resonance. A combustor modification solved the resonance problem, but unfortunately had adverse effects on emission levels. Sound level frequency analysis of "before-and-after-fix" runs are shown in Figure 82. The modification reduced maximum combustor frequency peak from 107 db (sound pressure level, Ref. $20\mu N/m^2$) to 94 db at 109 lb/hr fuel flow (full power). Figure 83 distinguishes noise components of the combustor at an off-exit location.

The test conditions were:

- Fan inlet guide vanes: installed
- Microphone position and orientation: (1) on fan axis three feet in front of inlet at 45 degrees to axis for runs shown in Figure 82. (2) Data in Figure 83 is taken 12.5 feet radially from combustor exit, five feet from ground, 45 degrees orientation. (See Fig. 84).
- Surroundings: Outside, ten feet from brick wall (See Fig. 84).
- Equipment: Same as described for fan noise tests (Section 6).
- Background noise: Figure 82 indicates noise levels with only fan power generator operating. Figure 83 includes operational fan as part of background noise so that combustor components can be separated.

Table V summarizes the significant frequency peaks of the test series.

Summary of Results

1. Before modification, combustor resonance shows a frequency shift from 240 cps to 310 cps with a change of fuel flow from 20 lb/hr to 109.5 lb/hr. The sound level remains approximately the same at 106 to 107 db.

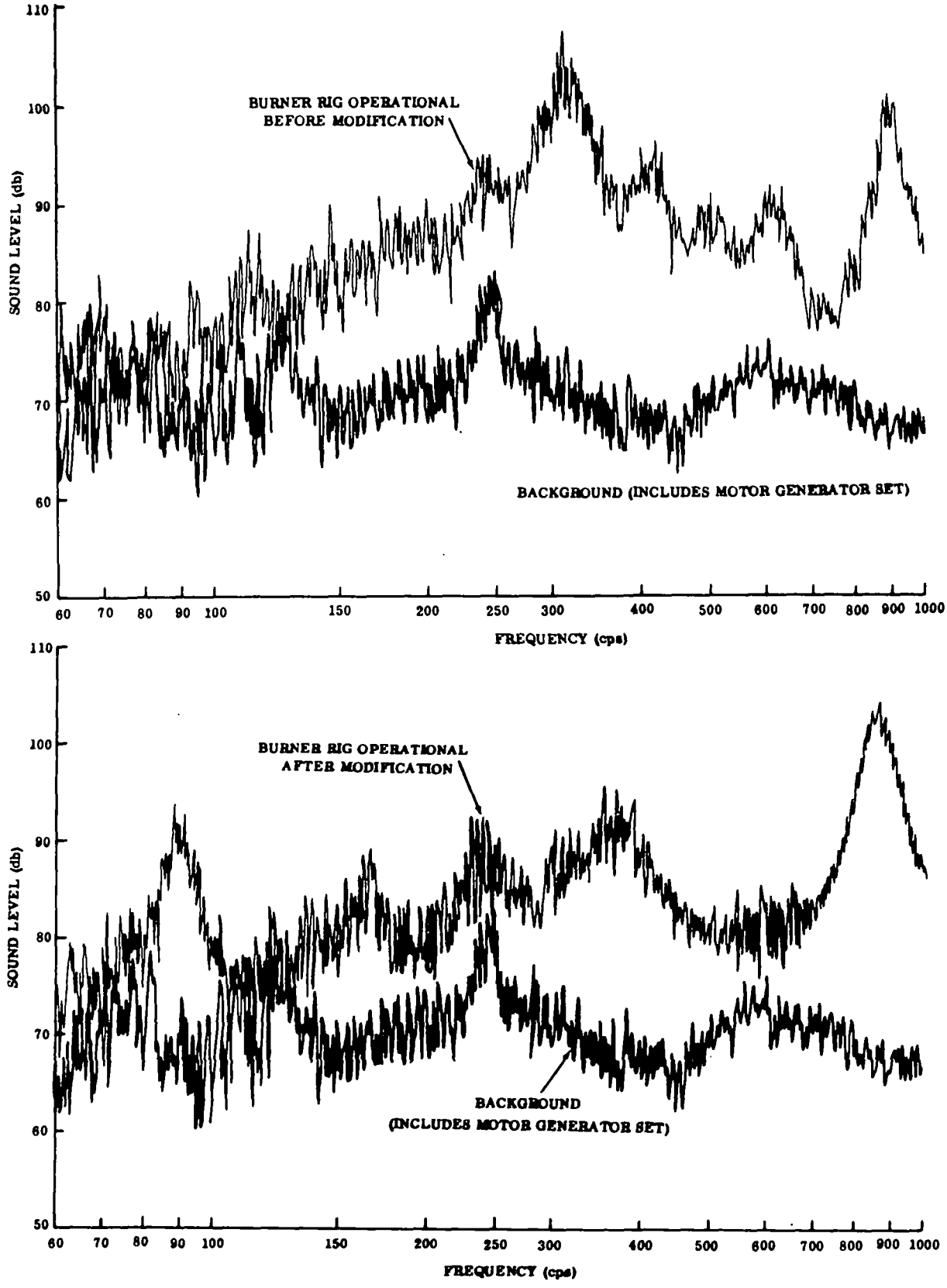

FIGURE 82. BEFORE AND AFTER MODIFICATION BURNER NOISE AT LOCATION "A"

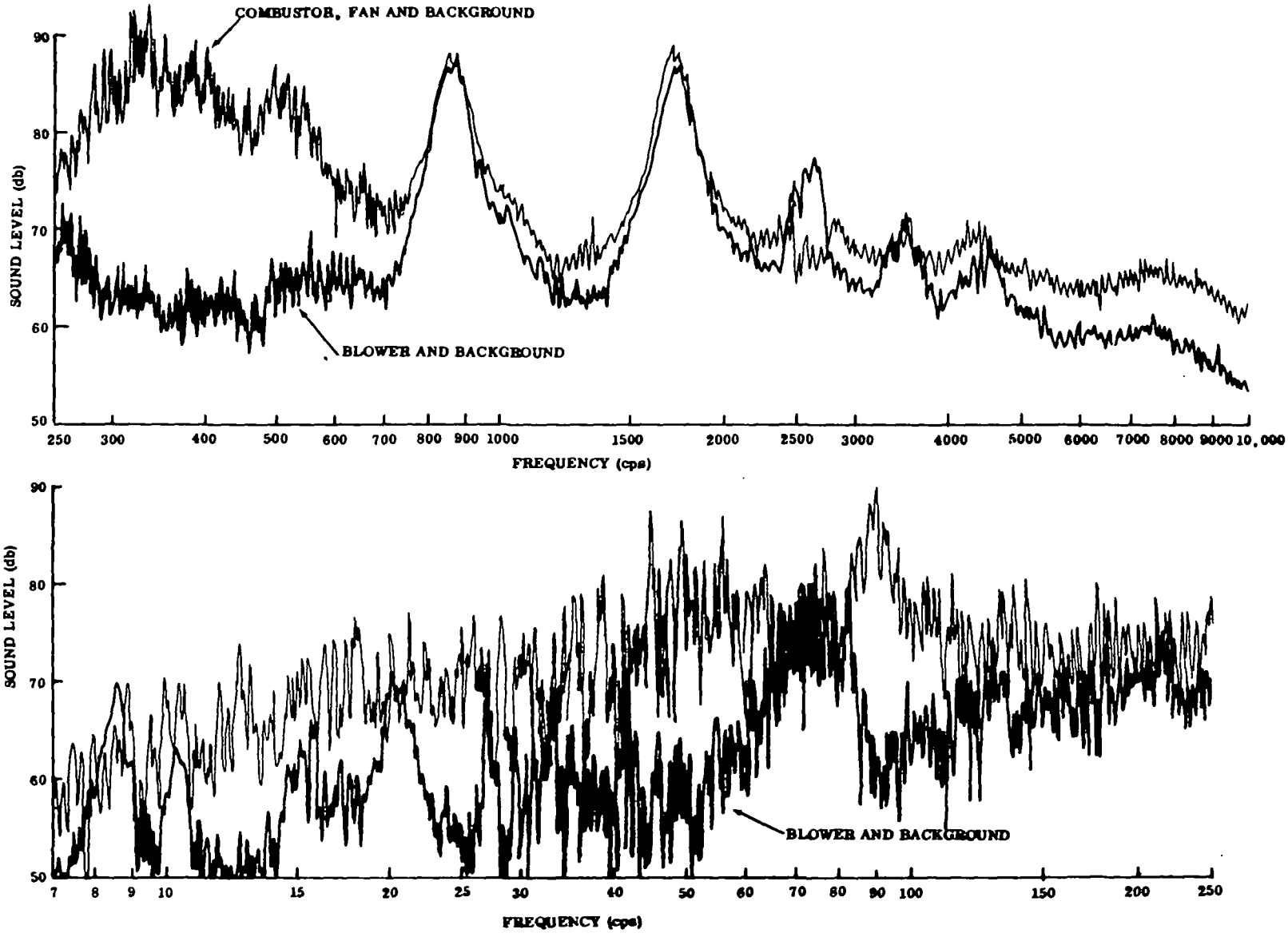

FIGURE 83. IDENTIFICATION OF COMBUSTOR NOISE AT LOCATION "B"

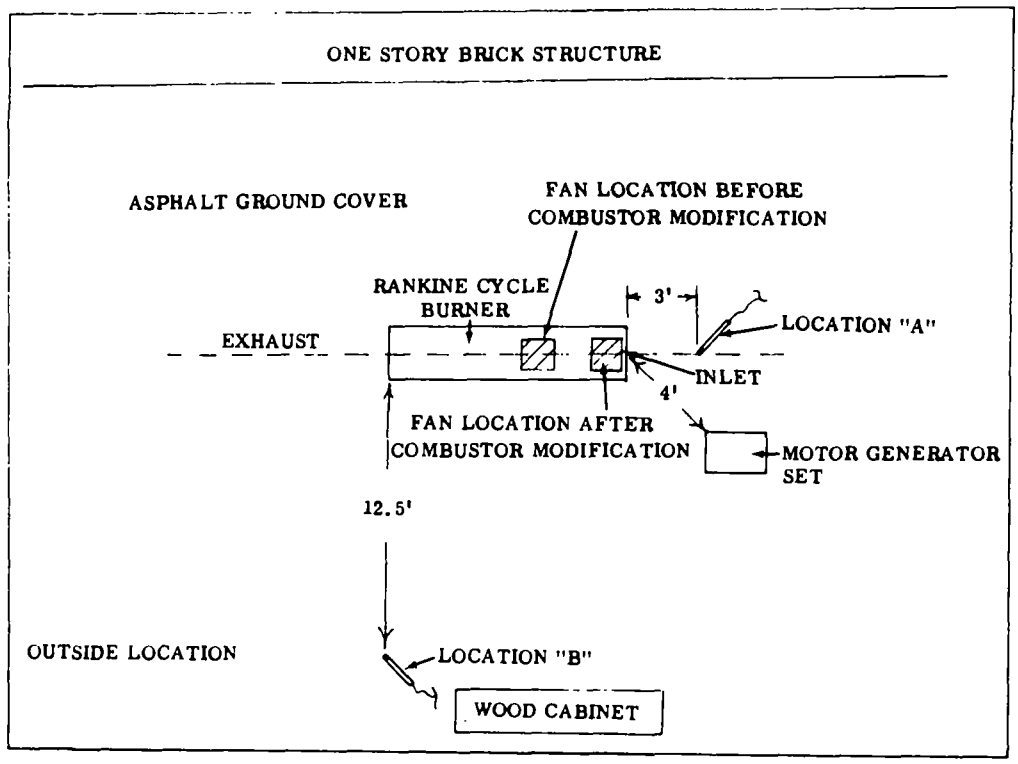

FIGURE 84. DIAGRAM OF COMBUSTOR ACOUSTIC TEST LOCATION

TABLE V

SIGNIFICANT NOISE FREQUENCY PEAK LEVELS

Frequency (cps)	Before Combustor Modification		After Modification			Source
	Inlet Axis Location "A"			Off Exit Location "B"		
	20 lb/hr Fuel Flow	109.5 lb/hr Fuel Flow				
	Fan and Combustor				Fan Only	
90	None	None	94 db	89 db	None	Combustor
240	106 db	95.5 db	93 db	None	None	
310	No Peak	107 db	91 db	92 db	None	
350	94 db	94 db	94 db	93 db	None	
900	100 db	101 db	104 db	88 db	88 db	Fan and Harmonics
1750	90 db	90 db	88 db	89 db	87 db	
2700	None	98 db	94 db	None	78 db	

2. The combustor modification eliminates the combustor as the dominant noise source as measured at location "A". A new 94 db peak at 90 cps occurs after the change and the 107 db peak at 310 cps is significantly reduced to 91 db.

3. After modification with fan and combustor operating a measurement to be 99 db at location "B". (Measured in the all frequency pass mode, flat frequency response mode-weighting contours not used.)

   (It should be noted that the change in the fundamental fan peak level at 900 cps from 101 db to 104 db before and after combustor modification is due to a relocation of fan position. See Figure 84 for details.)

7.3.8 Ignition Tests

A prime source of hydrocarbon emissions is cold light off. Ignition must be instantaneous otherwise resultant emissions are unacceptable. Throughout all the tests ignition procedures were monitored and, at all times, good ignition occurred and no failures to light were seen. Tests were done, simulating cold day starts at -40° F with kerosene,by using a heavy, less volatile fuel of 17 centistokes viscosity (the highest viscosity likely). Good ignition could be obtained and the flame performance at maximum fueling rate appeared similar to that obtained with JP-5 (no emission data was taken). However, ignition reliability was only 50 percent and it is suspected that a reduction in fuel flow at ignition (nominally 10 lb per hour of fuel) due to viscous effects on the fuel control system was the cause of this. At high fuel flows this viscous effect is reduced (it is a function of Reynolds number) and fuel flow was satisfactory. Some further investigations are indicated.

7.3.9 Aldehydes and Smoke

No instrumentation was available to measure either aldehydes or smoke. Throughout the tests reliance had therefore to be placed on sight and smell to assess these emissions. In steady state operation the flame was odorless and smoke free. Indicating that aldehydes and smoke were at a very low level or perhaps nonexistant. During transient decelerative operations, at low levels of fuel flows it was seen that some smoke was emitted though emissions of CO, NO_2 and HC were maintained low. The level of smoke was a direct function of deceleration and it was therefore a likely result of differing response characteristics of the fuel and air flow. The problem was minimized by controlling the deceleration rate in transient tests as a function of fuel flow. At high flow rates deceleration was maintained at a higher rate than at low flows. This fits in well with the response requirements of the system in that vaporizer response at high fuel rates must be quicker than at low fuel rates. Future work must involve complete package testing if minimum smoke is to be obtained and synchronization of the air and fuel metering systems must be improved.

8

OPTIMUM DESIGN APPROACH FOR RANKINE CYCLE COMBUSTION SYSTEM

Based upon the results of the analysis, design and test program conducted on the demonstration system a number of specific conclusions may be formulated:

- The 1980 AAPS emission levels for automotive vehicles are feasible.
- A relatively small combustion system incorporating hydromechanical control components can operate at high response across a fully modulated heat release rate of 100 to 1 (2×10^6 to 2×10^4 BTU/hr).
- Emissions during the required high frequency automotive startup, power level transients and shutdown cycles can be maintained below emission level goals (start up in 3 seconds, combustor only, transient response 50%/sec).
- Air flow changes resulting from voltage, leakage and efficiency changes can be compensated to maintain correct air-fuel ratios for low emissions.
- Heavy fuels such as Diesel No. 1, Jet A, Kerosene or JP-5 can be burned across the full flow range.
- Parasitic power can be minimized at part loads by the fuel delta-P compensator.

A set of design factors determined to be of major importance in the development of a low emission combustion system have also been identified. Listed below are some of the major design guides determined by analysis and test results.

- Precise control of combustion in three axial zones with rapid time transitions between primary and secondary zones is necessary.
- Mixing must be rapid and uniform.

- Overall air-fuel ratio must be precisely controlled across the entire heat release range.

- Uniform air distribution into the air valve and combustor is essential for low emission combustion.

- Flame radiation losses are important factors in emission levels.

- High response of both air and fuel flow control is necessary throughout transients. Fan speed control is probably inadequate due to inertial lags.

- Air valve appears to require flow symetry to obtain 100 to 1 flow control.

- Fan design and configuration has a major effect upon the air valve design and combustor performance.

- Vaporizer effects on aerodynamics and radiation flame radiation heat loss may also have significant effects upon the design and emission performances of the combustion system.

An optimum system can be synthesized based upon results of the demonstration system tests. A major factor in determining the package configuration of the demonstration system was component availability and the need for design flexibility in this highly developmental program. Although the best fan found to be readily available has low volume (0.2 cubic feet) and low weight (13 pounds), it is not optimum. Initially, it was designed for aircraft applications. Weight and volume are emphasized in these designs with noise only as a secondary consideration. Thus, the unit is a small diameter, high speed fan having a high dynamic head. In order to obtain accurate air regulation across the 100 to 1 range, the adverse aerodynamic effects of the dynamic head must be eliminated. To do this, a relatively large volume cavity at the discharge side of the fan is needed to turn the flow and reduce its velocity. Another design feature that would also be eliminated in a production type unit would be a separate drive motor for the rotating cup atomization system. Its use in the demonstration unit is necessary due to rotational speed requirements and need for initial independent optimization of the atomization system. It also added to the length (~4 inches) and overall volume of the complete system.

The package design depends critically on the overall pressure drop through the system. The use of a low boiler pressure drop results in a different system than with a high boiler pressure drop. The effect on the combustor and control design philosophy is slight and it appears likely that the best system with either high or low loss boiler will incorporate a fan of larger diameter than currently used and which

will result in considerable improvements in performance and substantial reductions in length. The presence of a vapor generator could modify flame performance depending upon its design. By proper integration of the vapor generator, flame performance may not be effected and may even be improved.

Several significant areas for improvement can be identified by matching fan size and speed to the geometry and flow requirements of the air valve and combustion system. Optimizing the system will reduce volume, power and noise significantly. An optimum configuration of this type is compared to the demonstration system in Figure 85.

The optimum system considered is based on slight modifications to the demonstration system design. Basically a better aerodynamic interface is the key element in the optimum configuration. Lower turning and metering losses are expected together with a corresponding reduction of parasitic power. A small reduction in combustor pressure drop also appears quite feasible by increasing the outside diameter of the basic combustor. As a result of use of a large diameter fan and a combined fan motor rotating cup drive, the overall length and volume can be reduced to as low as 14 inches. Parasitic power loss at full load could be as low as 1.25 HP with part load parasitic power drain well under 0.5 HP if voltage is reduced at lower power demands.

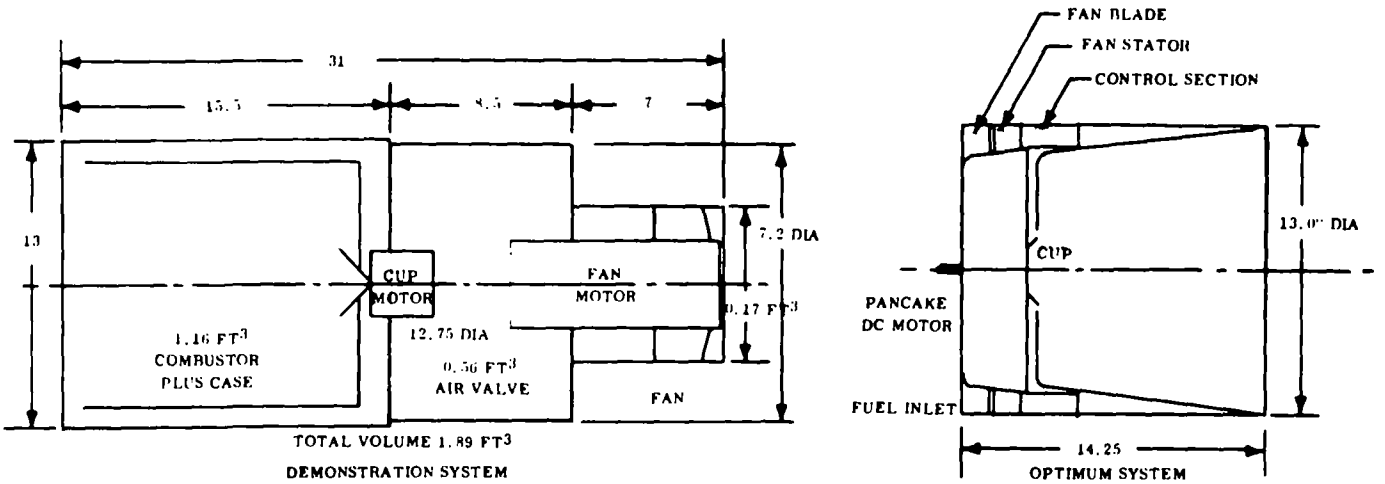

	Demonstration System Design	Optimum System Design	Spec
Total Volume (ft^3)	1.89	1.09	1.33
Length (Inch)	31.0	14.25	
Diameter (Inch)	13.00	13.00	
Combustor Volume (ft^3)	0.687	0.687	
Combustor Diameter (Inch)	11.00	12.00	
Horsepower	2.30	1.25	2.00
Combustor Loss (Inch Water)	8.00	6.0	
Diffuser Loss (Inch Water)	3.00	0.5	
Metering Loss (Inch Water)	2.00	1.5	
Overall Pressure Loss (Inch Water)	13.00	8.0	
Fan Efficiency (%)	75.0	85.0	
Motor Efficiency (%)	75.0	75.0	
Overall Efficiency (%)	56.2	68.0	
Motor Speed (rpm)	14000	7000	

Note: Ignition, Fuel and Air Regulators not included.

FIGURE 85. TWO FAN SKETCHES - PRESENT AND OPTIMUM

APPENDIX A

APPENDIX A

EMMISSION MONITORING EQUIPMENT AND PROCEDURES

Emission measurements were taken using three Beckman Model 315A infrared analyzers, Figure A-1, and a Beckman Model 402 hydrocarbon analyzer, Figure A-2. These instruments provided continuous and automatic determination of the exhaust components.

The infrared analysis system is based on a differential measurement of the absorption of infrared energy. An infrared radiation source is transmitted through two long cells one containing the exhaust sample and the other a reference gas. In operation, the presence of the infrared absorbing component of interest in the sample stream causes a difference in the radiation absorption levels between the sample and reference sides of the system. Due to this difference the gas in the reference cell is heated more, thus raising the pressure and causing a metal diaphragm to distend. This metal diaphragm is part of a capacitor circuit, as the IR source beams are alternately blocked and unblocked, it pulses, thus causing a cyclic change in the detector capacitance (Luft Principle). The resultant signal is then routed to the amplifier control section, and finally to the recorder.

The hydrocarbon sensor is a burner where a regulated flow of sample gas passes through a flame sustained by regulated flow of a fuel gas and air. Within the flame, the hydrocarbon components of the sample stream undergo a complex ionization that produces electrons and positive ions. Polarized electrodes collect these ions, causing current to flow through measuring circuitry located in the electronics unit. The ionization current is proportional to the rate at which carbon atoms enter the burner and is therefore a measure of the concentration of hydrocarbons in the original sample.

The following conditions were employed for all analysis:

Gas	Detection	Range
NO	IR-41" cell	0-150 ppm
CO	IR-10" cell	0-1000 ppm
CO_2	IR-0.25" cell	0-16%
Hydrocarbons	FID	0-500 ppm, 0-10 ppm

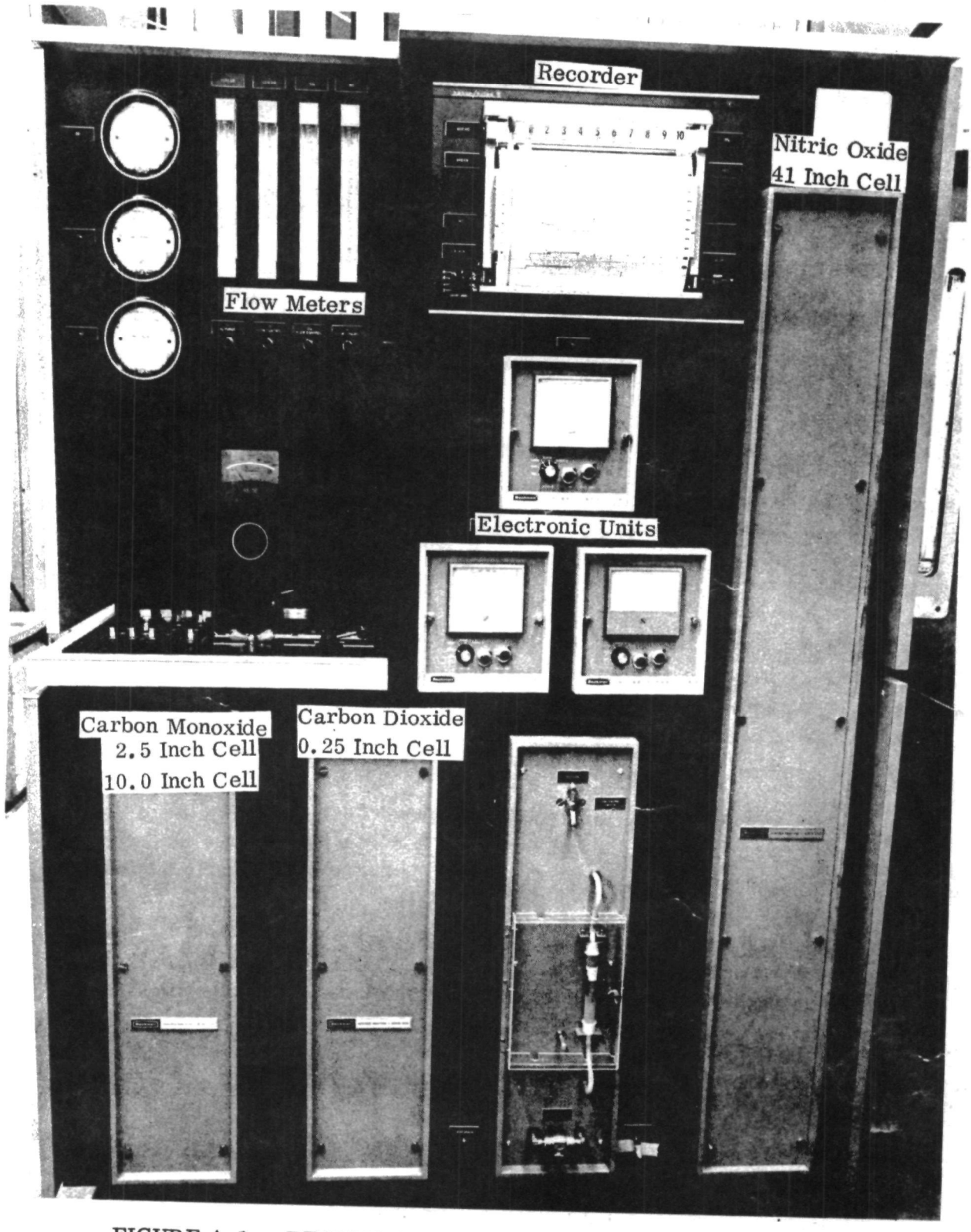

FIGURE A-1. BECKMAN MODEL 315A INFRARED ANALYZER

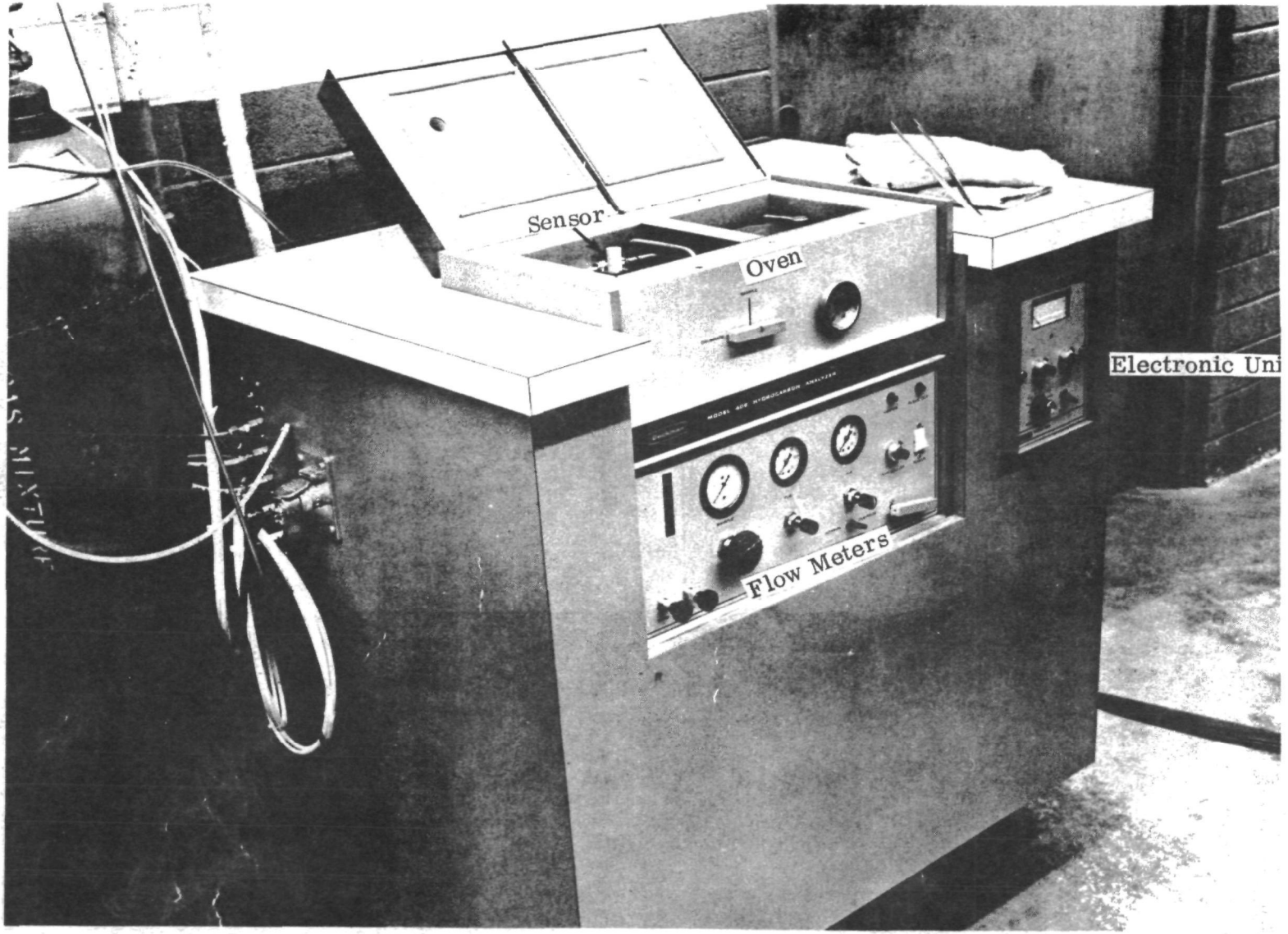

FIGURE A-2. BECKMAN MODEL 402 HYDROCARBON ANALYZER

Each instrument was calibrated and maintained per manufacturer's recommendations. Calibration curves supplied by Beckman were cross checked each day with known gases to determine the validity of these curves. The NDIR unit was kept on at all times in order to permit maximum stabilization. No difficulties or large variances were encountered in maintaining day-to-day gain settings, and zero settings.

Certified calibration gases as received from the vendor were within ±0.5 percent of the stated values with the exception of the nitric oxide standards. Nitric oxide calibration gases have an analytical accuracy of ±5.0 percent. Each NO standard gas was analyzed by the modified Saltzman* method employing the evacuated bottle sampling technique.

Table A-I shows the nitric oxide values obtained by the Saltzman method as compared to the vendor's analysis. (Average of a minimum of 5 determinations.)

TABLE A-I

NDIR COMPARED TO SALTZMAN

Stated Value	Infrared	Saltzman
140	---	144 ppm
105	100 ppm	118 ppm
53	45 ppm	47 ppm

The flame ionization hydrocarbon analyzer was calibrated immediately prior to each run and set up according to the manufacturer's specifications. Eight ranges are available on the instrument varying from 0-10 ppm to 0-50,000 ppm. All determinations required the lower two ranges. The heated sample line was maintained at 350° F and the detector at 400° F to avoid condensation problems.

Intensive investigations were performed at the start of the program to evaluate the sampling technique. The following facts were observed:

- Each analyzer unit required its own probe. Attempts to tee off from one probe showed adverse flow effects.

* Cornelius, W., and Wade, W. R., "The Formation and Control of NO in a Regenerative Gas Turbine Burner", SAE Report N_0. 700708.

- A filter (glass-wool)-dryer (Drierite-nonindicating) was used between the NDIR and the probe.

- Sample line length (20-200 ft) had little if any effects on the measurements, other than flowrate.

- The use of the pre-drier, plus the refrigerator and additional NO drier were more than adequate to remove all the water. (Aquasorb was used just prior to the NO cell).

- An air-quenched averaging probe was determined suitable for the combustor tail pipe.

The accuracy of the NDIR is dependent upon the accuracy of the calibration gases used. Each of the calibration gases were analyzed by the supplier using "gold" standards. These primary standards were prepared using National Bureau of Standards weights.

Reproducibility of the instrument is within one percent. Reproducibility tests were performed on separate days and under varying sampling conditions. The results showed that the measurements were reproducible.

TABLE A-II

REPRODUCIBILITY TEST

Power Setting	ppm NO	ppm CO	% CO_2	Flow $ft^3/m.$	Remarks
10-28-29					
50%	56	128	7.9	4	Probe Preheated
↓	61	120	7.9	2	↓
↓	60	120	7.8	1	↓
↓	60	128	7.9	4	↓
↓	56	120	7.7	2	↓ ~200' Sample Line
↓	59	120	7.7	3	Probe Not Heated
75%	64	282	7.7	3	Probe Heated
↓					↓ 200' Sample Line
↓	55	305	7.9	3	
25%	47	53	6.8	3	Probe Heated
↓	47	53	6.5	3	Probe Unheated
10-29-70					
50%	59	120	7.5	3	Probe Heated
↓	47	143	7.9	3	Probe Unheated
75%	62	295	7.8	3	Probe Heated
↓	56	335	7.9	3	Probe Unheated
25%	49	45	6.0	3	Probe Heated
↓	47	38	6.5	3	Probe Unheated

Because of the very low emission levels obtained with this combustor (compared to Otto cycle engines), special attention was required to calibrate the measurement system at the low ranges. Calibration gases in the actual ranges being recorded were obtained to establish the validity of the instrument deflection to volumetric concentration supplied by Beckman. Gases used for calibration were certified by the span gas suppliers to be within the following concentrations:

Nitric oxide

Concentration	Certified Accuracy
10.5 ± 0.5 ppm	± 5.0% of component
103.0 ± 2.1 ppm	± 2.0% of component
140.0 ± 2.8 ppm	± 2.0% of component

Carbon dioxide

Concentration	Certified Accuracy
14.31 ± 0.29%	± 2% of component
4.31 ± 0.09%	± 2% of component
2.10 ± 0.04%	± 2% of component
1.12 ± 0.02%	± 2% of component

Carbon monoxide

Concentration	Certified Accuracy
115 ppm ± 2 ppm	± 2% of component
225 ppm ± 4 ppm	± 2% of component
850 ppm ± 17 ppm	± 2% of component

(Recorder deflection error is ± 0.5% full scale.)

Results of calibration tests are shown plotted in Figures A-3, A-4, and A-5. The basic curve was supplied by Beckman. Data points used by Beckman to verify the basic curve slope are shown as open circles. Solar calibration points including the zero span gas point are shown with the closed circles. Good correlation was obtained throughout the range required to measure emissions with the Rankine cycle combustor.

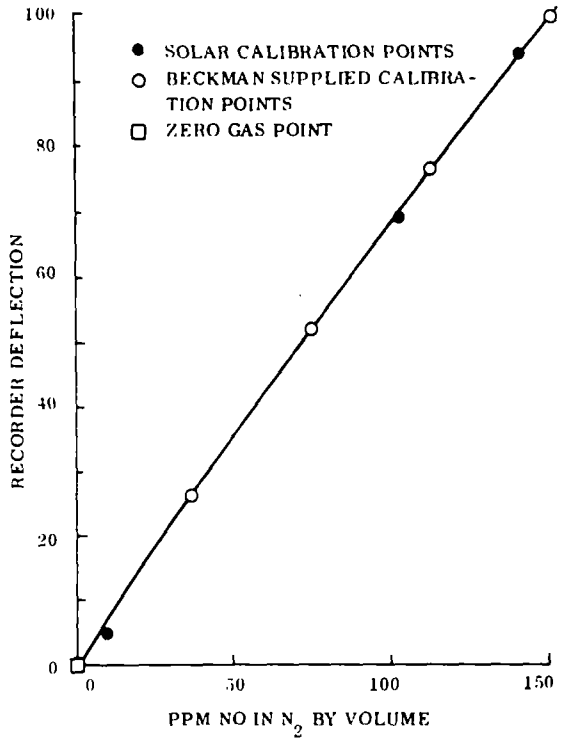

FIGURE A-3. NO CALIBRATION RESULTS

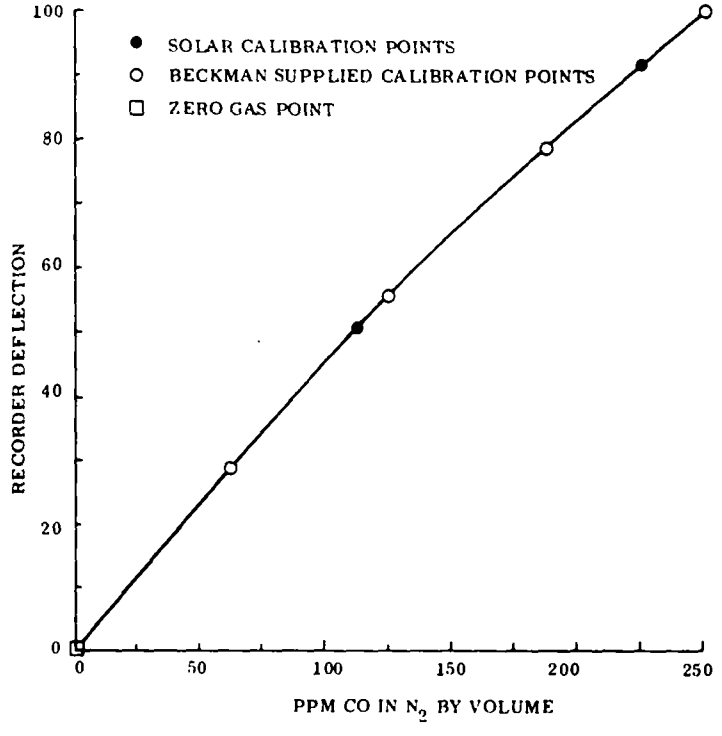

FIGURE A-4. CO CALIBRATION RESULTS

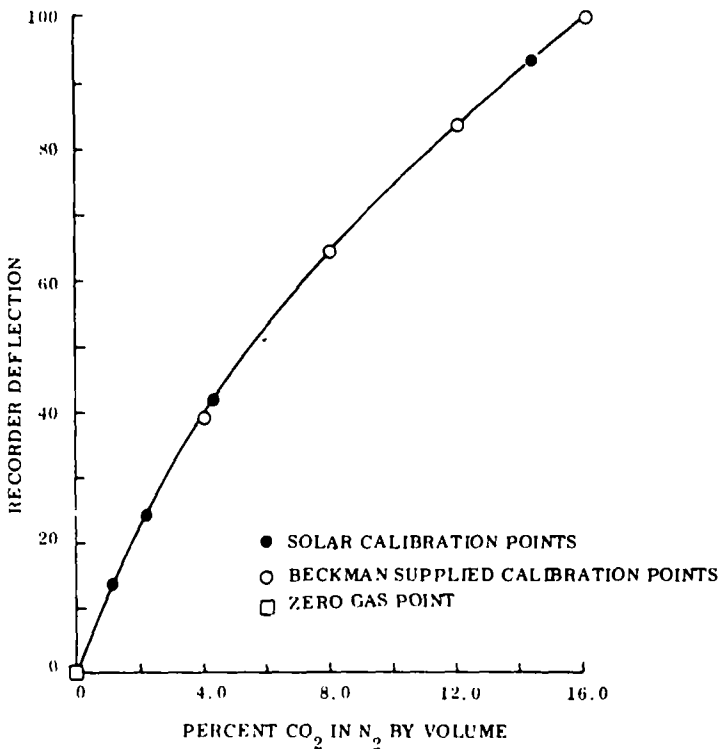

FIGURE A-5. CO_2 CALIBRATION RESULTS

APPENDIX B

APPENDIX B

TEST FUEL SPECIFICATIONS

The fuels specified to be used for combustion tests are #1 Diesel, kerosene and Jet A. These fuels can vary widely in their combustion characteristics because their specifications are loose. Refineries in differing locations can produce different fuels, meeting the same spec, because their production is guided by economics dictated by local conditions of demand and the type of crude that is available.

Solar is using JP-5, which is a more rigorously controlled fuel than those specified by EPA. It is a fuel that typically will be more difficult to burn than those specified. In addition, JP-4 and #2 diesel will be used to provide information with fuels that are respectively considerably more and less difficult to burn than those specified (Fig. B-1).

The Government has recognized this problem of fuel variability in regard to the testing of diesel engines* and has proposed a fuel spec for #1 diesel as follows:

	Specification		
Fuel Property	ASTM D-975 Grade 1-D	Proposed Government Spec	MIL-T-5624 Grade JP-5
Cetane	40 min.	48-54	
Distillation ° F			
Initial Boiling Point		330-390	
10%		370-430	400 min.
50%		410-480	
90%	550 max.	460-520	
End Point		500-560	550 max.
Gravity °API		40-44	
Total Sulfur %	0.5 max.	.05-.2	
Aromatics %		8-15	
Paraffins, Napthenes, Olefins		Remainder	
Flash Point ° F (min.)	100 or legal	120	140
Viscosity (Centistokes), at 100° F	1.4-2.5	1.6-2.0	

* Federal Register, Volume 35, Number 136, Part II.

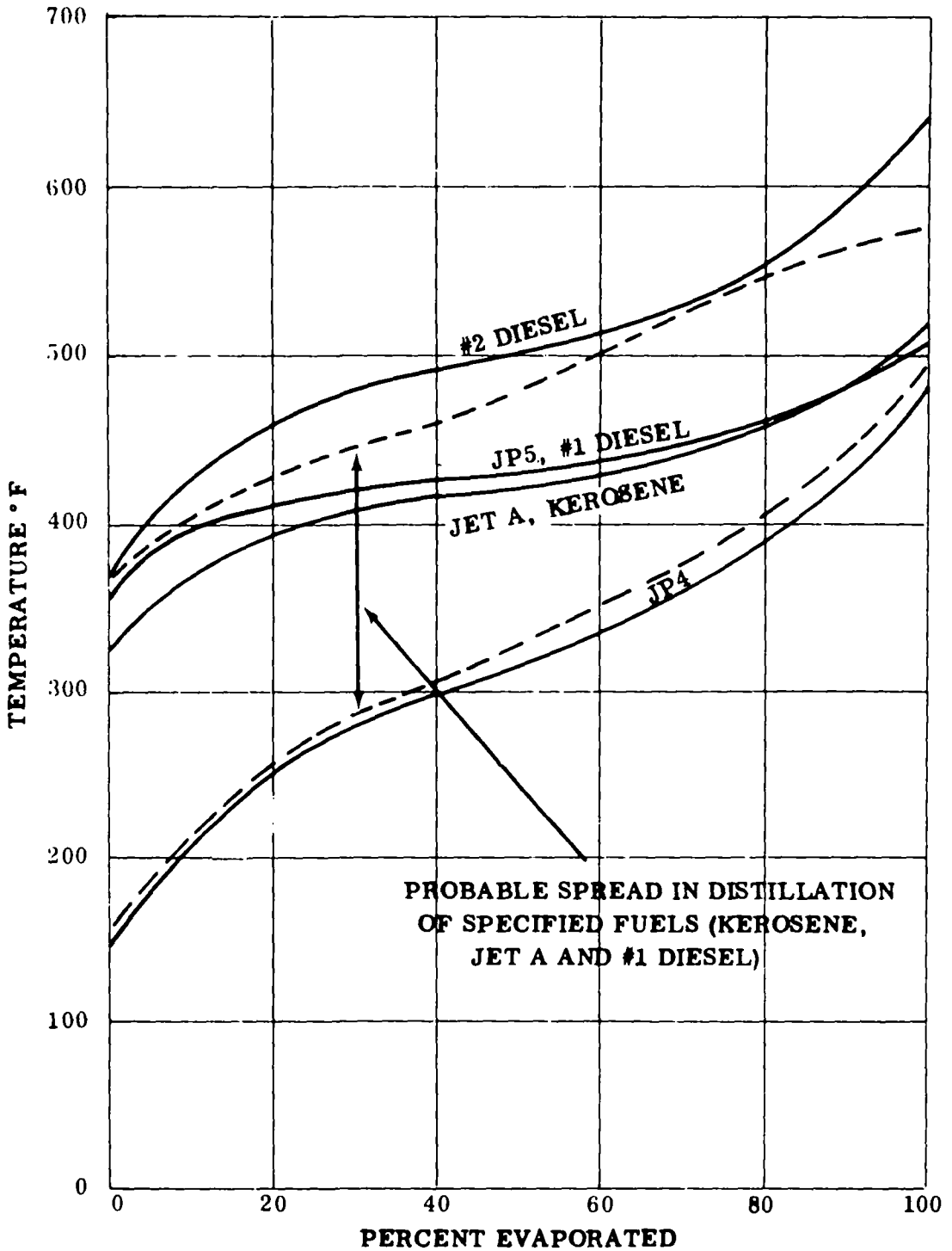

FIGURE B-1. VARIATION OF ASTM DISTILLATION TEMPERATURES FOR THE TEST FUELS (AVERAGE VALUES)

The proposed fuel is more rigorously controlled than current ASTM specs, agrees closely to the JP-5 fuel used by Solar and is representative of a typical grade of kerosene that could ordinarily be available. As the combustion characteristics of a diesel engine are different from those of an atmospheric combustor, it is likely that the specification above should be modified so as to highlight any combustion difficulties inherent in an atmospheric flame. Items that warrant more specific control are noted below with the reasons for such control

- Flash Point, °F, 140°F minimum, 150°F maximum

  A high flash point makes ignition more difficult and therefore should be controlled to the high end of typical practice. Current specs for fuels used have a maximum of 150° F but no bottom limit.

- End Point, °F, 550°F minimum, 600° F maximum

  A high end point tends to carbon build and smoke in exhaust. Current specs allow 575 °F maximum but a bottom limit is not specified.

- Aromatics, 20 to 25%

  High aromatics tend to cause smoke and carbon build. No specs currently apply and typically are lower than shown.

- Viscosity, 2.0 to 2.5 centistokes

  High viscosity makes control of fuel more difficult and makes for problems of fuel atomization with certain types of combustion systems. Typical values are less than shown and the range is 1.4 to 2.5.

- Olefins and Diolefins, 5 to 10%

  High diolefins tend to cause deterioration of fuel with resultant gum formation. This causes unreliability in fuel metering and fuel injection. No specs exist and typical values are below 5%.

Tests have indicated that most of the problems seen with burning a heavy grade of fuel such as JP-5 will tend to diminish with the lighter grades of kerosene.

The current specifications of the fuels to be used and of JP-5 are as follows:

	Jet A (ASTM D1655)	Kerosene (VV-K-211)	Kerosene (VV-K-220)	JP5 (MIL-T-5624)
Flash Point	110-150°F	115°F Min.	125°F Max.	140°F Min.
10% Point	400°F Max.			400°F Min.
50% Point	450°F Max.			
End Point	550°F Max.	572°F Max.	510°F Max.	550°F Min.

Of these fuels, Jet A and JP5 are the most tightly controlled. JP5 will inevitably be heavier than Jet A as flash point and 10 per cent point tend to be higher.

The specifications for the fuels to be used to monitor the limits of typical fuels are as follows:

#2 Diesel (ASTM D975)	JP4 (MIL-T-5624)
Flash Point 125°F or Legal	20% Point 290°F Max.
90% Point 540°F min., 640°F max.	50% Point 370°F Max.
	90% Point 470°F Max.

APPENDIX C

APPENDIX C

FAN NOISE REDUCTION METHODS

The National Air Pollution Control Administration Division of Motor Vehicle Research and Development has recently established a goal of 77 dbA as the maximum noise generated by the vehicle. Either the combustor or compressor fan are likely to be the critical noise source in the Rankine cycle vehicle. Thus, a detail analysis of the fan and its noise generation mechanisms is necessary. Results of noise measurements on the fan currently being used (because of availability) are analyzed in Sections 6 and 7. These results in general indicate that significant noise reduction would be necessary in a production system. An optimum low noise fan could be designed also to provide better aerodynamic and mechanical matching to the air valve and combustor. A design analysis indicates that this could be accomplished by incorporating the following changes:

- Increased diameter (up to 13 inches O. D.)
- Decreased rotational speed
- Decreased pressure rise
- Larger number of blades
- High vane to rotor blade ratios
- Increased spacing between blades and rotors

An investigation into the mechanism and relative noise improvements that can be expected has been initiated. Recent advances in aerospace acoustic analysis technology have made the optimum design approach method relatively clear. Up to the recent work in acoustics on turbo fan engines, the best empirical method to predict noise of fans was:

$$PWL = 90 + 10 \log HP + 10 \log P_S \quad (1)$$

or

$$PWL = 55 + 10 \log Q + 20 \log P_S \quad (2)$$

or

$$PWL = 125 + 20 \log HP - 10 \log Q \quad (3)$$

where PWL - db - overall sound power level re 10^{-12} watt

HP - hp - rated motor horsepower

Q - cfm - fan discharge flow

P_s-in. H_2O - fan total to static pressure rise *

These equations indicate the importance of maintaining as low a pressure rise (P_s) as possible. A more comprehensive approach to axial vane fans has recently been published by M. J. Benzakein and S. B. Kazin**. The following important design information has been abstracted from this work.

A study of various fan/compressor noise reduction methods is presented. The analytical treatment of the basic mechanisms of fan/compressor noise generation is described. The results are presented in parametric form and indicate the effects of fan/compressor design, number of blades, vane/blade ratio, aerodynamic parameters, and blade row spacing on pure tone noise reduction. These results are based on non-steady aerodynamic treatment of wake and potential interaction effects and theoretical extensions of spinning mode theories.

A listener in the vicinity of an axial-flow fan may distinguish two distinct sound components known as "discrete-frequency noise" and "broadband noise". The first component consists of a number of pure, or nearly pure, tones which combine to form a high frequency noise, best described as a whine. The second component is a background hissing noise, caused by a superposition of sounds over a continuous band of frequencies from the lower audible range to the higher, and without pronounced peaks at any particular frequencies.

The relative importance of the two noise components depends on the type of fan or compressor. Noise from a many-bladed fan, working at subsonic tip speed in an unobstructed airflow, has broadband characteristics. Noise from a high speed propeller has predominantly discrete-frequency characteristics. From a compressor in which the rotor interacts with stators, or a fan with bearing support struts or other obstacles near the rotor face, the noise is a mixture of the two components. Generally, however, the discrete-frequency noise dominates the frequency spectrum. The object of this paper is to present different methods by which the blade passing frequency tones can be reduced.

BASIC NOISE GENERATION MECHANISMS

The complexity of the fan/compressor noise generation phenomena lead many researchers to a largely empirical approach to the problem. Some broad understanding of the various sound sources has been derived from experimental data in the last

---

* Beranek, L. L., "Noise Reduction", McGraw Hill, New York, 1960.

** ASME 69-GT-9 Fan Compressor Noise Reduction, March 1969, M. J. Benzakein and S. B. Kazin.

ten years. It is felt, however, that a basic knowledge of the different noise sources is indispensable if fan/compressor noise is to be reduced at the source.

Different mechanisms are involved in the pure tone generation in fans and compressors. These different mechanisms vary in importance from configuration to configuration, and in a design, from speed to speed. Each particular mechanism can become the main noise contributor for a particular fan design at a particular speed. The major mechanisms are defined later.

Rotor Alone Noise

"Rotor alone noise" arises from the pressure field that surrounds each blade as a consequence of its motion. In a moving blade, the pressure distribution on each section along the blade span produces force fluctuations on the surrounding air. The force produced on the air by each blade is equal and opposite to the force produced on each blade by the air, and the latter force can be resolved into lift and drag components of the force on the blade along its aerodynamic axis.

The rotor alone noise is similar in nature to the propeller noise which has been extensively studied by Gutin, Garrick, and Watkins, and other investigators. The propeller noise theories are based, primarily, on three mechanisms: (a) thickness noise, (b) lift noise, and (c) vortex noise. The experimental results on fan/compressor noise showed however, that the lift (blade loading) portion is the primary contributor of the rotor alone noise. Attention has therefore been directed towards a prediction of rotor noise due to steady aerodynamic loading. The analysis consists of an extension of Gutin's work that includes the effect of a many-bladed rotor and the presence of the duct. It was assumed in this work that the blades do not interact. That is, each blade carries its own discrete pressure profile, and this periodic disturbance (in an absolute frame of reference) is mathematically described as an impulse occurring at the blade passing frequency.

Wake Interaction Noise

Turbomachinery aerodynamicists have long recognized that the airfoils arranged in rotating and stationary cascades of axial flow machinery, do not operate in steady flow. A distinction should be made, however, between the unsteadiness in the flow field created by the presence of an adjacent blade row which is characterized by the generation of pure tones at the blade passing frequency, and the unsteadiness due to the flow turbulence along the airfoils and in their wakes which represents the primary source of broadband noise in the machine. The broadband noise generated, is in general, of a lower order of intensity. A brief look will first be taken at the noise created by the interaction of the wakes shed by a stationary or rotating cascade with the following blade row. The wakes leaving a rotor or stator row necessarily impinge on the adjacent blade row as they pass downstream. Within the wake there is a reduction in velocity, and the primary effect of this velocity defect is to cause a fluctuating incidence at the downstream blade. This fluctuating incidence gives rise

to a fluctuating force which results in sound radiation.

PARAMETRIC STUDY OF ROTOR ALONE NOISE

Sound pressure levels generated by a rotor alone are a direct function of the circulation around the blade row. The larger the circulation the higher the pure tone levels. This is consistent with aircraft propeller experience. A study has been made to investigate these effects, parametrically, from a turbomachinery standpoint. Some of the results are shown in Figures C-1 and C-2.

- Figure C-1 shows that if the tip speed is held constant and the pressure ratio is increased, the fundamental frequency sound power levels increase.

- Figure C-2 shows that as the number of rotor blades is increased, the sound power levels generated decrease. This seems to indicate that a high blade design is favorable.

PARAMETRIC STUDY OF INTERACTION NOISE

A parametric study was carried out to determine the functional relationship between the pure tone noise generated in the fan by the wake interactions and the primary turbomachinery aerodynamic and geometric parameters. This study was restricted to fans and compressors without inlet guide vanes which, at the present time, tend to produce lower noise levels than comparable machines with inlet guide vanes. The study was also directed towards designs incorporating large blade row spacings, where the wake and not the potential interaction is the major source of noise.

Pressure Ratio Effect

In an initial study, the tip speed of the machine and the fan geometry (number of blades and vanes, spacing/chord, and so on) were kept constant. Different designs with pressure ratios varying from 1.2 to 1.4 were investigated. When the pressure ratio is increased at a particular speed, more turning has to be done in the blade row and the loading goes up. The terms V_1/V_2 abd sin 8 in the expression for the coefficient of unsteady upwash subsequently increase; this is translated into an increase of pure tone levels. It can be seen from C-3 that when the fan design pressure ratio is increased from 1.2 to 1.4, the fundamental blade passing frequency power levels increase about 8 db for a fan of constant size, and 4 db for a fan of constant thrust. These results indicate that pressure ratio is an important parameter that cannot be neglected. The use of simple correlation formulas that do not take this effect into account may lead to erroneous results.

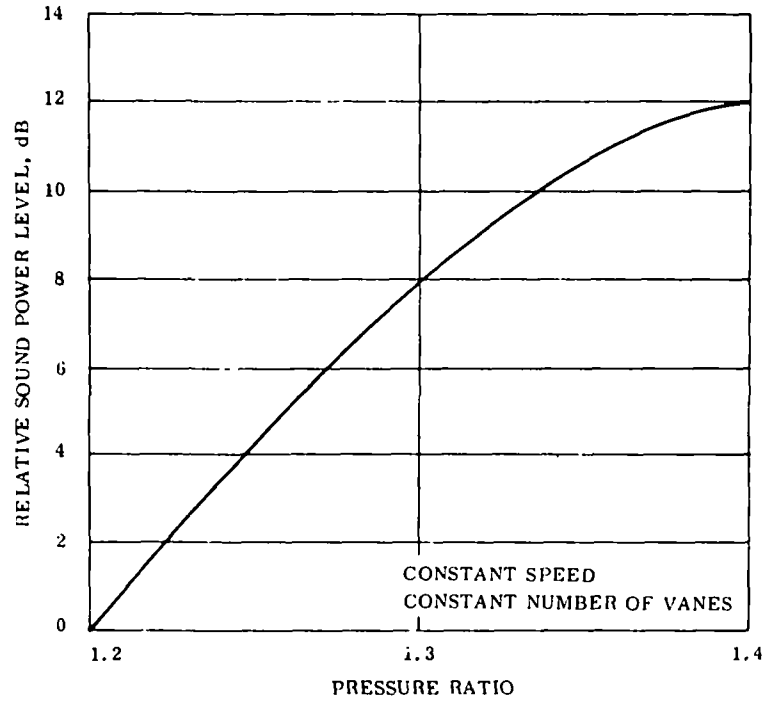

FIGURE C-1. EFFECT OF PRESSURE RATIO ON ROTOR ALONE BLADE PASSING FREQUENCY NOISE

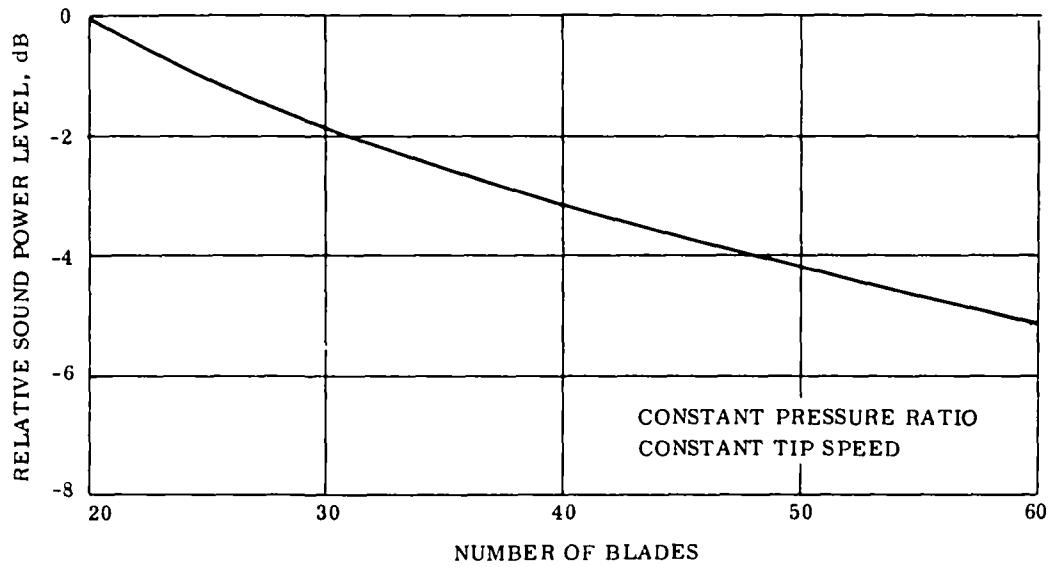

FIGURE C-2. EFFECT OF NUMBER OF BLADES ON ROTOR ALONE BLADE PASSING FREQUENCY NOISE

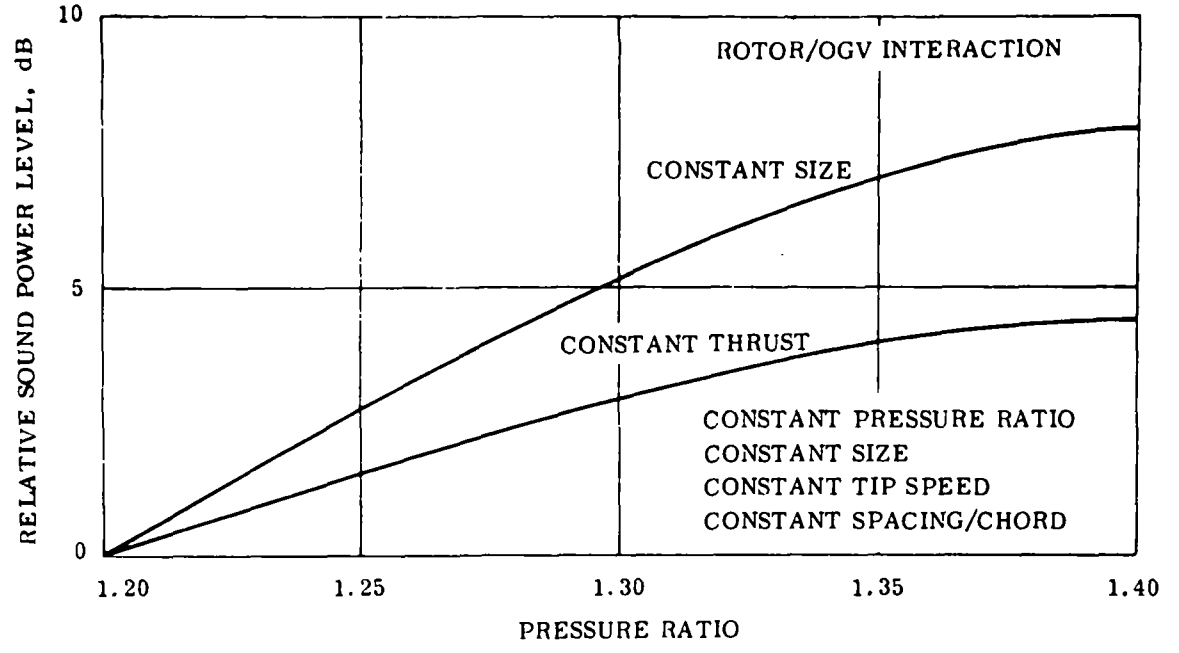

FIGURE C-3. EFFECT OF PRESSURE RATIO ON INTERACTION NOISE GENERATED AT THE BLADE PASSING FREQUENCY

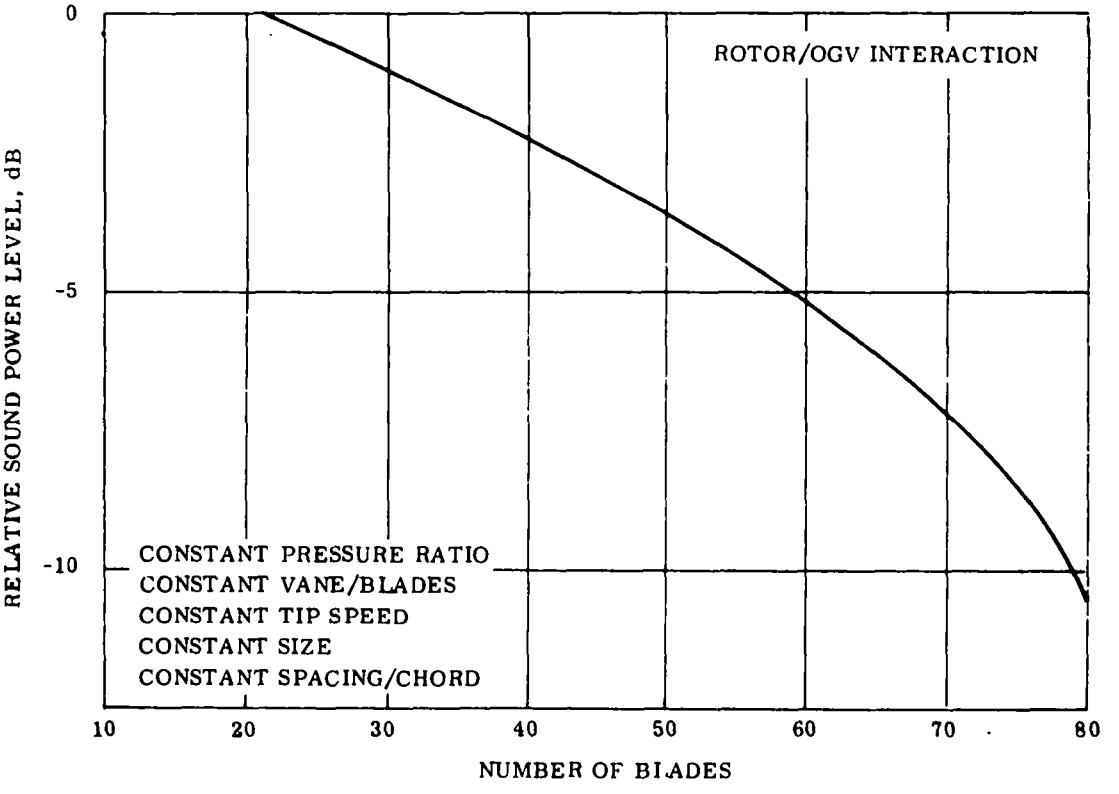

FIGURE C-4. EFFECT OF NUMBER OF BLADES ON INTERACTION NOISE GENERATED AT THE BLADE PASSING FREQUENCY

Number of Rotor Blades Effect

The number of rotor blades is an important parameter in the noise generation and can easily be modified (within certain vibration and aerodynamic bounds) to suit the acoustic designer. Should fan designs, therefore, be oriented toward a high or a low number of blades? The final answer depends upon the fan size. The number of blades and the fan rpm will determine the pure tone frequency, which should be kept out of the critical area of the NOY curve. Therefore, the size, as well as the blade tip speed of the fan, must be known before a final selection of the number of blades can be made. An investigation can be done, however, of the effect of the number of blades on the sound power levels generated at the blade passing frequency. In the following study, the pressure ratio, tip speed, blade row spacing, and the vane/blade ratio were kept constant and the number of blades were varied from 20 to 80. The results are shown in Figure C-4. It can be seen that a design incorporating a high number of blades will reduce the fundamental frequency tones. The fan size and rpm will determine the optimum configuration from a PNdb viewpoint.

Vane/Blade Ratio Effect

The analysis of the sound generation shows that the number of interaction diametral modes (or in other terms, the vane/blade combination) has a major effect on the blade passing frequency tones. Figure C-5 shows that a high vane/blade ratio can be beneficial, not only from a sound transmission, but from a sound generation viewpoint, as well.

Blade Row Spacing Effect

It is well known that increasing the spacing between blade rows will decrease the interaction noise. Several experimental investigations have determined the reduction in pure tone levels that can be obtained when the blade row spacing is increased. Some researchers show a 2 db reduction in sound pressure levels per doubling of the axial separation, while others prescribe 4 or even 6 db SPL. This inconsistency can be explained first by the fact that several other parameters besides axial spacing are involved in the interaction process, and second, because the concept of "per doubling" is not strictly correct.

In the present study, a particular rotor/OGV configuration was chosen and the spacing varied from 0.1 to 2.0 spacing/chord ratio. The results are shown in Figure C-6. It can be seen that an appreciable reduction in pure tone power levels can be obtained with large blade row spacings.

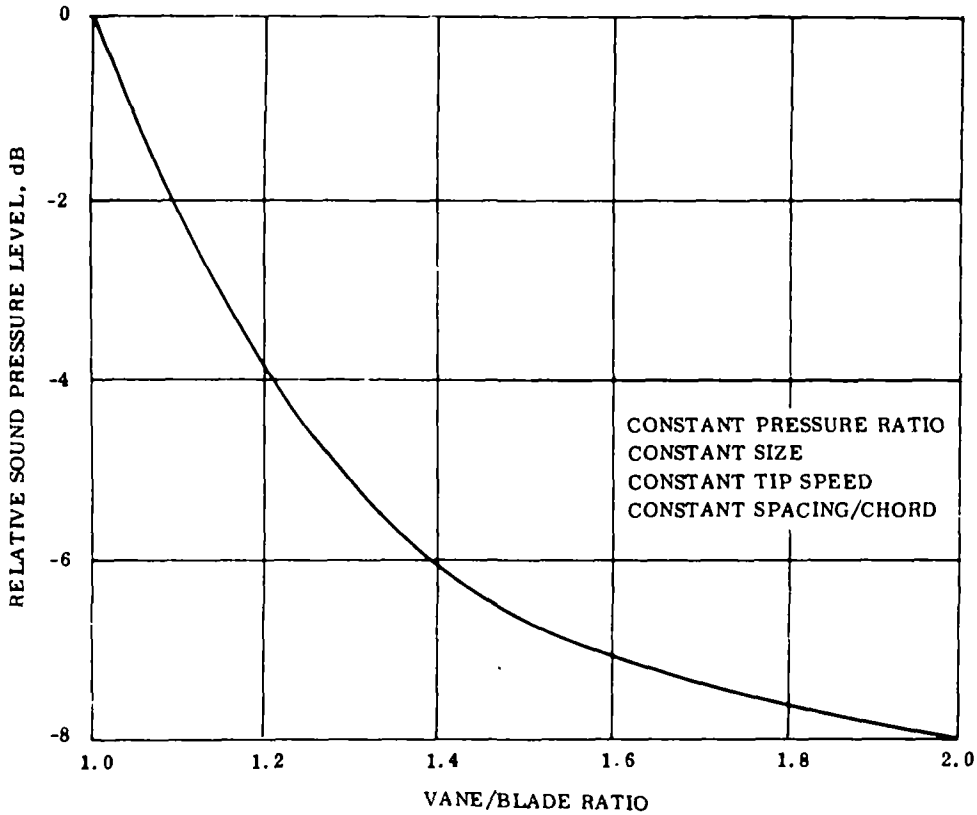

FIGURE C-5. EFFECT OF VANE/BLADE RATIO ON INTERACTION NOISE GENERATED AT THE BLADE PASSING FREQUENCY

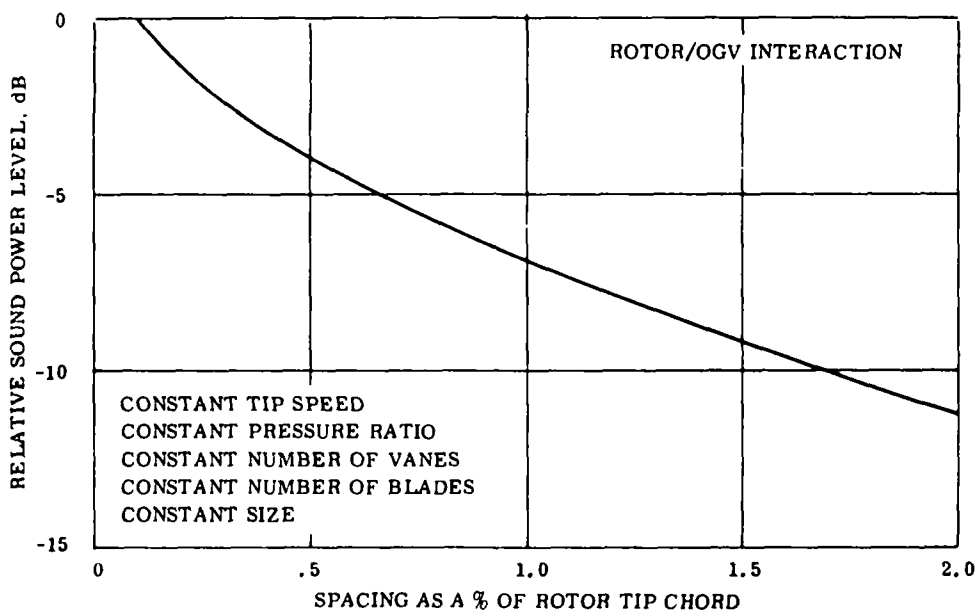

FIGURE C-6. EFFECT OF SPACING ON INTERACTION NOISE GENERATED AT THE BLADE PASSING FREQUENCY

SUMMARY AND CONCLUSIONS

Some theoretical methods have been developed to predict fan and compressor sound power levels generated at the blade passing frequency. These prediction techniques have been used to study the effects of different aerodynamic and geometric parameters on fan and compressor noise. The results indicate that low sound power levels will be obtained for:

- Low pressure ratios
- Low rotor blade loadings
- Low rotor diffusion factors
- High number of rotor blades
- High vane/blade ratios
- Large blade row spacings

An appreciable reduction in pure tone levels can be obtained by judicious selection of design parameters. This reduction of noise at the source can be quite attractive and should be incorporated in low noise fan and compressor designs.

By incorporation of this latest state-of-the-art design data, an optimum fan could be designed to interface with the Rankine combustor.

APPENDIX D

APPENDIX D

EMISSION DATA REDUCTION

The raw emissions data are read from the strip chart on the Beckman instrumentation cart and converted to observed values in parts per million (ppm) by volume or percent by volume from the previously obtained calibration curves for the instruments.

These observed values for carbon monoxide (CO), nitric oxide (NO), carbon dioxide (CO_2), and unburned hydrocarbons (H/C) together with the other pertinent rig operational parameters are utilized as input data for the data reduction program carried out on an IBM 360 Model 40 computer.

The program performs several correctional operations to the volumetric concentrations before conversion to mass concentrations.

- The observed CO and NO readings are corrected for other gaseous component interferences which produce higher readings. The interference correction factors are obtained from the emissions instrumentation manufacturer.

- A correction is made to the nitric oxide value for ambient humidity. This factor is contained in Section 1201.86 of the February 27, 1971 Federal Register (Volume 35, Number 40), and is normalized at a humidity corresponding to a water content of 75 grains water per pound of dry air.

- An exhaust water vapor correction is applied to put the volumetric concentrations on a wet rather than a dry basis. The wet volume concentrations are used for conversion to mass concentrations and flow rates of the individual species. The correction factor is calculated as a function of test point air-fuel ratio and fuel ultimate analysis.

- The volume concentrations are converted to unity equivalence ration, i.e., are quoted at a stoichiometric air-fuel ratio. This correction is thus a ratio of the actual test air-fuel ratio to the stoichiometric air-fuel ratio,

the latter being calculated from the fuel ultimate analysis. The volume concentrations are normally quoted as ppm or percent dry, corrected to stoichiometric (and to standard humidity conditions in the case of NO).

As noted, the wet volume concentrations are used to convert to the mass concentration using the test air-fuel ratio and the appropriate specie molecular weight. The molecular weight of the exhaust gas is assumed to be that for air.

A calculated value of CO_2 is obtained from a knowledge of the test air-fuel ratio and the fuel compositions assuming complete combustion. This calculated CO_2 value is compared to the measured value and in this manner any spurious results due to irregularities in the air, fuel, or emissions measurements can be eliminated.

It can be seen from the attached sample sheet of program output that the measured nitric oxide volumetric concentration is expressed on a weight basis in terms of the oxidized product, nitrogen dioxide (NO_2). This assumes that all the nitric oxide ultimately reacts in the atmosphere to nitrogen dioxide.

The unburned hydrocarbons are quoted on a weight basis as an "average" hydrocarbon, $CH_{1.85}$, as contained in the Federal Register requirements for light duty vehicles. This pseudo hydrocarbon was proposed for gasoline fueled power plants and is unlikely to represent the "average" unburned hydrocarbons while operating on JP-5 but its use does form a basis for comparison.

The horsepower figure used in the input data and in the brake specific emissions output is actually the test point fuel flow for convenience and has no other significance.

DATA POINT 1 ENGINE SPEED % 0.0

FUEL % CARBON	85.09999	CO2 %	6.80000
% HYDROGEN	14.90000	HORSEPOWER	109.00000
LHV BTU/LB	18400.0	WA LB/SEC	0.94110
HUMIDITY GN/LB	75.0000	WF LB/HR	109.00000

-*-*-*-*-* CORRECTION FACTORS *-*-*-*-*-*

WATER VAPOUR	0.93305
EQUIVALENCE	2.08027
HUMIDITY FED	1.00000
HUMIDITY CAL	0.99981

	NO	CO	H/C AS C1
VOLUMETRIC CONCENTRATION			
PPM OBSERVED	34.500000	53.000000	21.000000
PPM CORR INT	30.397934	48.375992	21.000000
PPM WET	28.362762	45.137177	21.000000
PPM DRY	30.397934	48.375992	22.506851
PPM DRY& STOICH	63.235901	100.635101	43.685654
PPM DRY,STOIC&HUM	63.235901	100.635101	43.685654
PPM WET&HUM	28.362762	45.137177	21.000000

	CO	H/C AS CH1.85	NO2
MASS CONCENTRATION			
GM/KG FUEL	1.399999	0.322611	1.444906
GM/HR	69.363571	15.983922	71.588562
GM/HR BHP	0.636363	0.146641	0.656776
LB/HR	0.152918	0.035238	0.157823
LB/HR BHP	0.001403	0.000323	0.001448
MM GM/M**3	53509.9414	12330.6563	55226.3906

COMBUSTION EFFICIENCIES	
E COMB CO	99.966553
E COMB H/C	99.969254
E COMB CO&H/C	99.935791

CARBON BALANCE	
CO2 RATIO MEAS/CALC IGNORING CO&H/C	0.993188
CO2 RATIO MEAS/CALC WITH CO&H/C	0.994216